Exploring the non-innocent character of electron rich π-extended 8-oxyquinolate ligands in ruthenium(II) bipyridyl complexes

Supporting Information

Stephanie Bellinger-Buckley,[†] Tse-Cing Chang,[‡] David Schweinfurth,[¥] Seema Bag,[†] Weihong Zhou,[†] Bela Torok,[†] Biprajit Sarkar,[¥] Ming-Kang Tsai,[‡] Jonathan Rochford[†]**

[†]Department of Chemistry, University of Massachusetts Boston, 100 Morrissey Boulevard, Boston, MA 02125. [‡]Department of Chemistry, National Taiwan Normal University, Taipei, Taiwan ROC. [¥]Institut für Chemie und Biochemie, Anorganische Chemie, Freie Universität Berlin, Fabeckstraβe 34-36, Berlin, Germany.

Jonathan.Rochford@umb.edu

Contents ***page #***

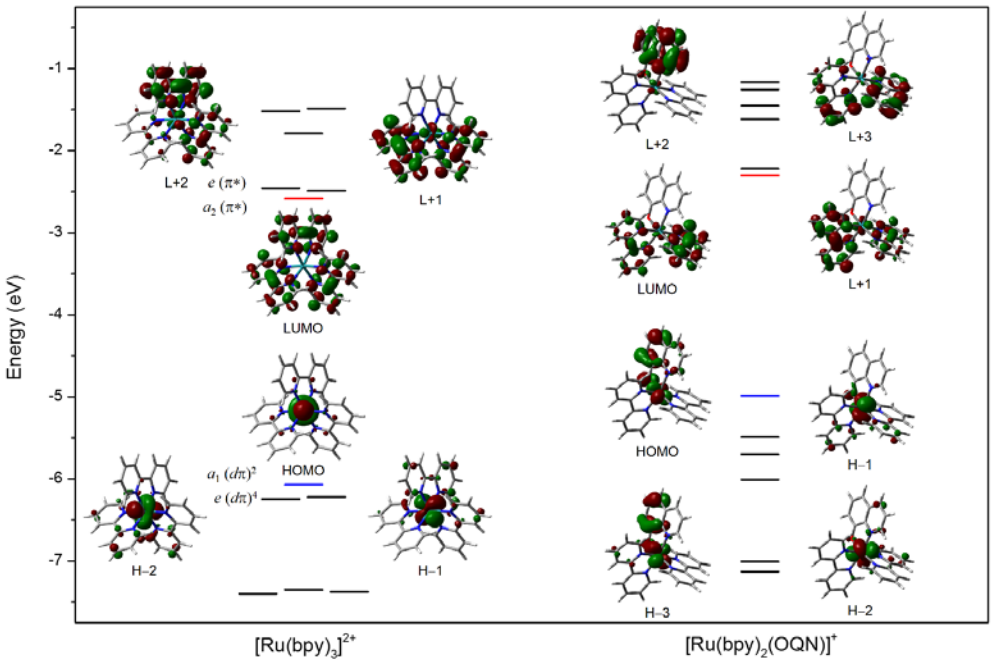

Figure SI-1. Molecular orbital correlation diagrams for 12+ [Ru(bpy)3]2+ (D3 symmetry) and 2+ [Ru(bpy)2(OQN)]+ (C1 symmetry) calculated by DFT with an acetonitrile polarizable continuum model [B3LYP/6-31g(d,p) (C,H,N,O), LANL08 (Ru)].

UV/Vis electronic absorption spectra.

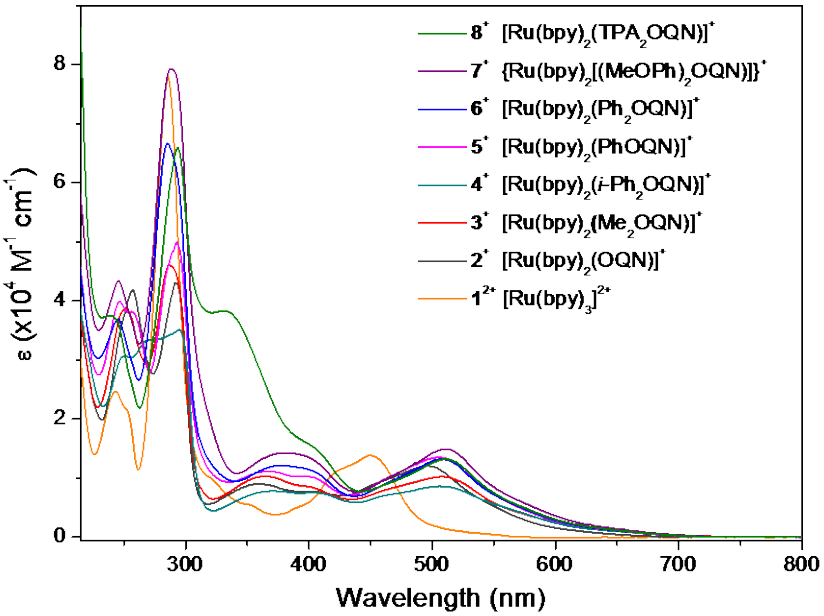

Figure SI-2. Overlay of all electronic absorption spectra $\mathbf{1}^{2+}$ **–** $\mathbf{8}^+$ recorded acetonitrile at room temperature.

Excitation and emission spectra.

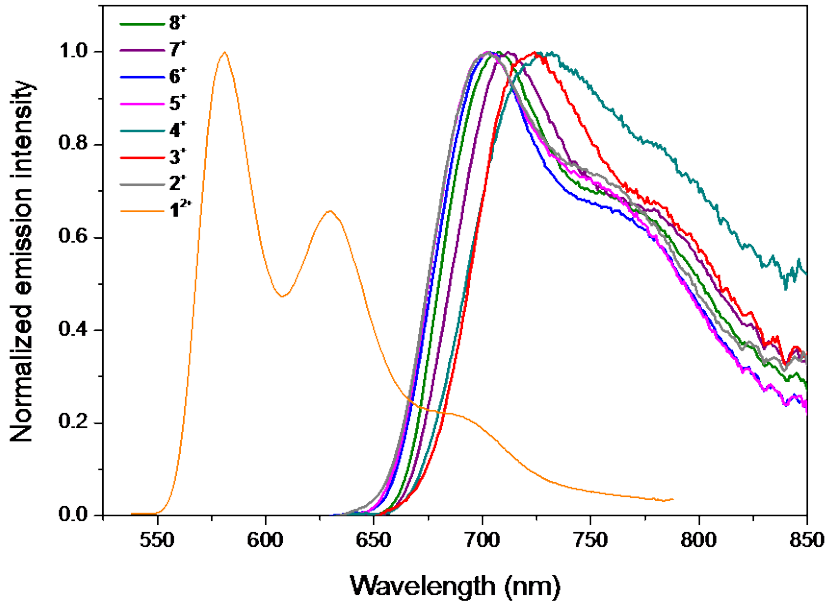

Figure SI-3. An overlay of corrected emission spectra for $\mathbf{1}^{2+}$ - $\mathbf{8}^{+}$ recorded in EtOH:MeOH frozen glass at 77 K.

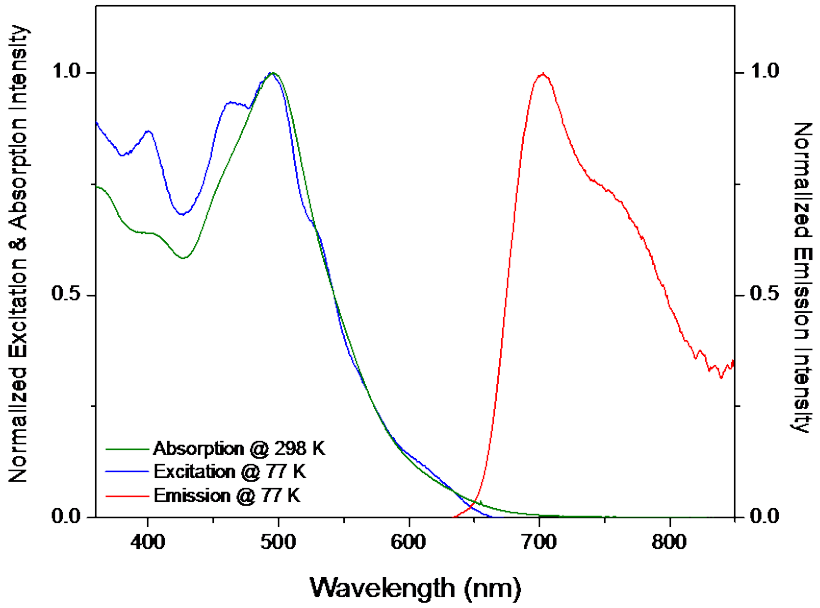

Figure SI-4. An overlay of absorption (298 K in acetonitrile), corrected excitation and emission spectra for $\mathbf{2}^{+}$ recorded in a EtOH:MeOH frozen glass at 77 K.

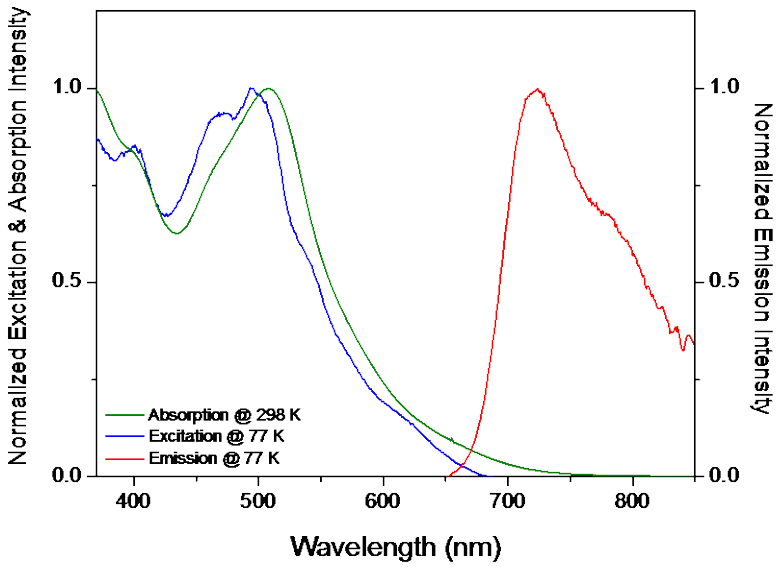

Figure SI-5. An overlay of absorption (298 K in acetonitrile), corrected excitation and emission spectra for $\mathbf{3}^{+}$ recorded in a EtOH:MeOH frozen glass at 77 K.

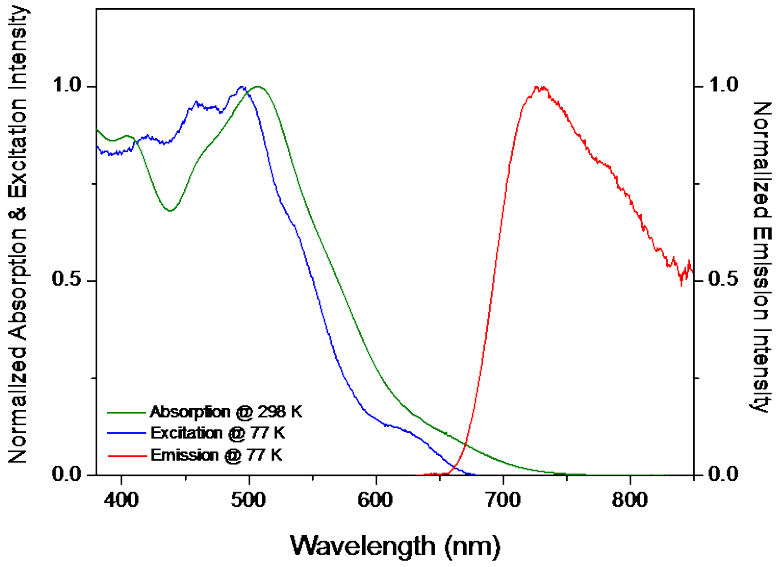

Figure SI-6. An overlay of absorption (298 K in acetonitrile), corrected excitation and emission spectra for $\mathbf{4}^{+}$ recorded in a EtOH:MeOH frozen glass at 77 K.

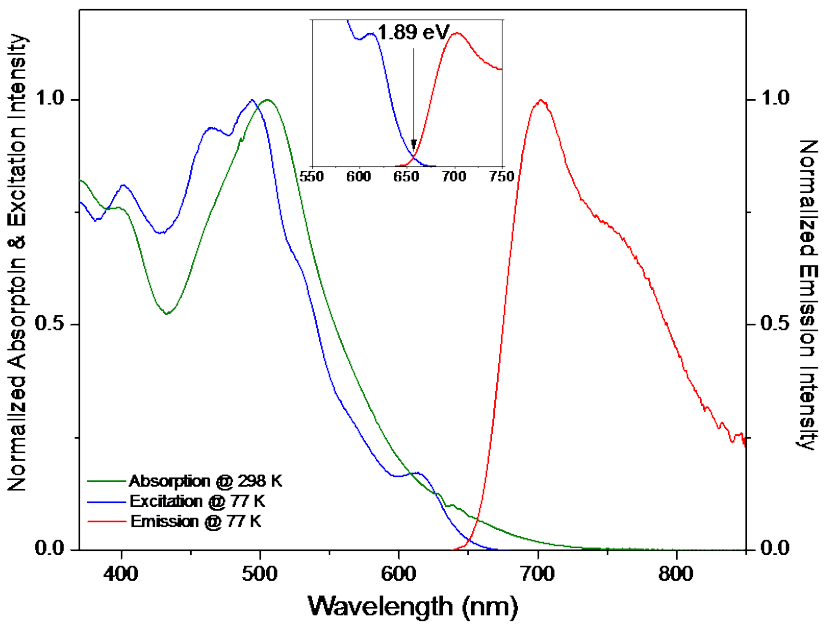

Figure SI-7. An overlay of absorption (298 K in acetonitrile), corrected excitation and emission spectra for $\mathbf{5}^{+}$ recorded in a EtOH:MeOH frozen glass at 77 K.

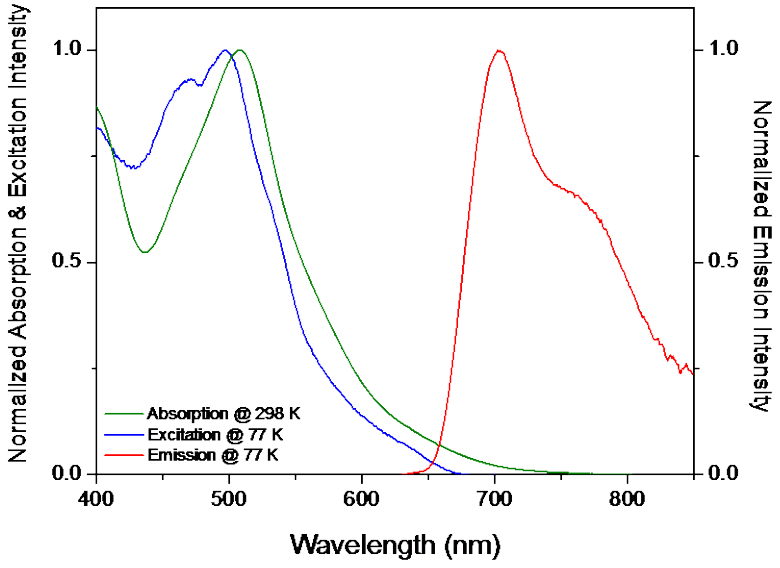

Figure SI-8. An overlay of absorption (298 K in acetonitrile), corrected excitation and emission spectra for $\mathbf{6}^{+}$ recorded in a EtOH:MeOH frozen glass at 77 K.

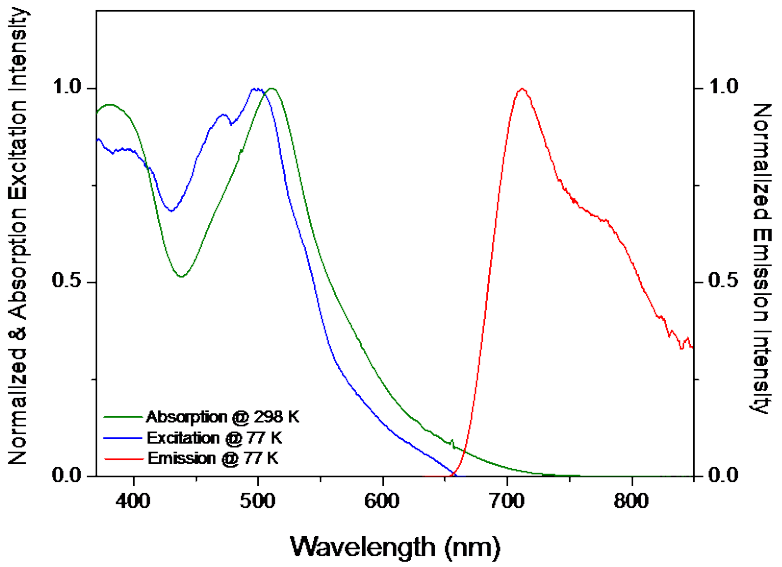

Figure SI-9. An overlay of absorption (298 K in acetonitrile), corrected excitation and emission spectra for $\mathbf{7}^{+}$ recorded in a EtOH:MeOH frozen glass at 77 K.

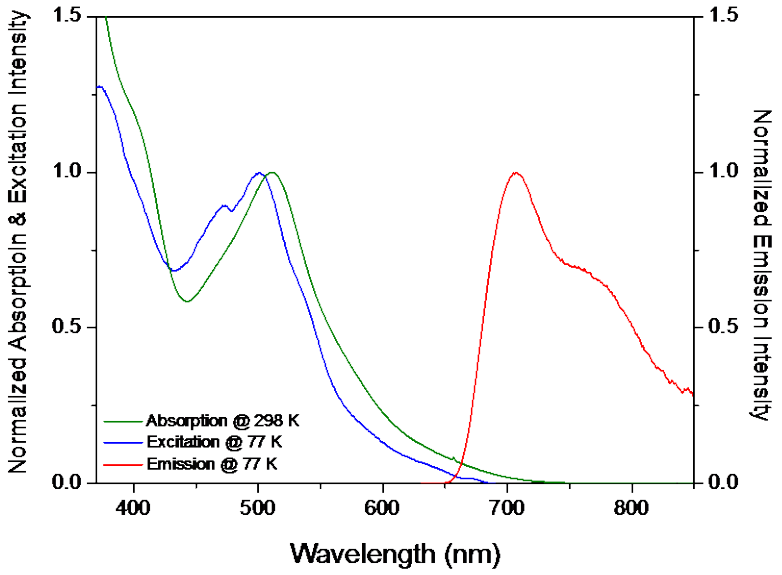

Figure SI-10. An overlay of absorption (298 K in acetonitrile), corrected excitation and emission spectra for $\mathbf{8}^{+}$ recorded in a EtOH:MeOH frozen glass at 77 K.

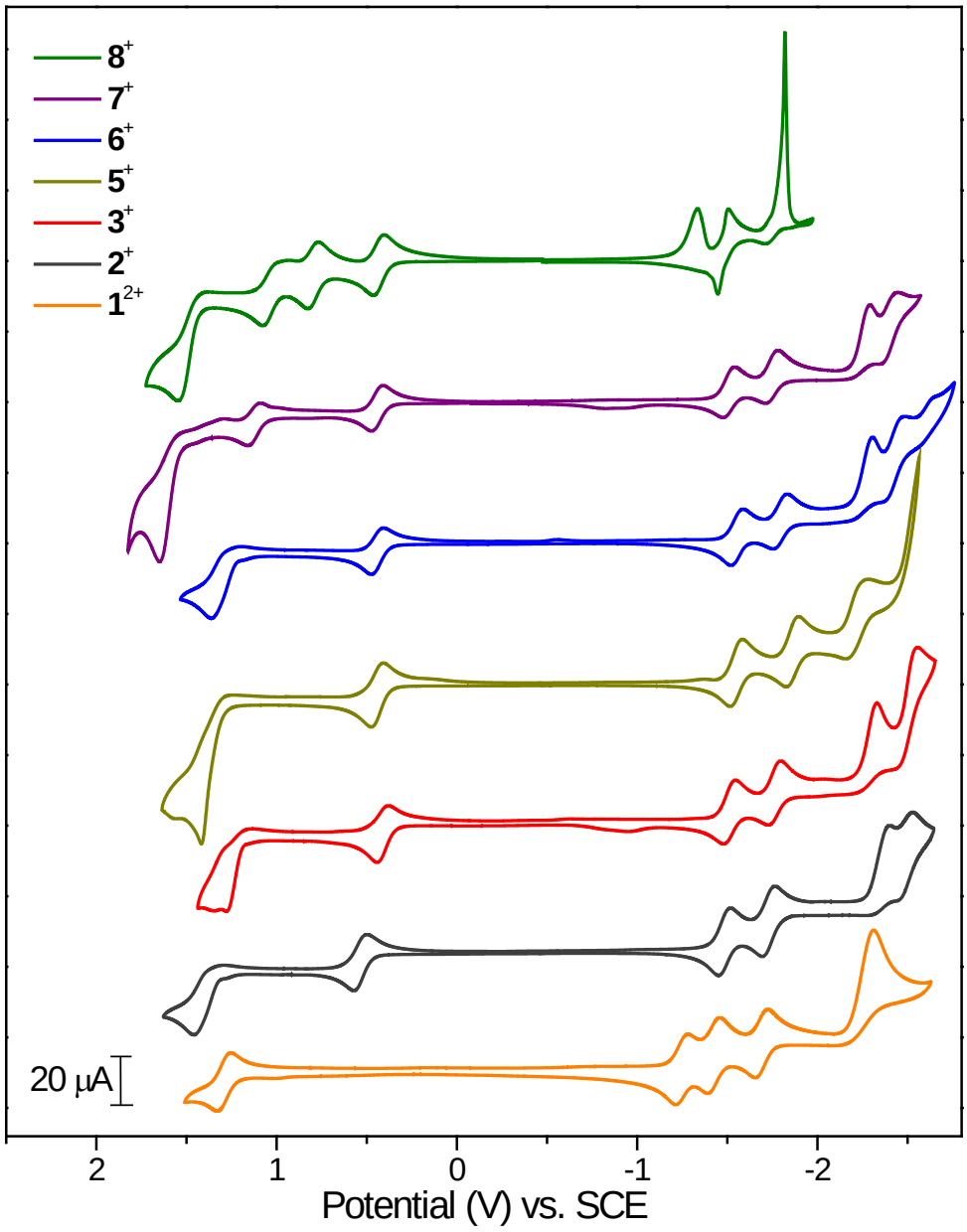

Figure S11. Overlay of cyclic voltammograms for all complexes $\mathbf{1}^{2+}$ – $\mathbf{8}^{+}$ recorded in acetonitrile (0.1 M Bu_4NPF_6) at a glassy carbon working electrode with scan rate of 50 mV s^{-1}.

Computational analysis of native $\mathbf{1}^{2+}$ - $\mathbf{8}^{+}$ *complexes*

All data was calculated with an acetonitrile polarizable continuum model using the B3LYP functional and 6-31g(d,p) (C,H,N,O) and LANL08 (Ru) basis sets.

$\mathbf{1}^{2+}$ $[Ru(bpy)_3]^{2+}$

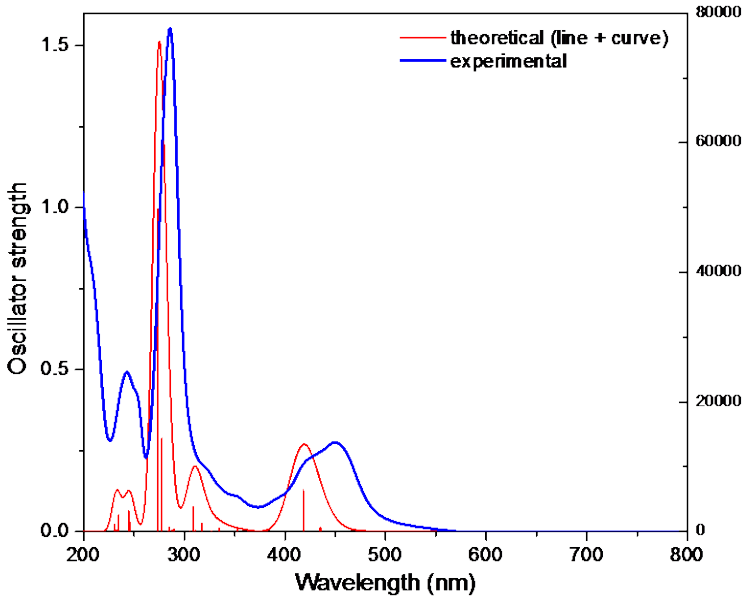

Figure SI-12. An overlay of experimental (acetonitrile) and theoretical spectra for $\mathbf{1}^{2+}$. TDDFT spectrum was calculated with an acetonitrile polarizable continuum model using the [B3LYP functional and 6-31g(d,p) (C,H,N,O), LANL08 (Ru) basis sets.

electronic transition (nm)	MO contributions (%)	oscillator strength (f)
309.02	H-2->L+5 (30%), H-1->L+4 (40%), H-1->L+6 (16%)	0.0765
309.05	H-2->L+4 (30%), H-2->L+6 (18%), H-1->L+5 (39%)	0.0773
317.42	HOMO->L+7 (29%), HOMO->L+8 (60%)	0.0272
334.35	H-1->L+3 (96%)	0.0116
417.99	H-2->LUMO (19%), H-2->L+1 (12%), H-2->L+2 (29%), H-1->L+1 (27%), H-1->L+2 (11%)	0.1297
418.5	H-2->L+1 (28%), H-2->L+2 (12%), H-1->LUMO (21%), H-1->L+1 (11%), H-1->L+2 (26%)	0.1261
434.82	H-1->LUMO (78%)	0.0135
435.4	H-2->LUMO (80%)	0.0117

Table SI-1 electronic transitions for $\mathbf{1}^{2+}$ calculated by TD-DFT.

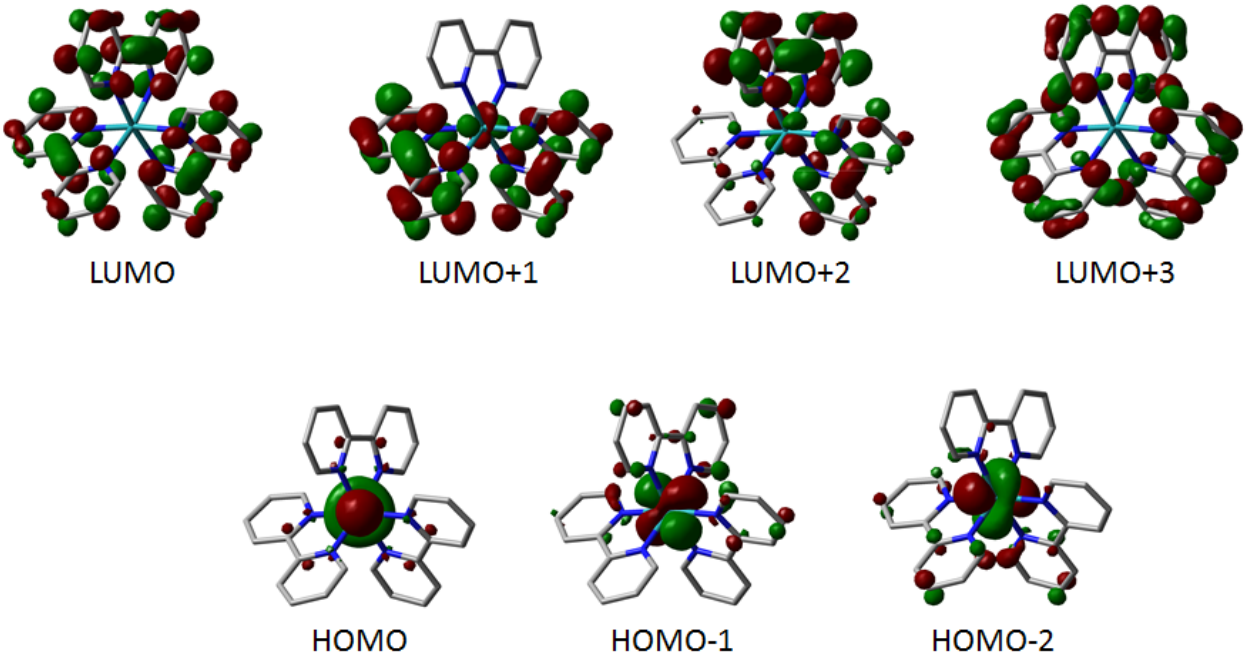

Fig. SI-13 Selected molecular orbitals for $\mathbf{1}^{2+}$.

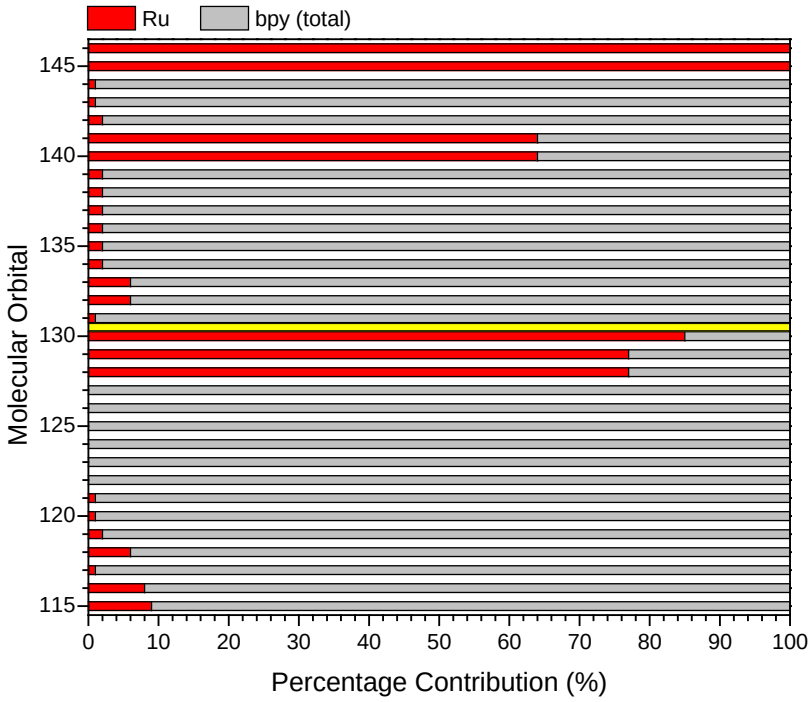

Fig. SI-14 Percentage contributions of Ru and bpy fragments to molecular orbitals of $\mathbf{1}^{2+}$. Filled and valence levels are separated by a yellow row between the HOMO (130) and LUMO (131) levels.

2^{+} $[Ru(bpy)_2(OQN)]^{+}$

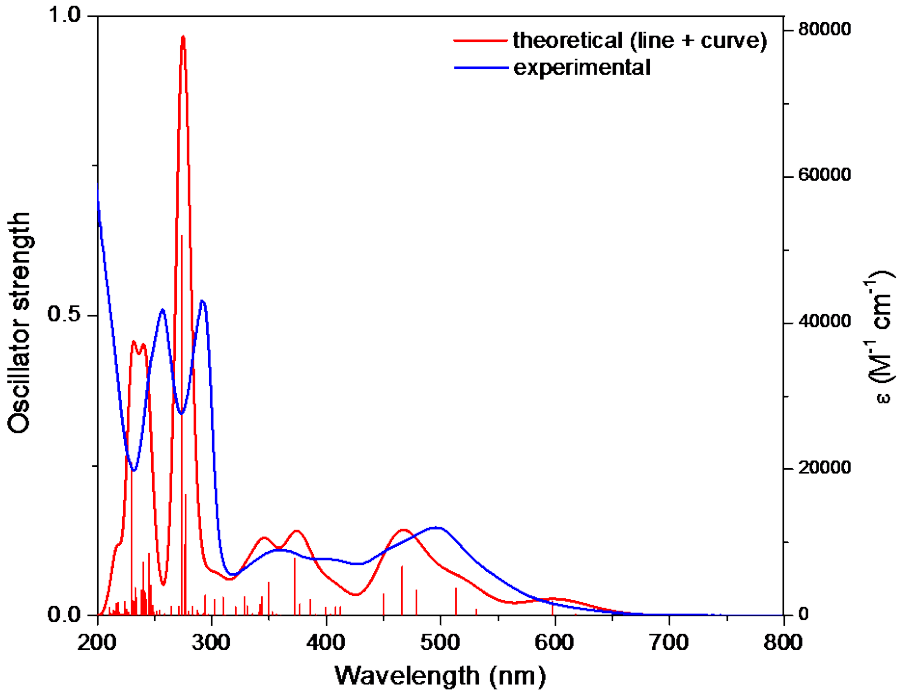

Figure SI-15. An overlay of experimental and theoretical spectra for **2**$^{+}$.

electronic transition (nm)	MO contributions (%)	oscillator strength (f)
309.70	H-3->L+3 (45%), H-2->L+4 (10%)	0.0313
344.15	H-3->L+2 (13%), H-1->L+5 (40%), H-1->L+10 (25%)	0.0319
349.63	H-2->L+3 (14%), H-1->L+5 (21%), H-1->L+6 (17%), H-1->L+10 (25%)	0.0556
372.62	H-2->L+2 (80%)	0.0967
399.64	H-3->LUMO (24%), H-3->L+1 (15%), HOMO->L+4 (33%)	0.0142
412.31	H-1->L+2 (82%)	0.0156
466.05	HOMO->L+2 (77%)	0.0825
512.94	H-2->L+1 (13%), H-1->LUMO (13%), H-1->L+1 (64%)	0.0468

Table SI-2 Electronic transitions for **2**$^{+}$ calculated by TD-DFT.

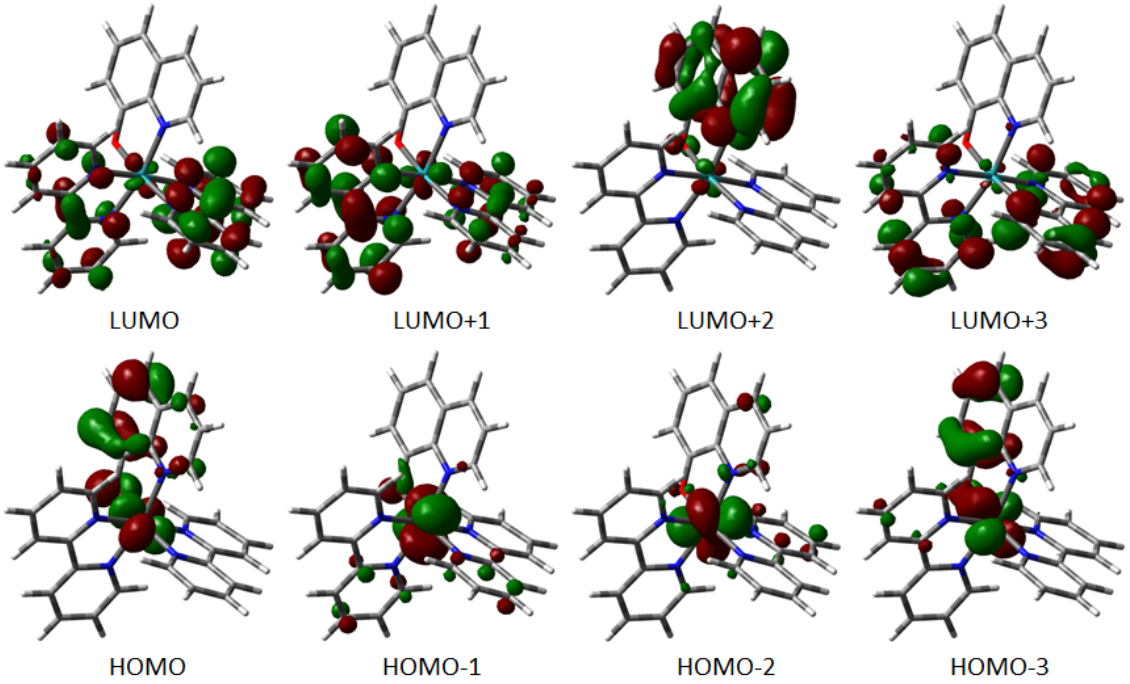

Fig. SI-16 Selected molecular orbitals for $\mathbf{2}^{+}$.

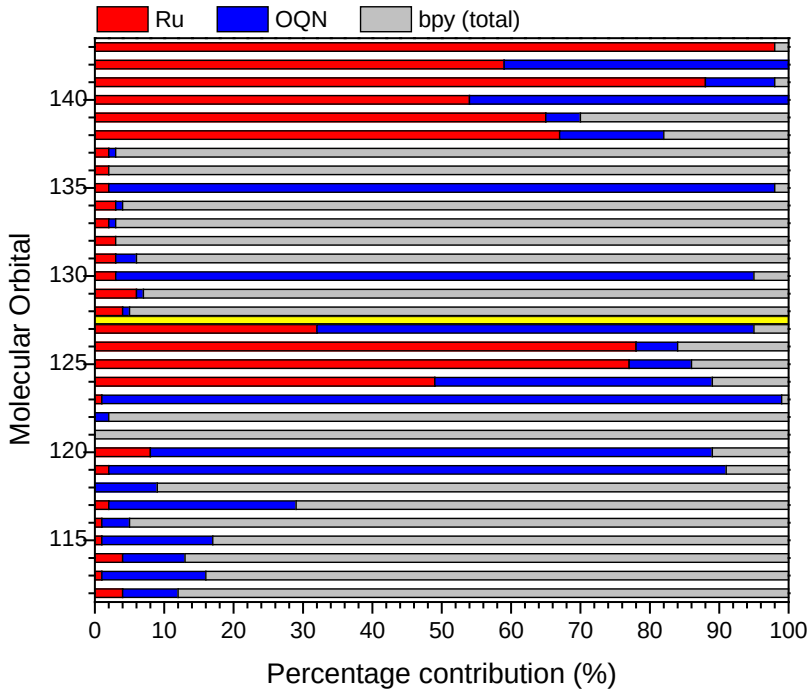

Fig. SI-17 Percentage contributions of Ru, OQN, and bpy fragments to molecular orbitals of $\mathbf{2}^{+}$. Filled and valence levels are separated by a yellow row between the HOMO (127) and LUMO (128) levels.

3^{+} $[Ru(bpy)_2(Me_2OQN)]^{+}$

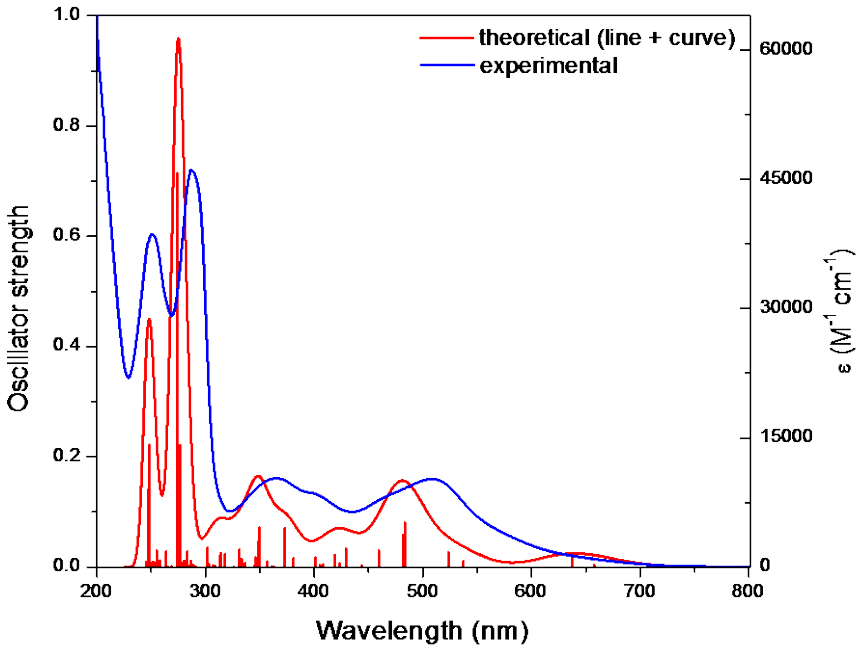

Figure SI-18. An overlay of experimental and theoretical spectra for **3**$^{+}$.

electronic transition (nm)	MO contributions (%)	oscillator strength (f)
309.02	H-2->L+5 (30%), H-1->L+4 (40%), H-1->L+6 (16%)	0.0765
309.05	H-2->L+4 (30%), H-2->L+6 (18%), H-1->L+5 (39%)	0.0773
317.42	HOMO->L+7 (29%), HOMO->L+8 (60%)	0.0272
334.35	H-1->L+3 (96%)	0.0116
417.99	H-2->LUMO (19%), H-2->L+1 (12%), H-2->L+2 (29%), H-1->L+1 (27%), H-1->L+2 (11%)	0.1297
418.5	H-2->L+1 (28%), H-2->L+2 (12%), H-1->LUMO (21%), H-1->L+1 (11%), H-1->L+2 (26%)	0.1261
434.82	H-1->LUMO (78%)	0.0135
435.4	H-2->LUMO (80%)	0.0117

Table SI-3 Electronic transitions for **3**$^{+}$ calculated by TD-DFT.

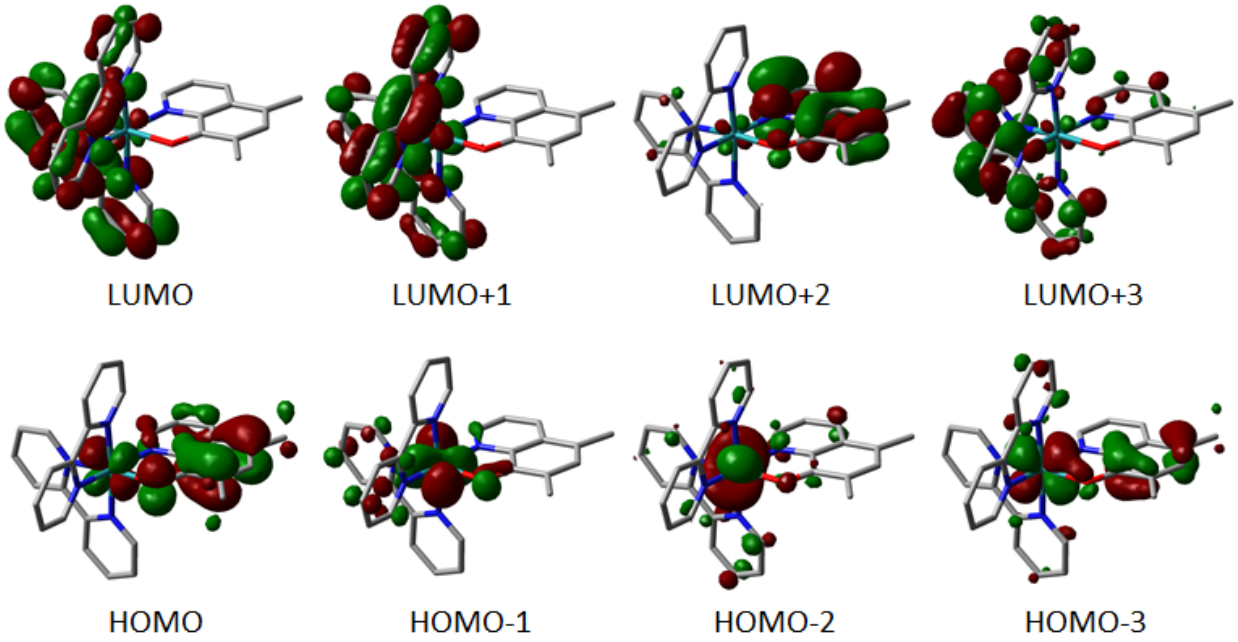

Fig. SI-19 Selected molecular orbitals for $\mathbf{3}^{+}$.

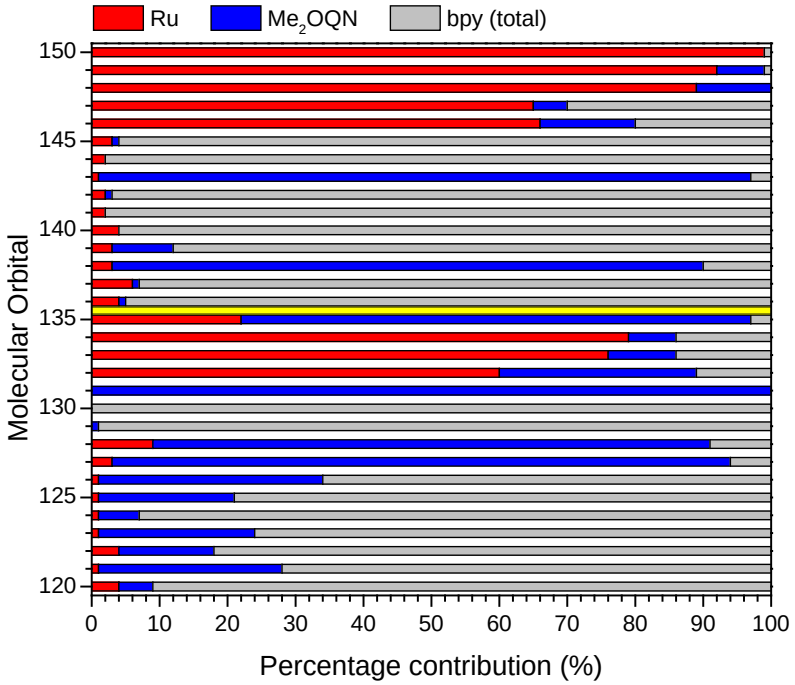

Fig. SI-20 Percentage contributions of Ru, Me_2OQN and bpy fragments to molecular orbitals of $\mathbf{3}^{+}$. Filled and valence levels are separated by a yellow row between the HOMO (135) and LUMO (136) levels.

4^{+} $[Ru(bpy)_2(i\text{-}Ph_2OQN)]^{+}$

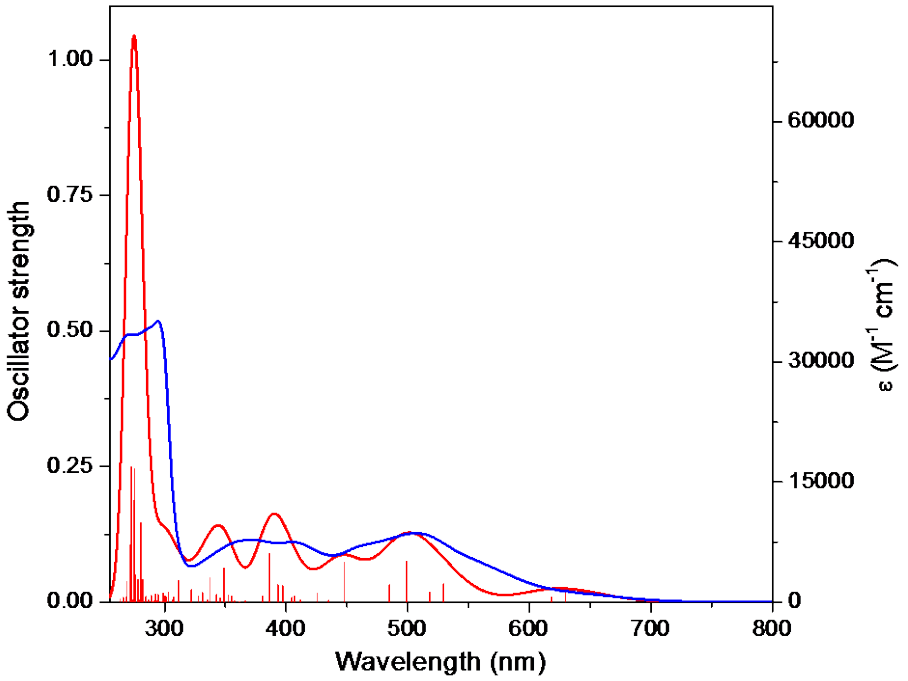

Figure SI-21. An overlay of experimental and theoretical spectra for **4**$^{+}$.

electronic transition (nm)	MO contributions (%)	oscillator strength (f)
311.74	H-3(A)->L+3(A) (26%),H-3(B)->L+3(B) (26%)	0.0401
337.21	H(A)->L+7(A) (40%),H(B)->L+7(B) (40%)	0.0451
349.08	H-1(A)->L+5(A) (32%),H-1(B)->L+5(B) (32%)	0.0637
386.39	H-2(A)->L+2(A) (33%),H-2(B)->L+2(B) (33%)	0.09
393.15	H(A)->L+6(A) (24%),H(B)->L+6(B) (24%)	0.0313
397.15	H(A)->L+5(A) (29%),H(B)->L+5(B) (29%)	0.0304
447.88	H-2(A)->L+1(A) (32%),H-2(B)->L+1(B) (32%)	0.0738
485.03	H-2(A)->L(A) (41%),H-2(B)->L(B) (41%)	0.0323
499.02	H(A)->L+2(A) (45%),H(B)->L+2(B) (45%)	0.0762
529.53	H-1(A)->L(A) (45%),H-1(B)->L(B) (45%)	0.0341

Table SI-4 Electronic transitions for **4**$^{+}$ calculated by TD-DFT.

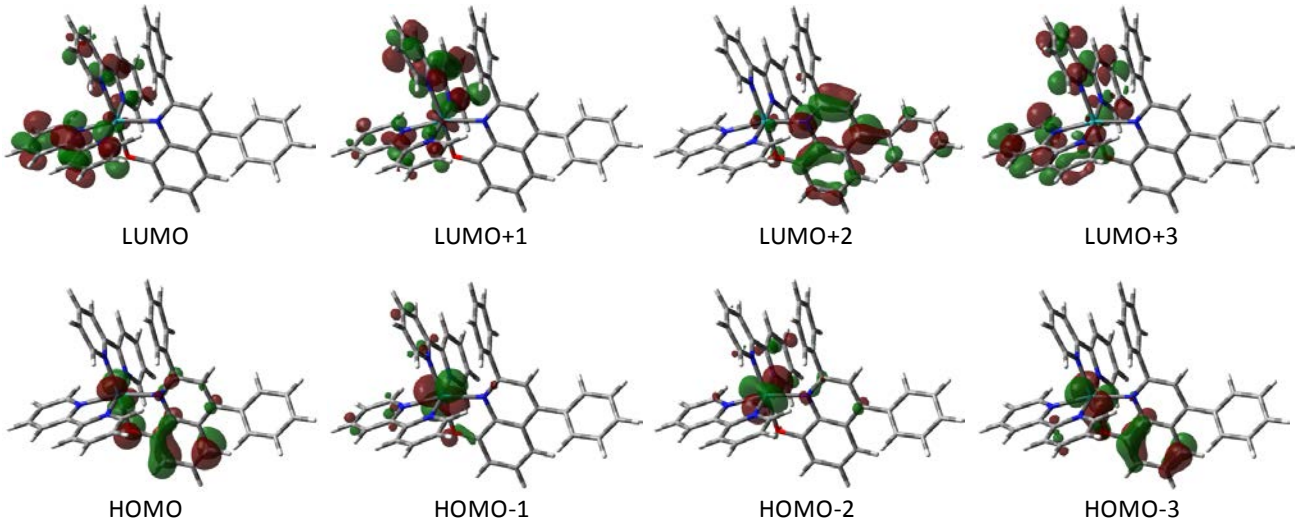

Fig. SI-22 Selected molecular orbitals for $\mathbf{4}^{+}$.

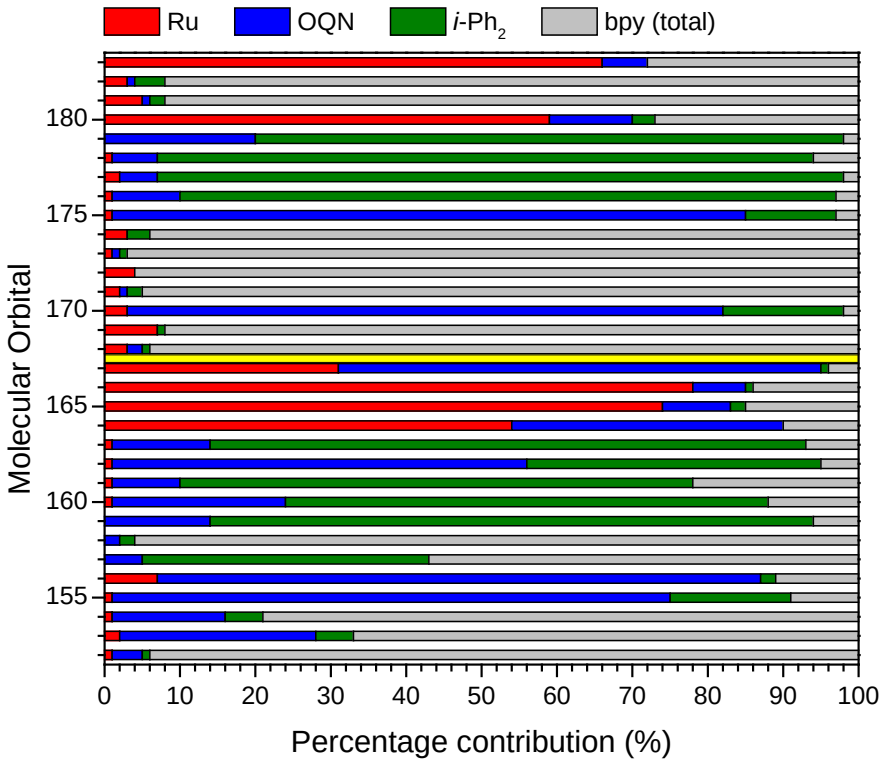

Fig. SI-23 Percentage contributions of Ru, OQN, *i*-Ph_2 and bpy fragments to molecular orbitals of $\mathbf{4}^{+}$. Filled and valence levels are separated by a yellow row between the HOMO (167) and LUMO (168) levels.

5^{+} $[Ru(bpy)_2(PhOQN)]^{+}$

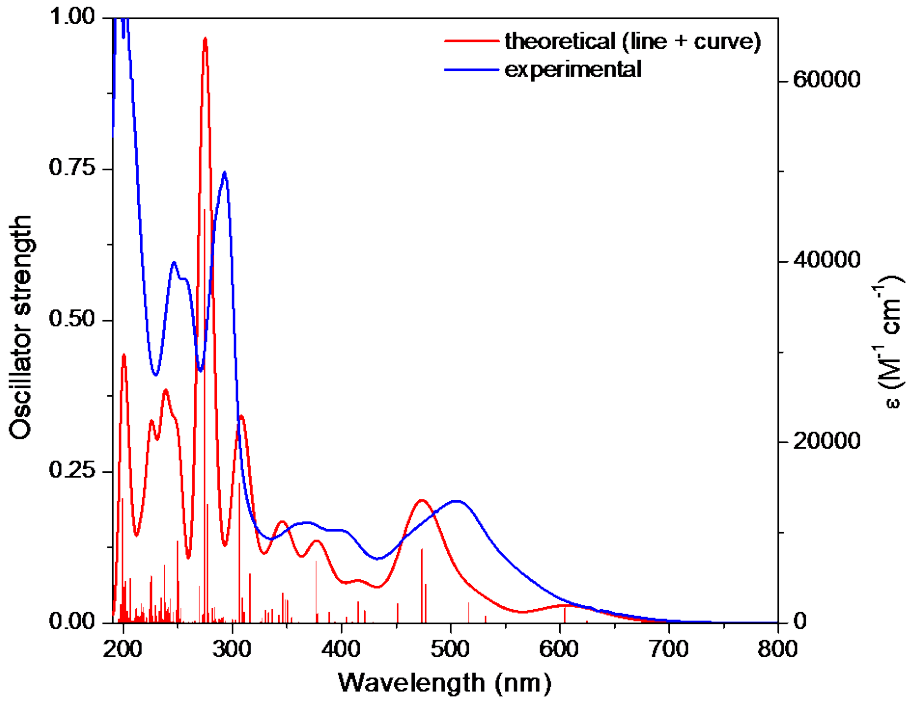

Figure SI-24. An overlay of experimental and theoretical spectra for **5**$^{+}$.

electronic transition (nm)	MO contributions (%)	oscillator strength (f)
306.12	H-3->L+5 (15%), HOMO->L+8 (76%)	0.2314
315.91	H-3->L+3 (34%)	0.0809
345.97	H-1->L+5 (46%), H-1->L+6 (21%), H-1->L+12 (14%)	0.0491
376.53	H-2->L+2 (87%)	0.1026
415.24	H-3->LUMO (10%), H-3->L+1 (41%), H-1->L+2 (37%)	0.0357
473.67	HOMO->L+2 (82%)	0.1222
476.9	H-2->LUMO (68%), H-2->L+1 (18%)	0.0638
516.53	H-2->L+1 (12%), H-1->LUMO (10%), H-1->L+1 (70%)	0.0337
604.38	HOMO->LUMO (19%), HOMO->L+1 (73%)	0.0251

Table SI-5 Electronic transitions for **5**$^{+}$ calculated by TD-DFT.

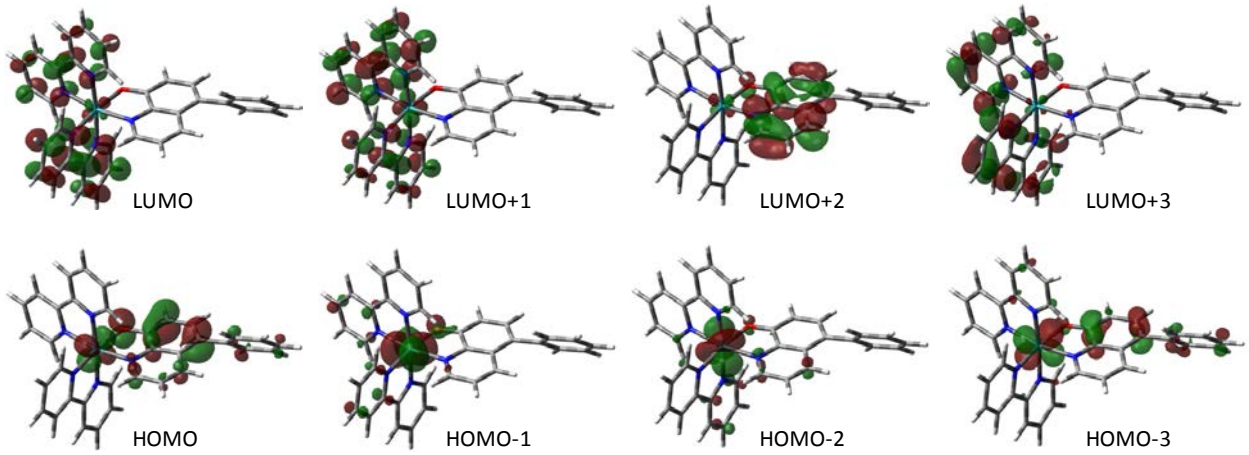

Fig. SI-25 Selected molecular orbitals for $\mathbf{5}^{+}$.

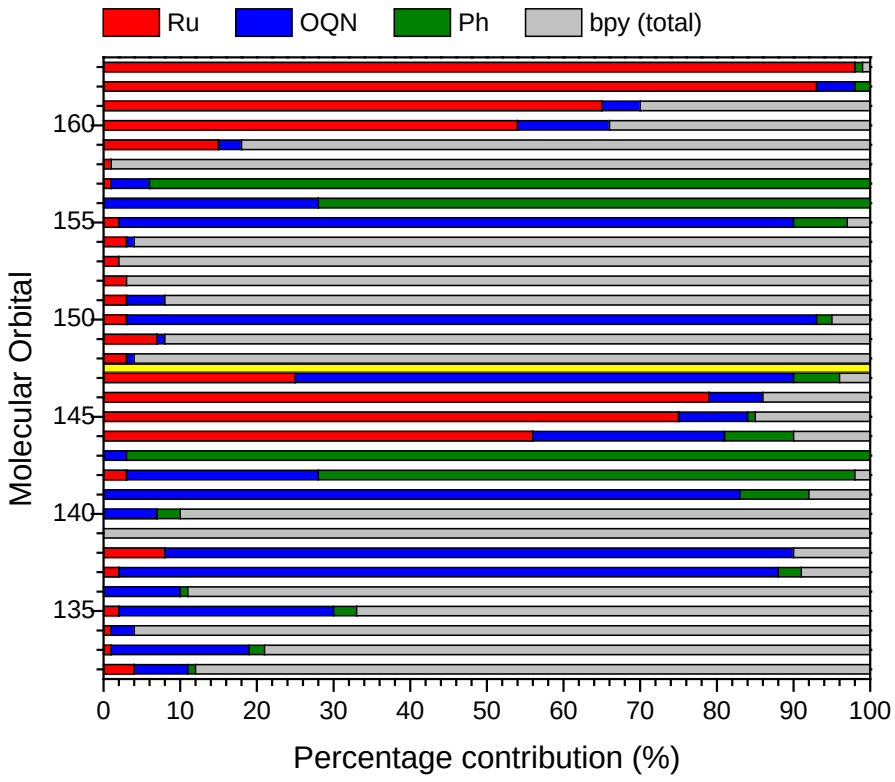

Fig. SI-26 Percentage contributions of Ru, OQN, Ph and bpy fragments to molecular orbitals of $\mathbf{5}^{+}$. Filled and valence levels are separated by a yellow row between the HOMO (147) and LUMO (148) levels.

6^{+} $[Ru(bpy)_2(Ph_2OQN)]^{+}$

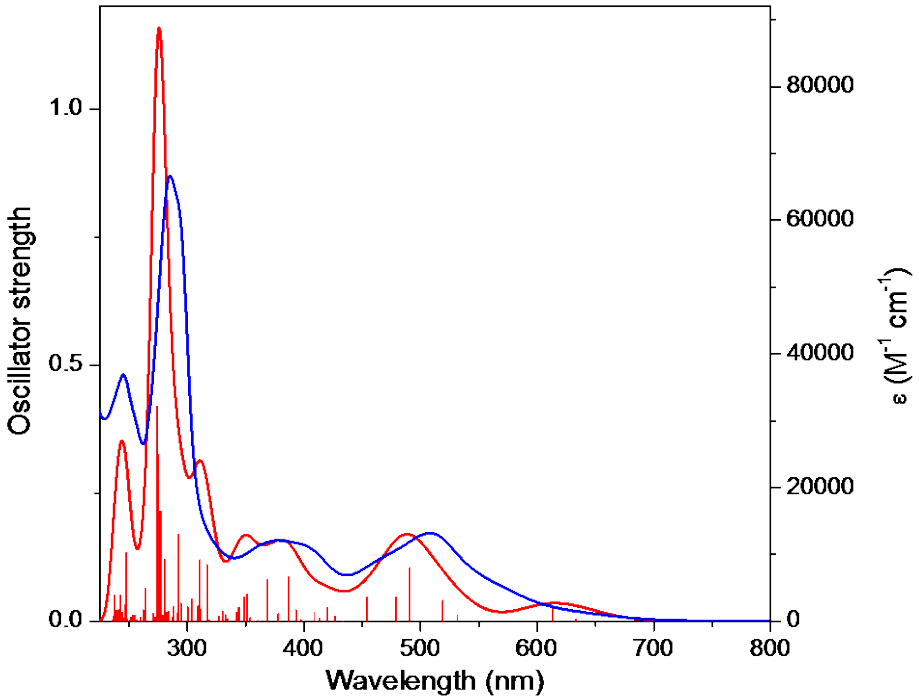

Figure SI-27. An overlay of experimental and theoretical spectra for **6**$^{+}$.

electronic transition (nm)	MO contributions (%)	oscillator strength (f)
310.78	HOMO->L+8 (58%)	0.1203
330.42	H-2->L+5 (80%)	0.0206
369.01	H-3->L+2 (16%), HOMO->L+7 (77%)	0.0815
386.68	H-2->L+2 (76%)	0.0869
420.21	H-3->LUMO (46%), H-3->L+1 (38%)	0.0277
454.25	H-2->LUMO (21%), H-2->L+1 (45%)	0.0477
490.82	H-2->L+1 (10%), HOMO->L+2 (85%)	0.1055
518.75	H-2->L+1 (10%), H-1->LUMO (11%), H-1->L+1 (69%)	0.0413
613.41	HOMO->LUMO (24%), HOMO->L+1 (68%)	0.0314

Table SI-6 Electronic transitions for **6**$^{+}$ calculated by TD-DFT.

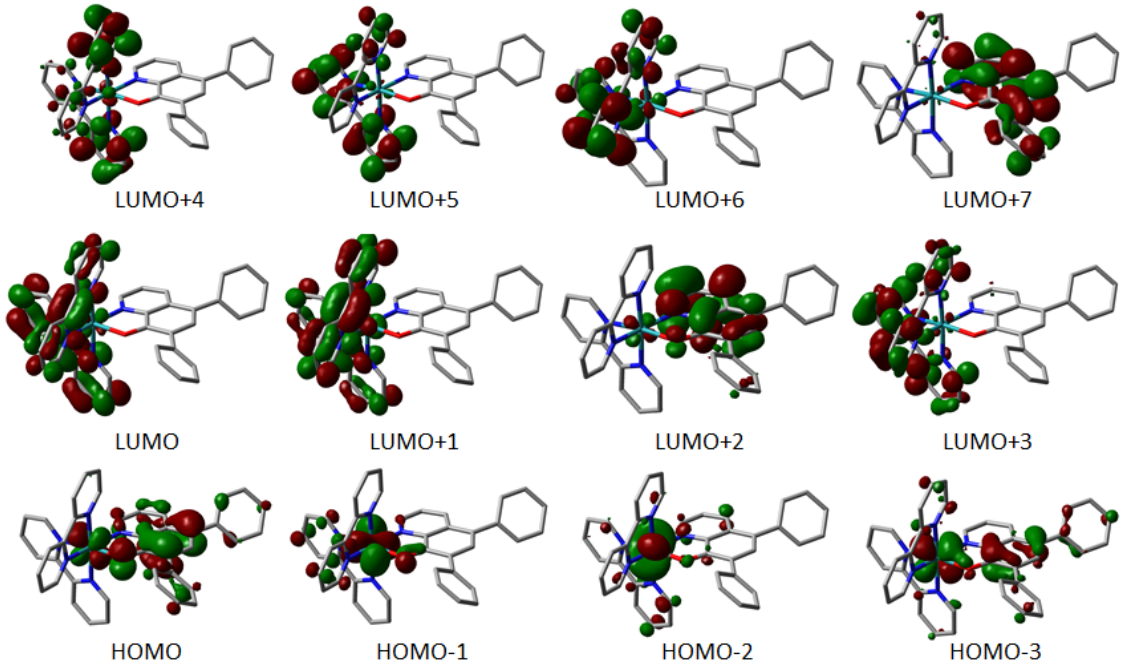

Fig. SI-28 Selected molecular orbitals for $\mathbf{6}^{+}$.

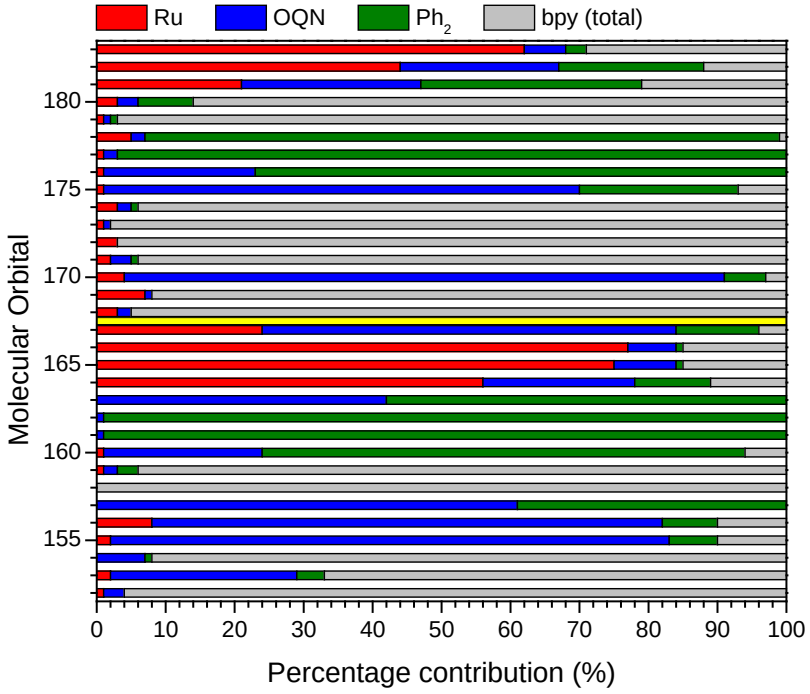

Fig. SI-29 Percentage contributions of Ru, OQN, Ph_2 and bpy fragments to molecular orbitals of $\mathbf{6}^{+}$. Filled and valence levels are separated by a yellow row between the HOMO (167) and LUMO (168) levels.

7^{+} $\{Ru(bpy)_2[(MeOPh)_2OQN]\}^{+}$

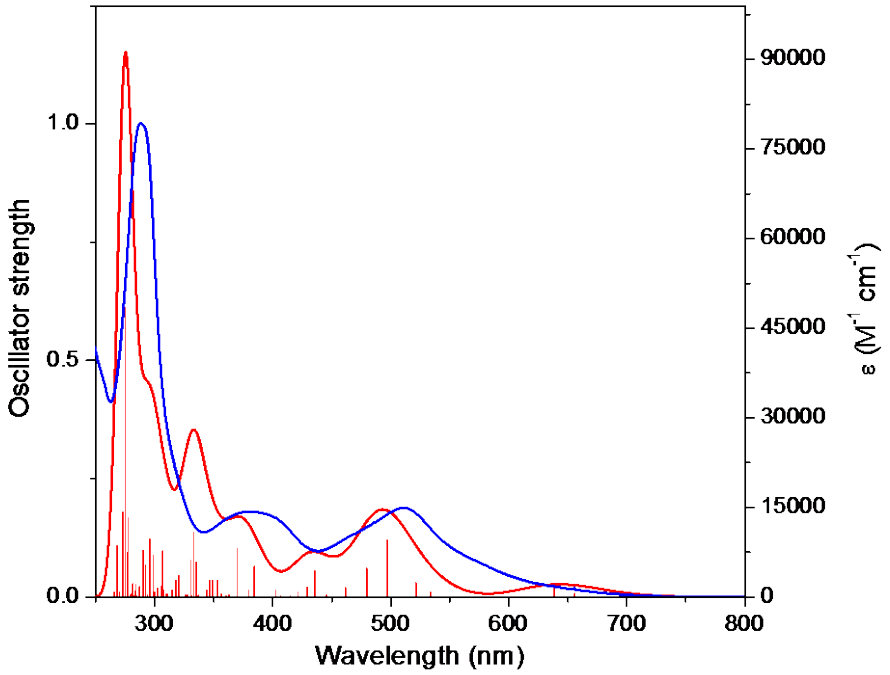

Figure SI-30. An overlay of experimental and theoretical spectra for **7**$^{+}$.

electronic transition (nm)	MO contributions (%)	oscillator strength (f)
306.73	H-3->L+5 (13%),H-3->L+6 (13%)	0.0979
330.71	H-2->L+5 (21%)	0.0786
333.05	H-4->L+2 (16%), H-2->L+5 (15%)	0.1373
335.14	H-4->L+2 (15%), H-2->L+6 (13%)	0.0734
369.8	H->L+7 (35%)	0.1016
384.23	H-2->L+2 (46%)	0.0648
435.46	H-3->L+1 (31%)	0.0553
479.77	H-2->L (38%)	0.0610
497.00	H->L+2 (44%)	0.1206
521.35	H-1->L+1 (36%)	0.0304
638.27	H->L+1 (42%)	0.0191
655.82	H->L (42%)	0.0079

Table SI-7 Electronic transitions for **7**$^{+}$ calculated by TD-DFT.

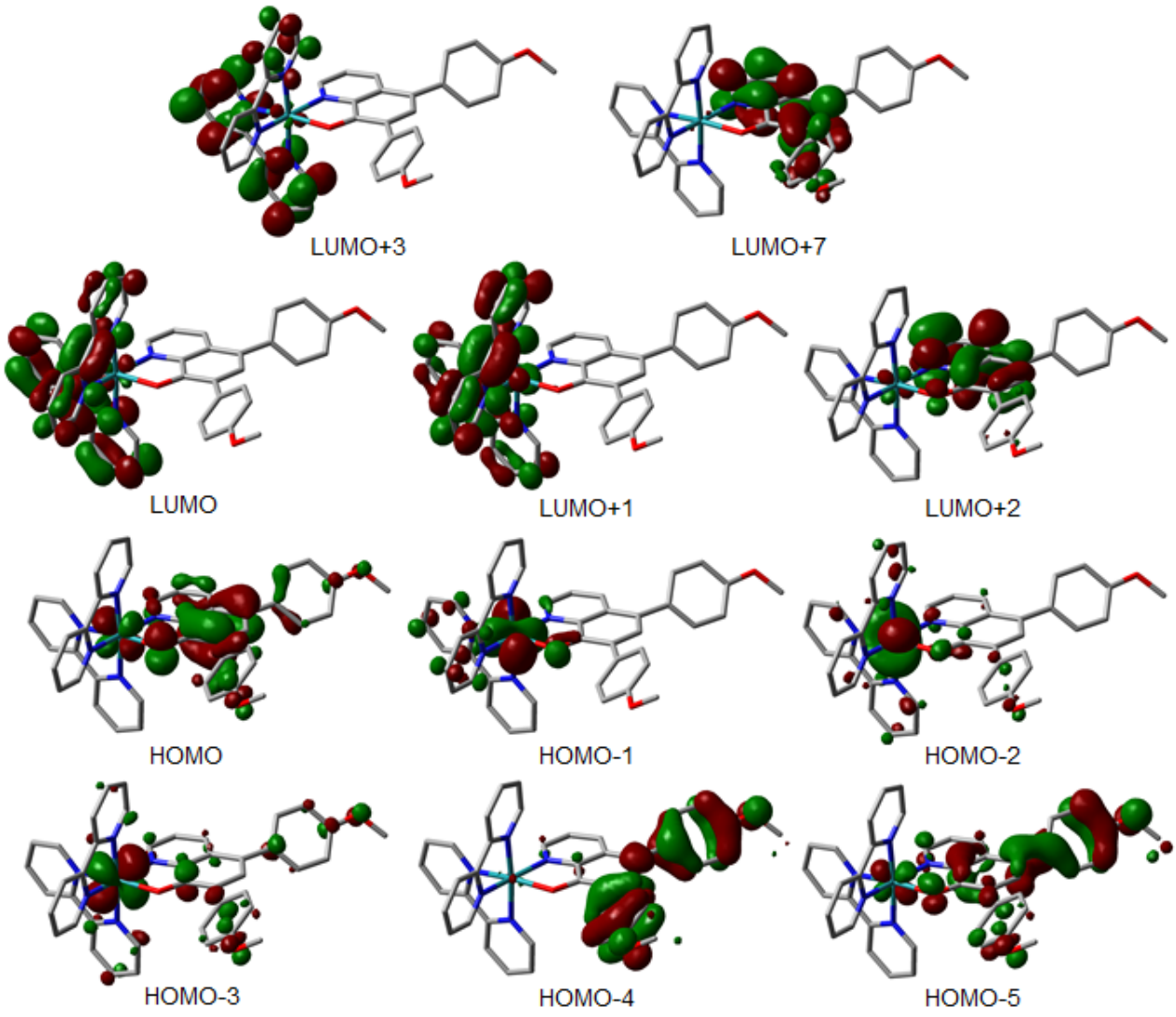

Fig. SI-31 Selected molecular orbitals for $\mathbf{7}^{+}$.

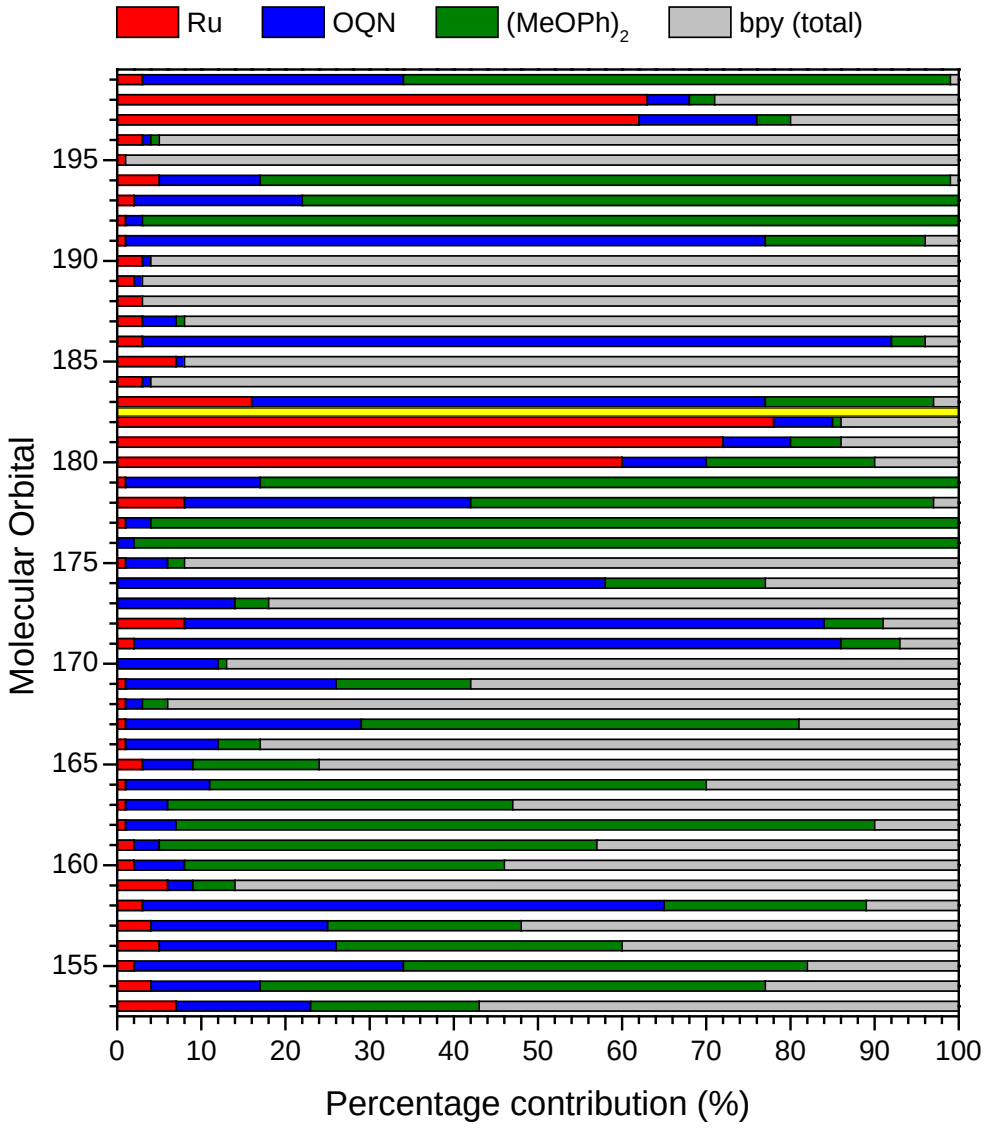

Fig. SI-32 Percentage contributions of Ru, OQN, $(MeOPh)_2$ and bpy fragments to molecular orbitals of $\mathbf{7}^+$. Filled and valence levels are separated by a yellow row between the HOMO (182) and LUMO (183) levels.

8^{+} $[Ru(bpy)_2(TPA_2OQN)]^{+}$

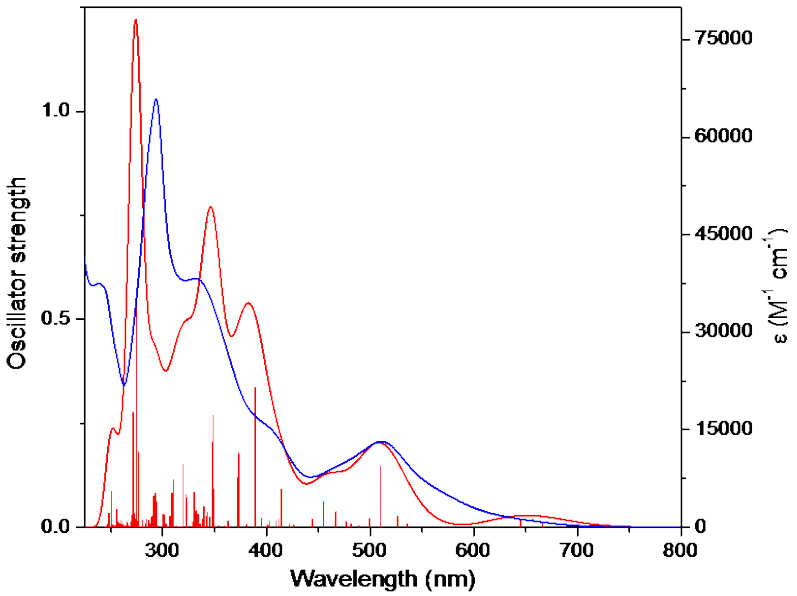

Figure SI-33. An overlay of experimental and theoretical spectra for **8**$^{+}$.

electronic transition (nm)	MO contributions (%)	oscillator strength (f)
319.66	H-1->L+11 (14%), HOMO->L+11 (82%)	0.1506
348.68	H-5->L+2 (16%), H-3->L+5 (26%), HOMO->L+8 (34%)	0.2696
373.02	H-4->L+2 (40%), H-2->L+2 (12%), H-1->L+3 (20%)	0.1781
389.12	H-4->L+2 (14%), HOMO->L+7 (74%)	0.3368
414.65	H-1->L+2 (92%)	0.0919
454.96	HOMO->L+3 (70%)	0.0614
476.76	H-4->LUMO (58%), H-4->L+1 (24%)	0.0146
510.11	HOMO->L+2 (84%)	0.1465
526.69	H-3->L+1 (70%)	0.027
645.1	HOMO->L+1 (86%), HOMO->LUMO (6%)	0.0202

Table SI-8 Electronic transitions for **8**$^{+}$ calculated by TD-DFT.

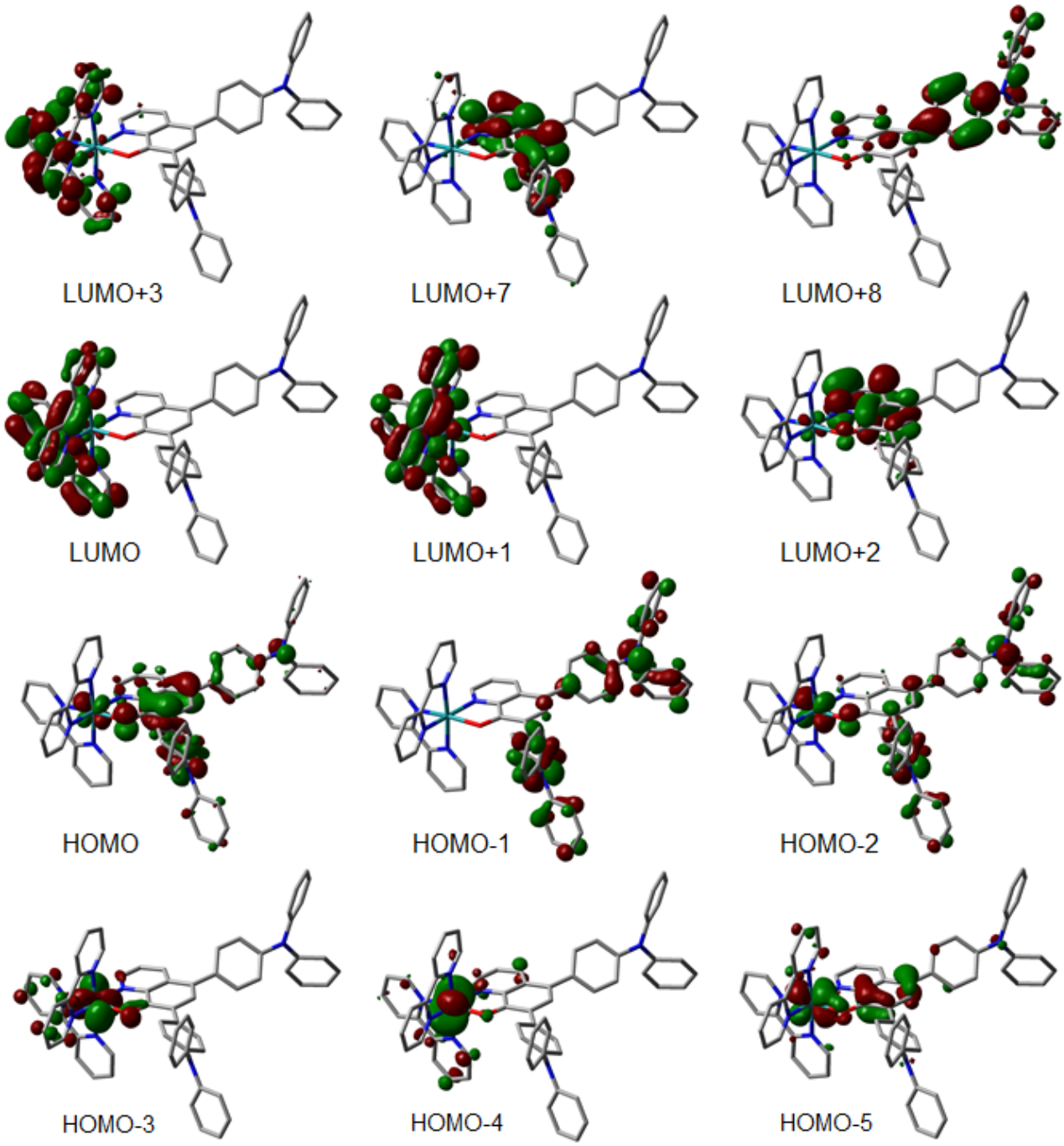

Fig. SI-34 Selected molecular orbitals for **8**$^{+}$.

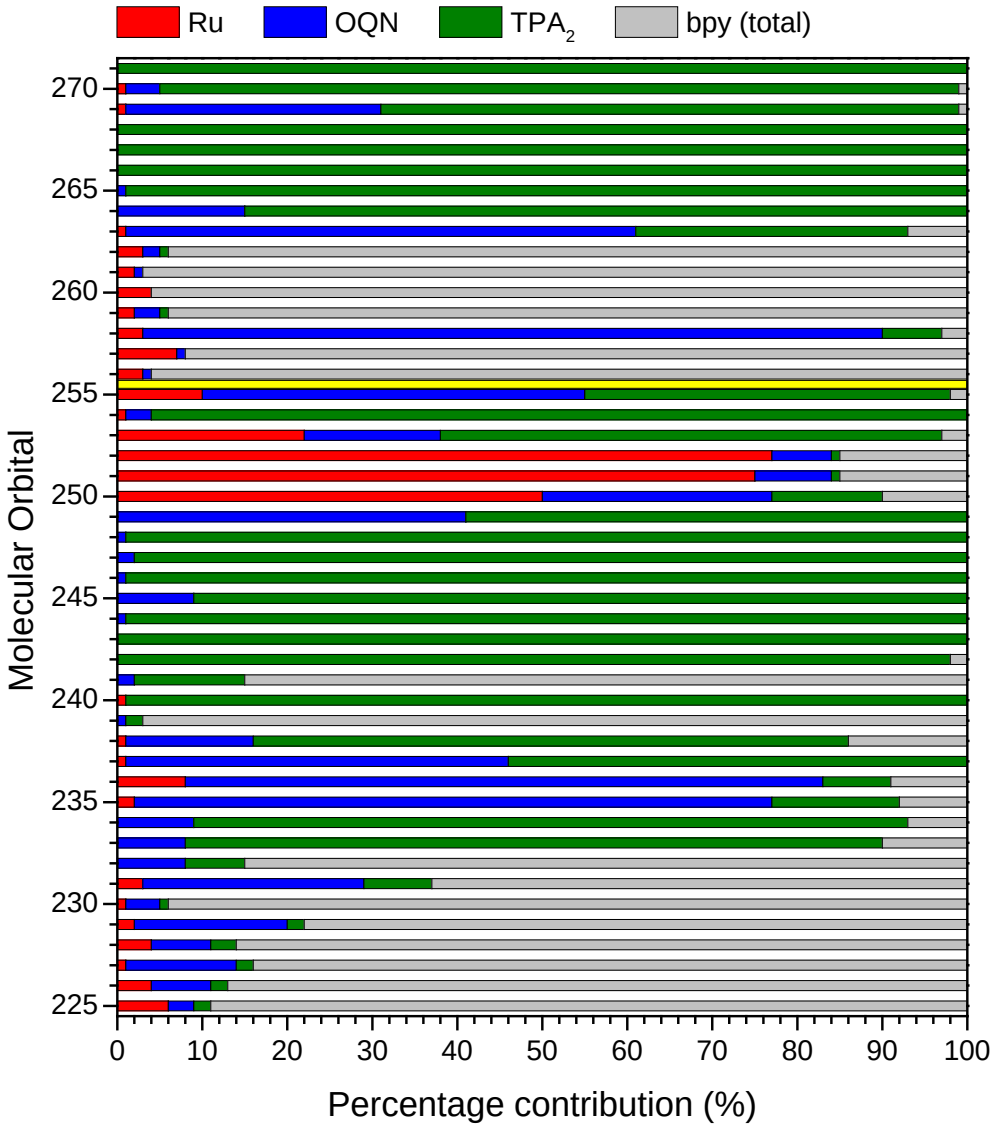

Fig. SI-35 Percentage contributions of Ru, OQN, TPA_2 and bpy fragments to molecular orbitals of $\mathbf{8}^+$. Filled and valence levels are separated by a yellow row between the HOMO (255) and LUMO (256) levels.

UV-vis-NIR and EPR spectroelectrochemistry.

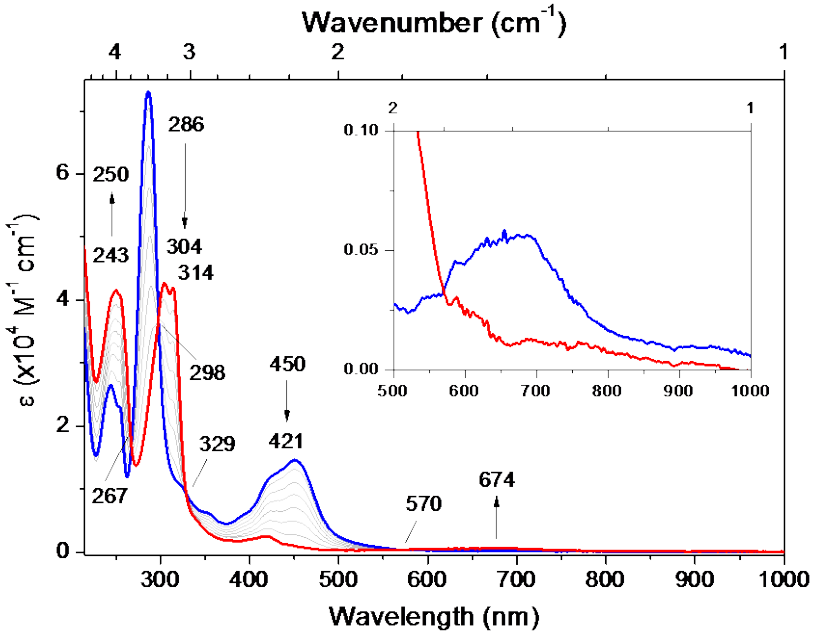

Figure SI-36. UV/Vis/NIR electronic absorption data of $\mathbf{1}^{3+}$ recorded during controlled potential electrolysis (+1.60 V vs. SCE) of $\mathbf{1}^{2+}$ in 0.1 M Bu_4NPF_6 acetonitrile electrolyte.

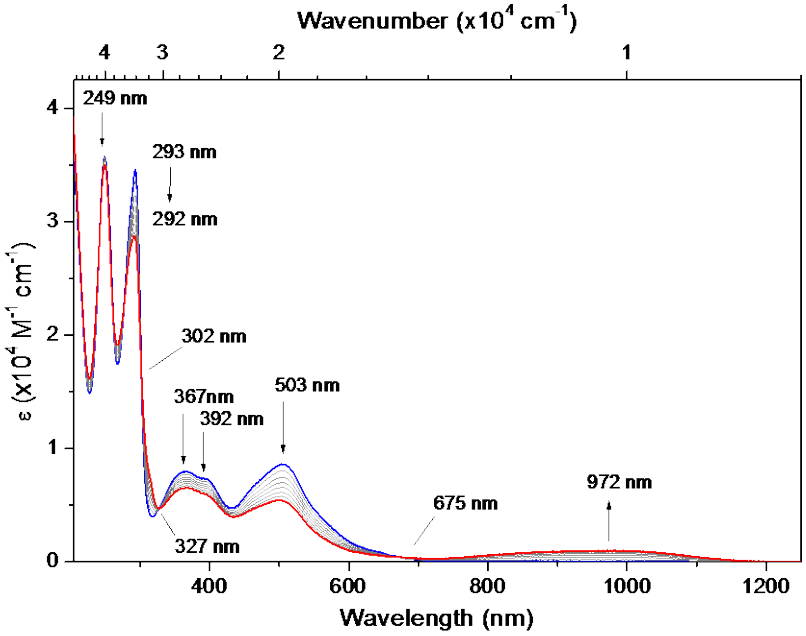

Figure SI-37. UV/Vis/NIR electronic absorption data of $\mathbf{2}^{2+}$ recorded during controlled potential electrolysis (+0.75 V vs. SCE) of $\mathbf{2}^{+}$ in 0.1 M Bu_4NPF_6 acetonitrile electrolyte.

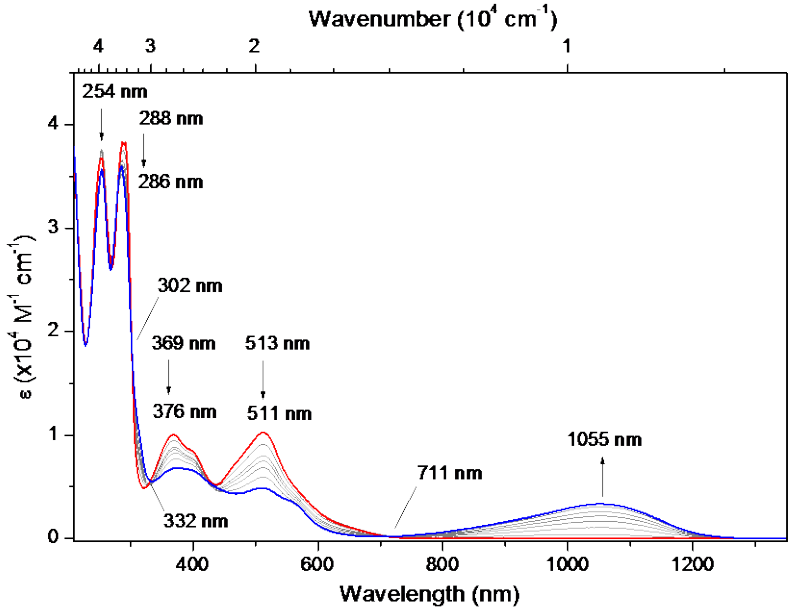

Figure SI-38. UV/Vis/NIR electronic absorption data of $\mathbf{3}^{2+}$ recorded during controlled potential electrolysis (+0.65 V vs. SCE) of $\mathbf{3}^{+}$ in 0.1 M Bu_4NPF_6 acetonitrile electrolyte.

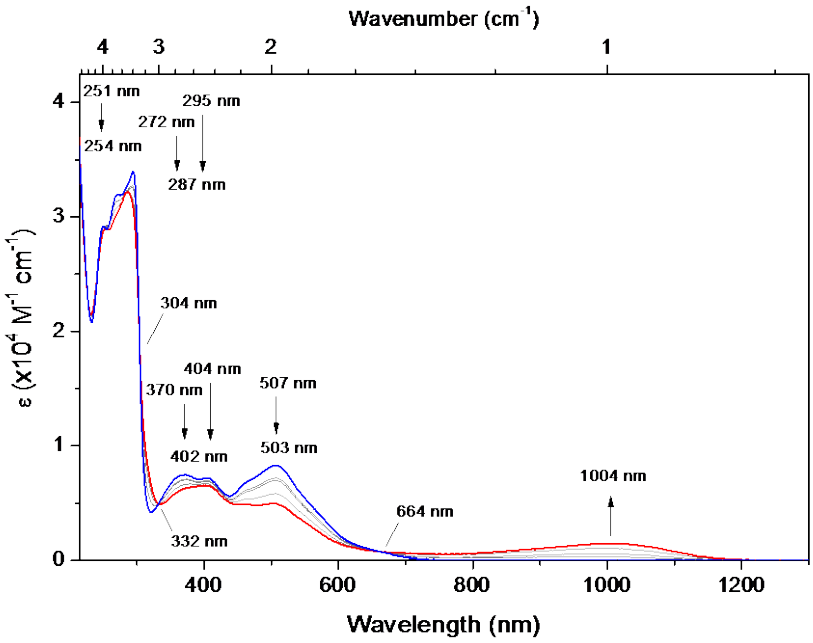

Figure SI-39. UV/Vis/NIR electronic absorption data of $\mathbf{4}^{2+}$ recorded during controlled potential electrolysis (+0.75 V vs. SCE) of $\mathbf{4}^{+}$ in 0.1 M Bu_4NPF_6 acetonitrile electrolyte.

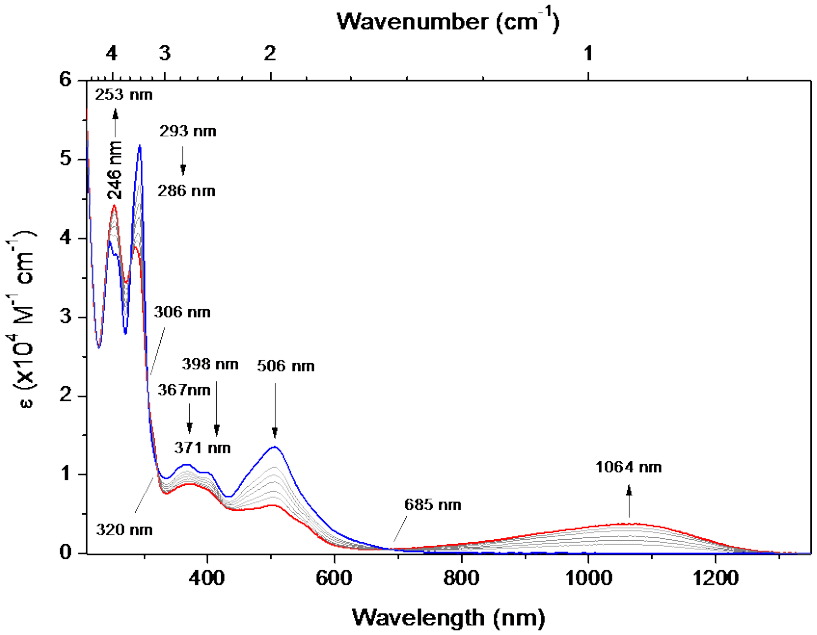

Figure SI-40. UV/Vis/NIR electronic absorption data of $\mathbf{5}^{2+}$ recorded during controlled potential electrolysis (+0.76 V vs. SCE) of $\mathbf{5}^{+}$ in 0.1 M Bu_4NPF_6 acetonitrile electrolyte.

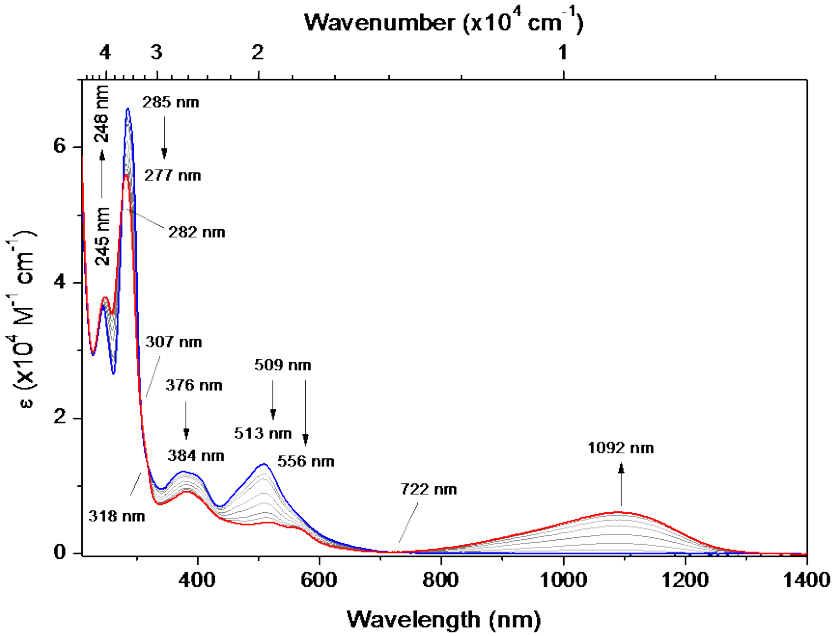

Figure SI-41. UV/Vis/NIR electronic absorption data of $\mathbf{6}^{2+}$ recorded during controlled potential electrolysis (+0.70 V vs. SCE) of $\mathbf{6}^{+}$ in 0.1 M Bu_4NPF_6 acetonitrile electrolyte.

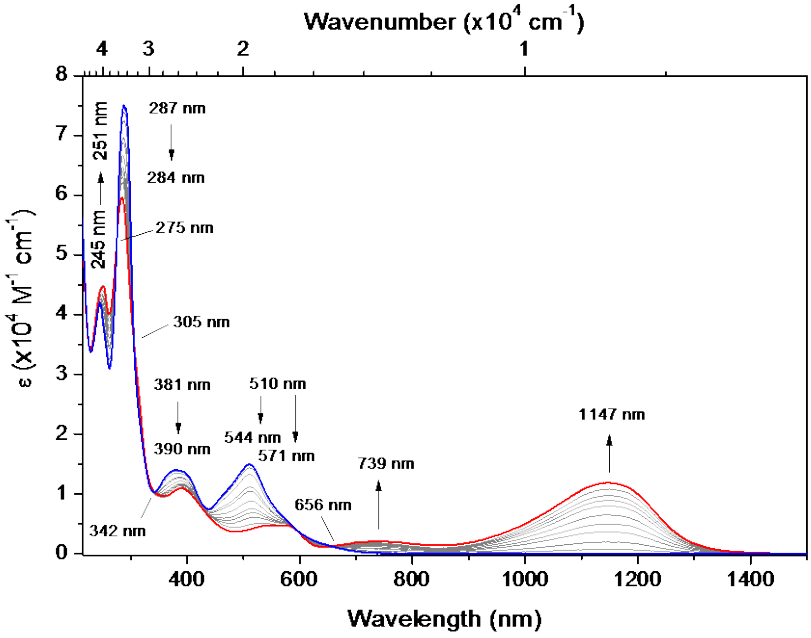

Figure SI-42. UV/Vis/NIR electronic absorption data of $\mathbf{7}^{2+}$ recorded during controlled potential electrolysis (+0.70 V vs. SCE) of $\mathbf{7}^{+}$ in 0.1 M Bu_4NPF_6 acetonitrile electrolyte.

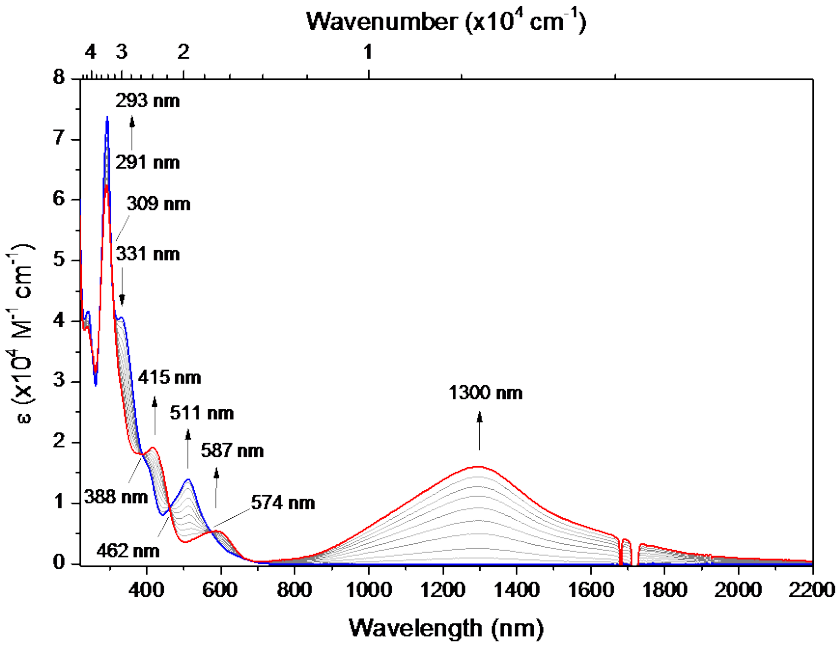

Figure SI-43. UV/Vis/NIR electronic absorption data of $\mathbf{8}^{2+}$ recorded during controlled potential electrolysis (+0.65 V vs. SCE) of $\mathbf{8}^{+}$ in 0.1 M Bu_4NPF_6 acetonitrile electrolyte.

Computational analysis of one-electron oxidized complexes $\mathbf{1}^{3+}$ - $\mathbf{8}^{2+}$

All data was calculated with an acetonitrile polarizable continuum model using the B3LYP functional and 6-31g(d,p) (C,H,N,O) and LANL08 (Ru) basis sets.

$\mathbf{1}^{3+}$ $[Ru(bpy)_3]^{3+}$

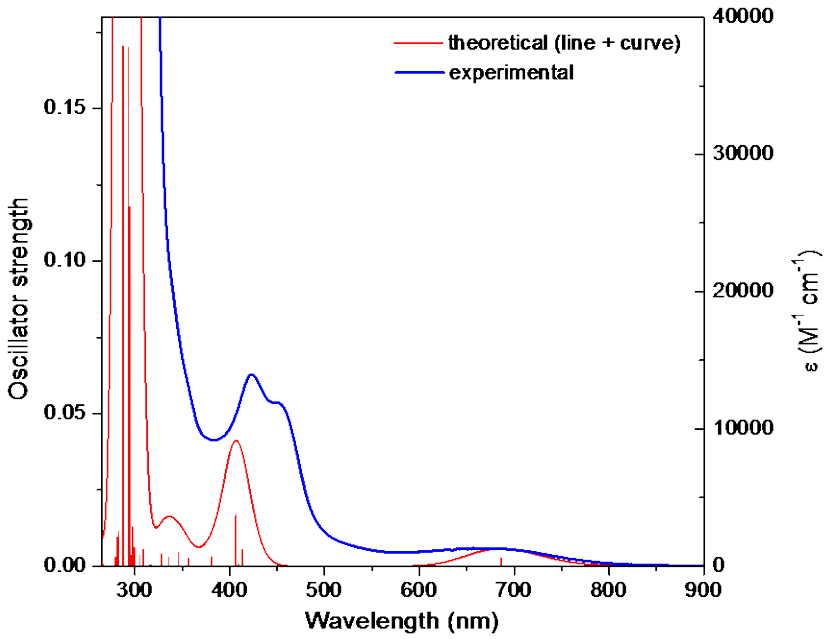

Figure SI-44. An overlay of experimental and theoretical spectra for $\mathbf{1}^{3+}$.

electronic transition (nm)	MO contributions (%)	oscillator strength (f)
293.30	H-2(B)->L+3(B) (28%)	0.1701
293.55	H-2(B)->L+1(B) (21%), H-3(B)->L+3(B) (11%), H-1(B)->L+3(B) (10%)	0.0816
294.30	H-2(A)->L+2(A) (24%), H-1(A)->L+2(A) (10%), H-1(B)->L+3(B) (10%)	0.1179
294.47	H(B)->L+2(B) (11%)	0.1002
294.60	H-2(B)->L+3(B) (23%), H-1(B)->L+1(B) (14%), H-1(A)->L+2(A) (11%)	0.0559
406.10	H-7(B)->L(B) (93%)	0.0167
406.49	H-6(B)->L(B) (93%)	0.0175
686.05	H-1(B)->LUMO(B) (89%)	0.0029
687.35	HOMO(B)->LUMO(B) (89%)	0.0028

Table SI-9 Electronic transitions for $\mathbf{1}^{3+}$ calculated by TD-DFT.

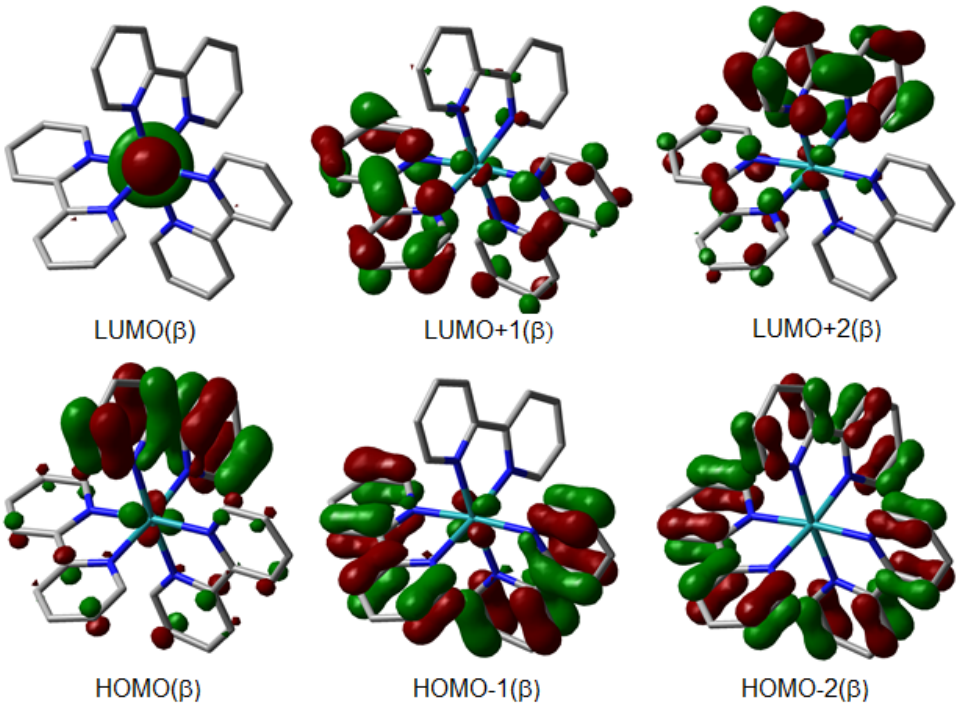

Fig. SI-45 Selected molecular orbitals for $\mathbf{1}^{3+}$.

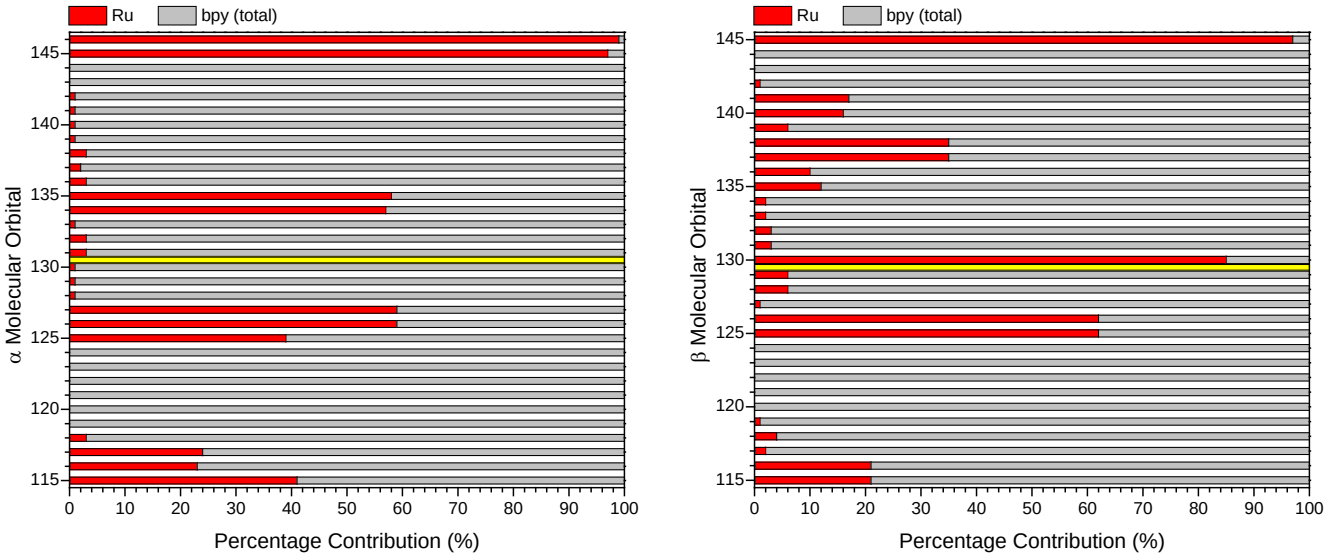

Fig. SI-46 Percentage contributions of Ru and bpy fragments for α (left) and β (right) molecular orbitals of $\mathbf{1}^{3+}$. Filled and valence levels are separated by a yellow row between the HOMO (α 130)/LUMO (α 131) and HOMO (β 129)/LUMO (β 130) levels.

2^{2+} $[Ru(bpy)_2(OQN)]^{2+}$

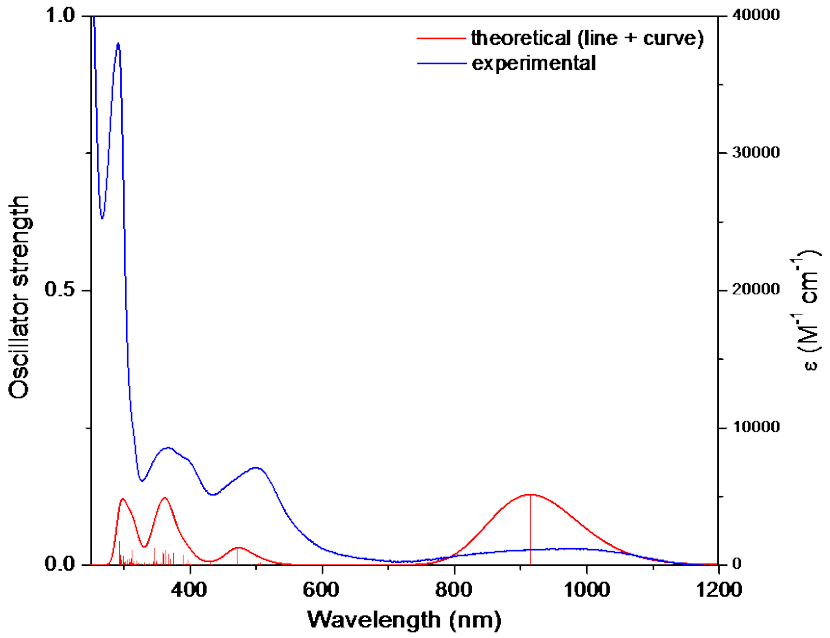

Figure SI-47. An overlay of experimental and theoretical spectra for **2**$^{2+}$.

electronic transition (nm)	MO contributions (%)	oscillator strength (f)
293.86	H(B)->L+7(B) (23%), H-1(A)->L+3(A) (11%), H(A)->L+6(A) (11%)	0.0431
312.58	H-2(A)->L+2(A) (21%), H-2(B)->L+3(B) (16%)	0.0262
346.62	H-2(A)->L+1(A) (23%), H-2(A)->L(A) (19%), H-2(B)->L+1(B) (14%)	0.0306
358.65	H-6(B)->L(B) (26%), H(A)->L+2(A) (13%), H(B)->L+3(B) (12%)	0.0228
363.04	H-2(B)->L+2(B) (50%), H-1(A)->L(A) (15%)	0.0268
368.41	H-1(A)->L+1(A) (25%), H-2(B)->L+1(B) (23%), H-2(B)->L+2(B) (19%)	0.0200
375.24	H-1(A)->L(A) (45%), H-1(B)->L+1(B) (19%)	0.0208
471.55	H(A)->L+2(A) (56%), H(B)->L+3(B) (26%)	0.0295
914.47	H(B)->L(B) (58%), H-2(B)->L(B) (23%), H-1(B)->L(B) (15%)	0.1284

Table SI-10 Selected electronic transitions for **2**$^{2+}$ calculated by TD-DFT.

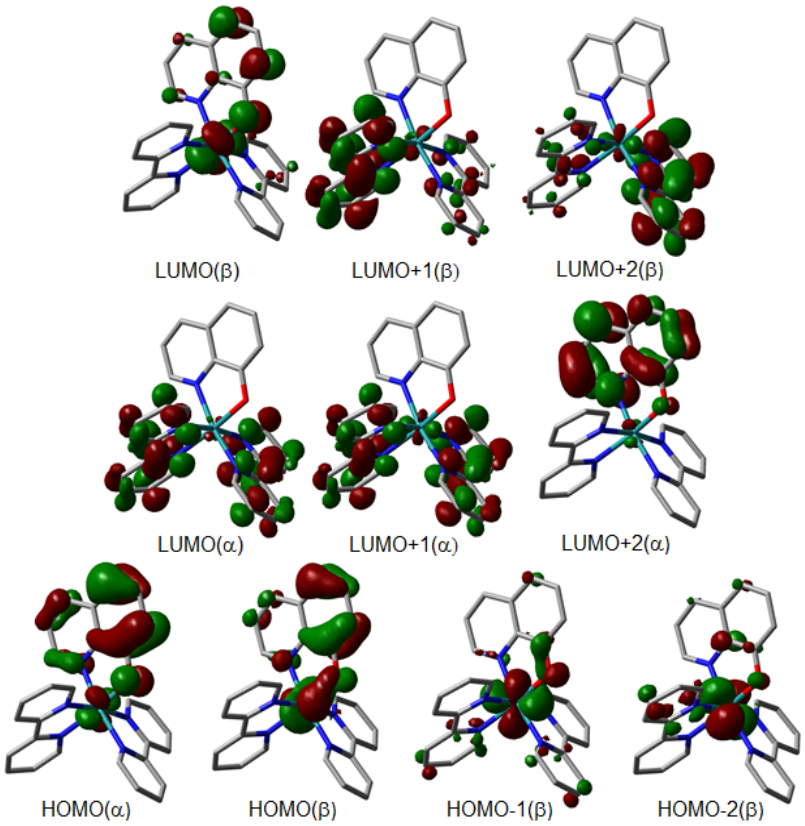

Fig. SI-48 Selected molecular orbitals for $\mathbf{2}^{2+}$.

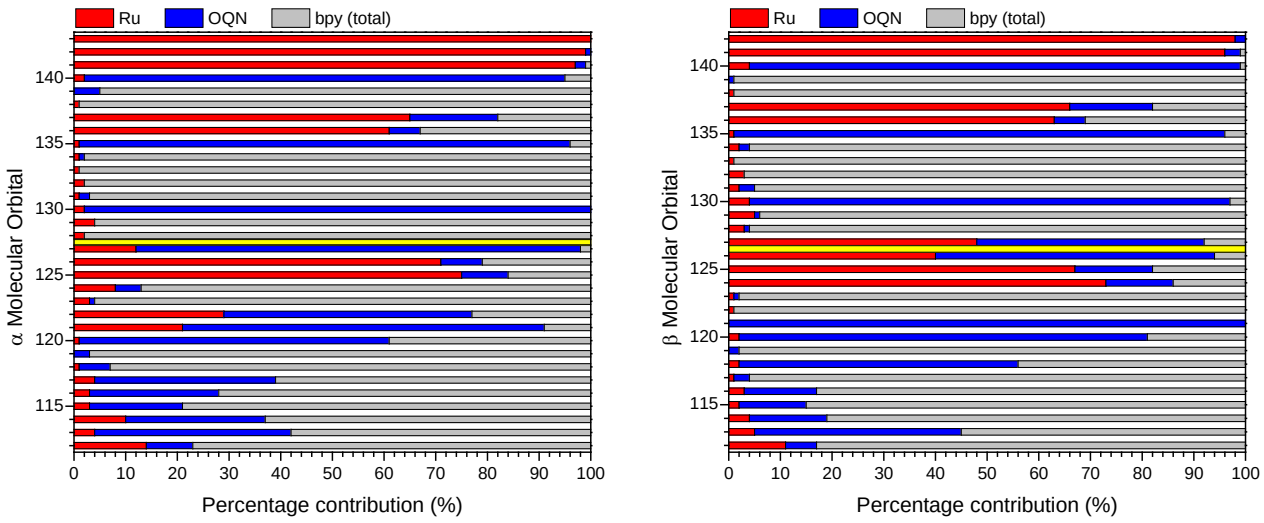

Fig. SI-49 Percentage contributions of Ru, OQN and bpy fragments for α (left) and β (right) molecular orbitals of $\mathbf{2}^{2+}$. Filled and valence levels are separated by a yellow row between the HOMO (α 127)/LUMO (α 128) and HOMO (β 126)/LUMO (β 127) levels.

3^{2+} $[Ru(bpy)_2(Me_2OQN)]^{2+}$

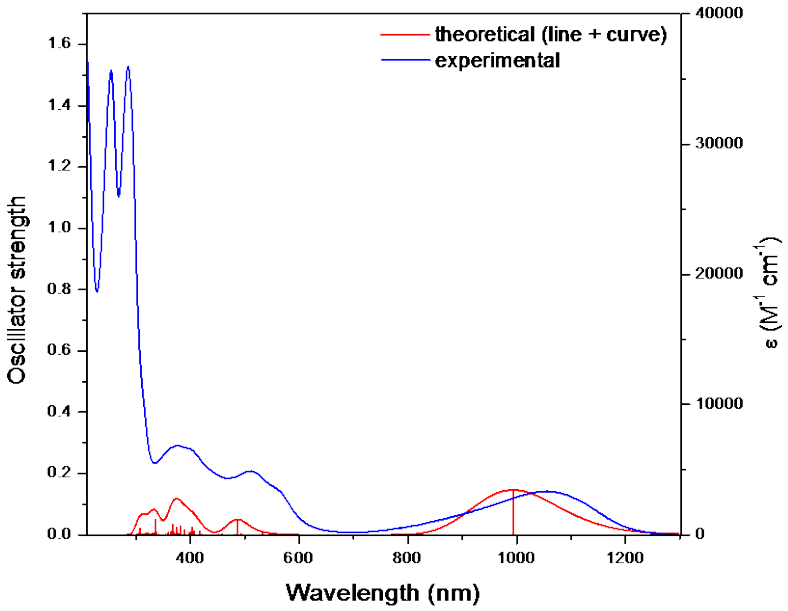

Figure SI-50. An overlay of experimental and theoretical spectra for **3**$^{2+}$.

electronic transition (nm)	MO contributions (%)	oscillator strength (f)
245.27	H-5(B)->L+3(B) (22%), H-6(A)->L+2(A) (16%), H-2(A)->L+7(A) (13%)	0.2929
254.76	H-2(A)->L+7(A) (42%), H-2(B)->L+8(B) (31%)	0.1095
269.10	H-2(A)->L+6(A) (16%), H-2(A)->L+5(A) (10%)	0.3040
274.40	H-1(A)->L+6(A) (12%)	0.1241
336.04	H-2(B)->L+3(B) (34%), H-2(A)->L+2(A) (32%)	0.0503
367.71	H-6(B)->LUMO(B) (35%), H-2(A)->L+1(A) (12%), H-1(A)->L+2(A) (12%)	0.0327
381.96	H-1(A)->LUMO(A) (12%), H-3(B)->L+2(B) (12%), H-1(A)->L+1(A) (10%)	0.0288
403.60	H-1(A)->LUMO(A) (30%), H-1(B)->L+1(B) (19%)	0.0251
486.32	HOMO(A)->L+2(A) (60%), HOMO(B)->L+3(B) (17%)	0.0443
993.30	HOMO(B)->LUMO(B) (56%), H-2(B)->LUMO(B) (23%), H-1(B)->LUMO(B) (18%)	0.1462

Table SI-11 Electronic transitions for **3**$^{2+}$ calculated by TD-DFT.

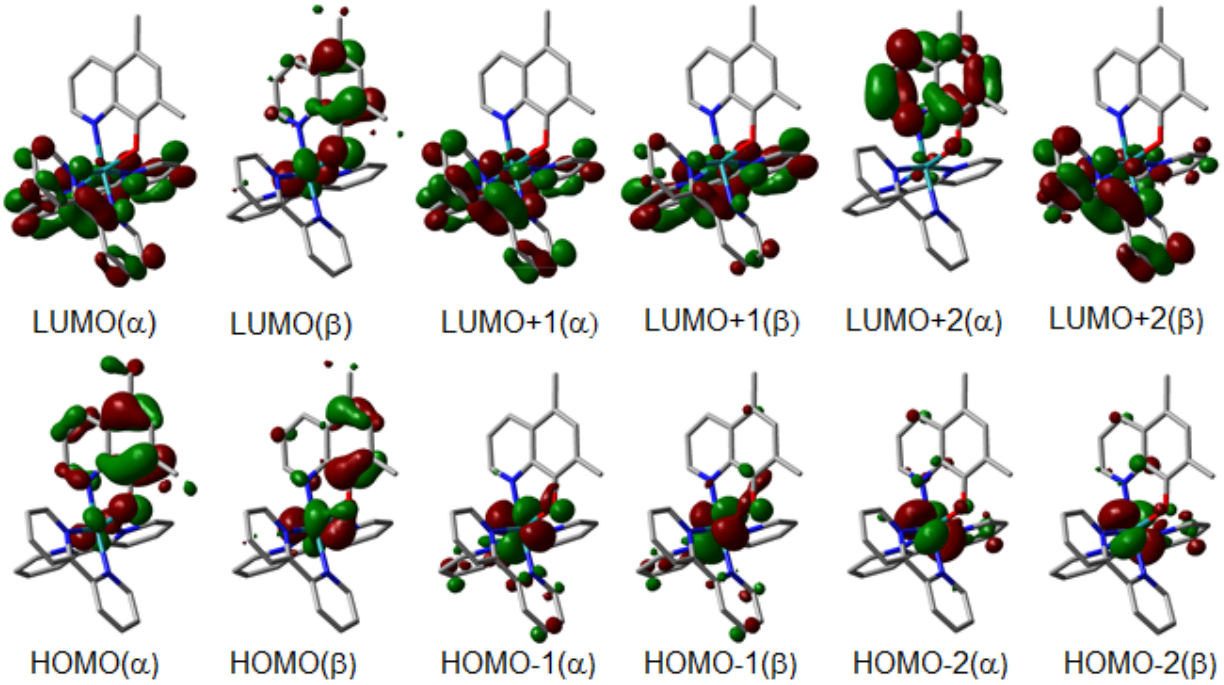

Fig. SI-51 Selected molecular orbitals for $\mathbf{3}^{2+}$.

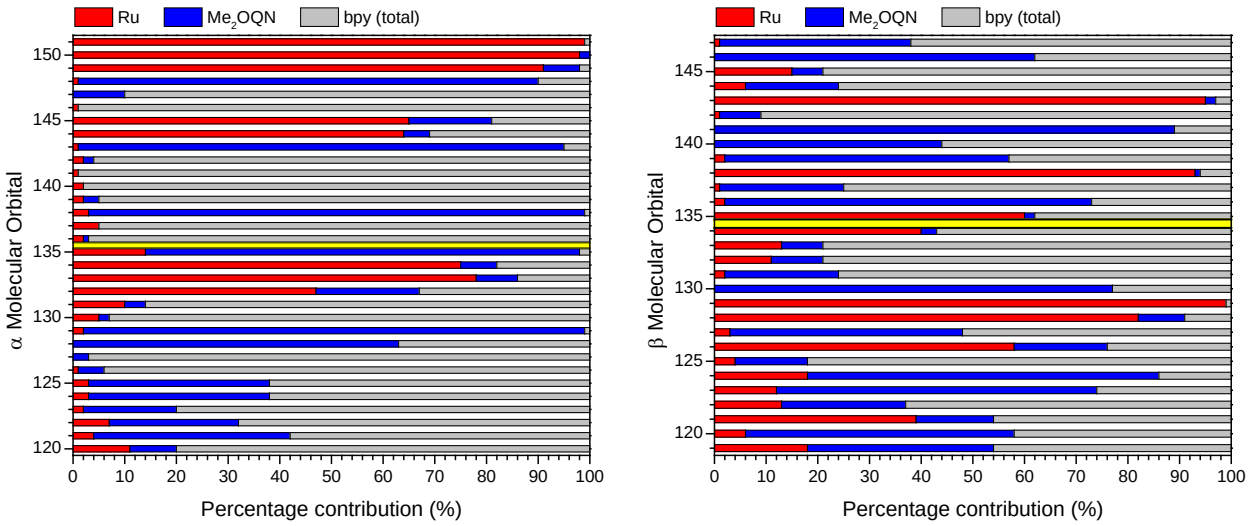

Fig. SI-52 Percentage contributions of Ru, Me_2OQN and bpy fragments for α (left) and β (right) molecular orbitals of $\mathbf{3}^{2+}$. Filled and valence levels are separated by a yellow row between the HOMO (α 135)/LUMO (α 136) and HOMO (β 134)/LUMO (β 135) levels.

4^{2+} $[Ru(bpy)_2(i\text{-}Ph_2OQN)]^{2+}$

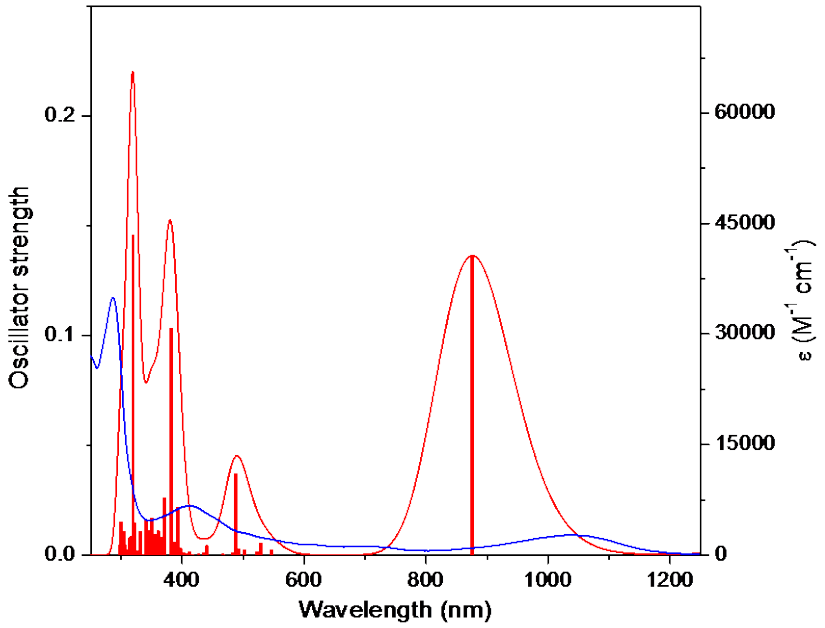

Figure SI-53. An overlay of experimental and theoretical spectra for **4**$^{2+}$.

electronic transition (nm)	MO contributions (%)	oscillator strength (f)
319.44	H-2(A)->L+2(A) (37%), H-2(B)->L+3(B) (30%)	0.1459
350.48	H-10(B)->L(B) (52%), H-1(B)->L+3(B) (11%)	0.0171
371.43	H-1(A)->L(A) (46%), H-2(B)->L+1(B) (11%), H-1(B)->L+1(B) (10%)	0.0263
381.58	H(B)->L+3(B) (50%), H(A)->L+2(A) (26%)	0.1034
393.35	H-1(B)->L+1(B) (46%)	0.0217
488.14	H(A)->L+2(A) (45%), H(B)->L+3(B) (24%)	0.0373
875.90	H(B)->L(B) (50%), H-2(B)->L(B) (37%)	0.1364

Table SI-12 Electronic transitions for **4**$^{2+}$ calculated by TD-DFT.

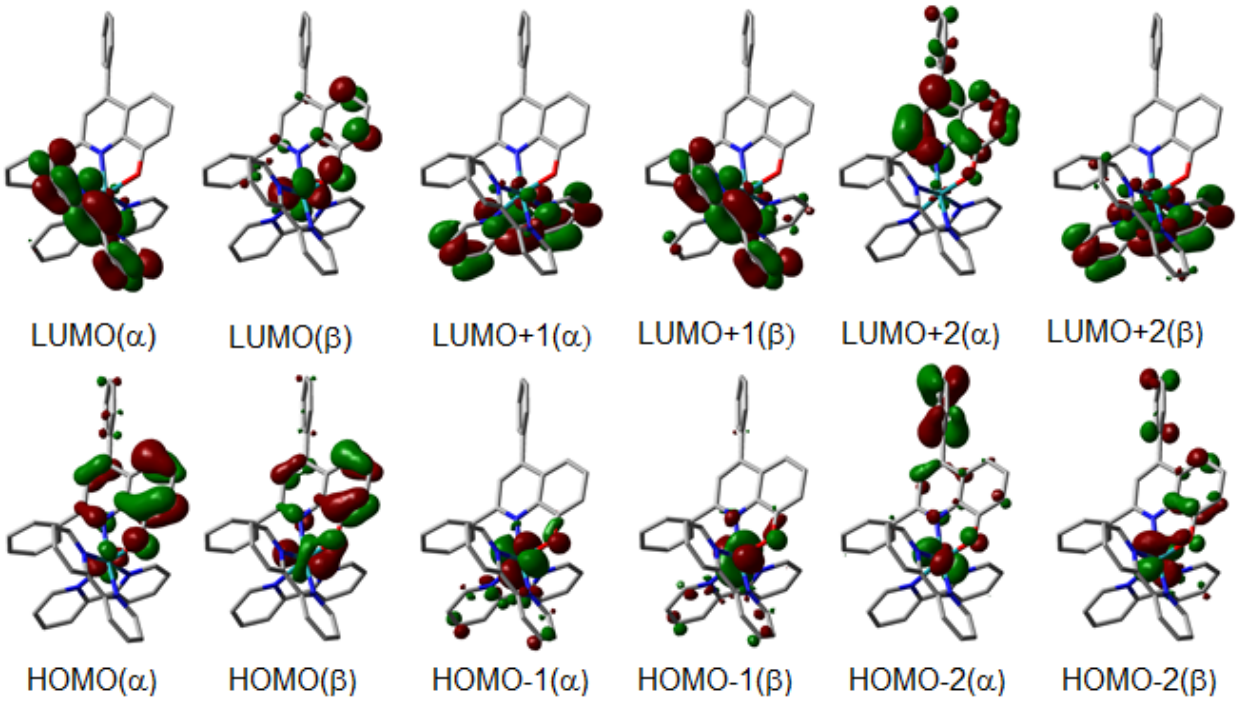

Fig. SI-54 Selected molecular orbitals for $\mathbf{4}^{2+}$.

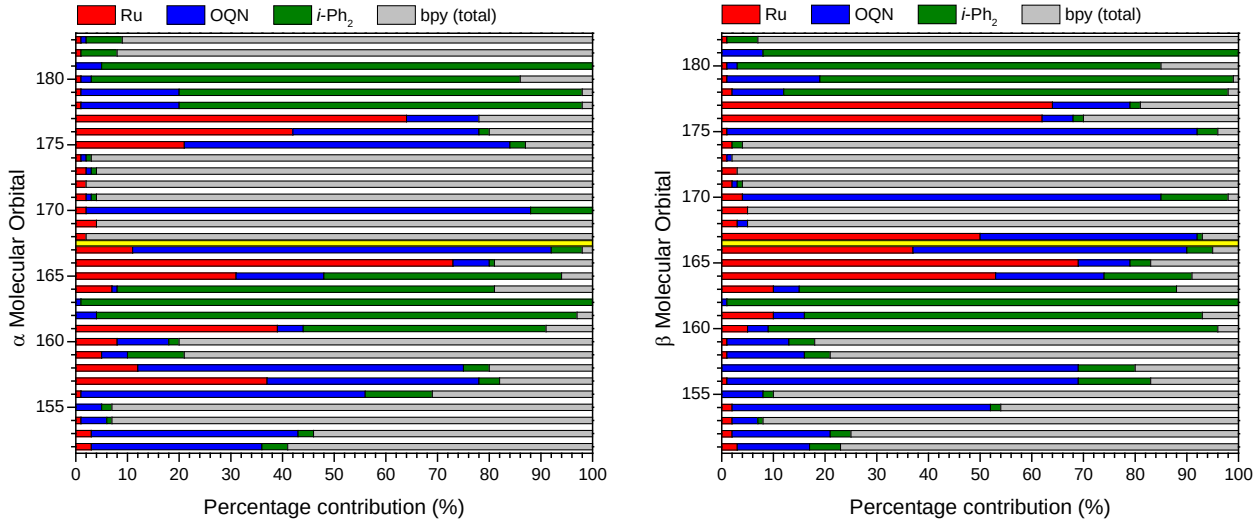

Fig. SI-55 Percentage contributions of Ru, OQN, *i*-Ph_2 and bpy fragments for α (left) and β (right) molecular orbitals of $\mathbf{4}^{2+}$. Filled and valence levels are separated by a yellow row between the HOMO (α 167)/LUMO (α 168) and HOMO (β 166)/LUMO (β 167) levels.

5^{2+} $[Ru(bpy)_2(PhOQN)]^{2+}$

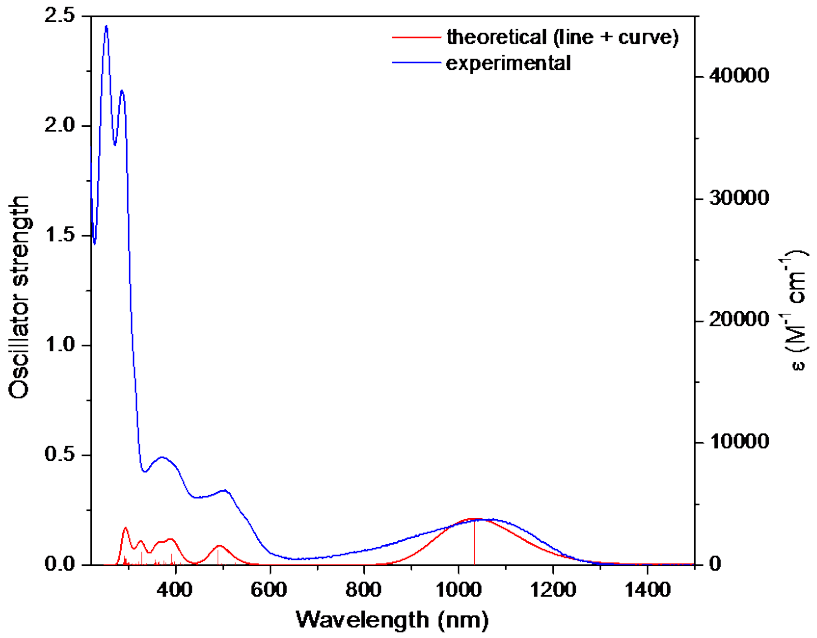

Figure SI-56. An overlay of experimental and theoretical spectra for **5**$^{2+}$.

electronic transition (nm)	MO contributions (%)	oscillator strength (f)
290.79	H(B)->L+8(B) (17%), H-16(B)->L(B) (15%)	0.0417
292.50	H-1(B)->L+6(B) (17%)	0.0304
295.39	H-17(B)->L(B) (11%), H-4(B)->L+3(B) (11%)	0.0298
328.40	H-2(A)->L+2(A) (30%), H-2(B)->L+3(B) (25%), H(B)->L+4(B) (11%)	0.0602
357.51	H-1(A)->L+2(A) (35%), H-2(A)->L+1(A) (22%), H-2(A)->L(A) (14%)	0.0248
375.46	H-2(B)->L+2(B) (18%), H-1(A)->L(A) (16%), H-1(A)->L+1(A) (14%)	0.0219
391.37	H(B)->L+3(B) (41%), H-10(B)->L(B) (14%), H(A)->L+2(A) (13%)	0.0509
490.32	H-7(B)->L(B) (38%), H(A)->L+2(A) (32%), H(B)->L+3(B) (12%)	0.0714
526.00	H-4(B)->LUMO(B) (92%)	0.0119
1033.37	HOMO(B)->LUMO(B) (70%), H-2(B)->LUMO(B) (15%), H-1(B)->LUMO(B) (10%)	0.2117

Table SI-13 Electronic transitions for **5**$^{2+}$ calculated by TD-DFT.

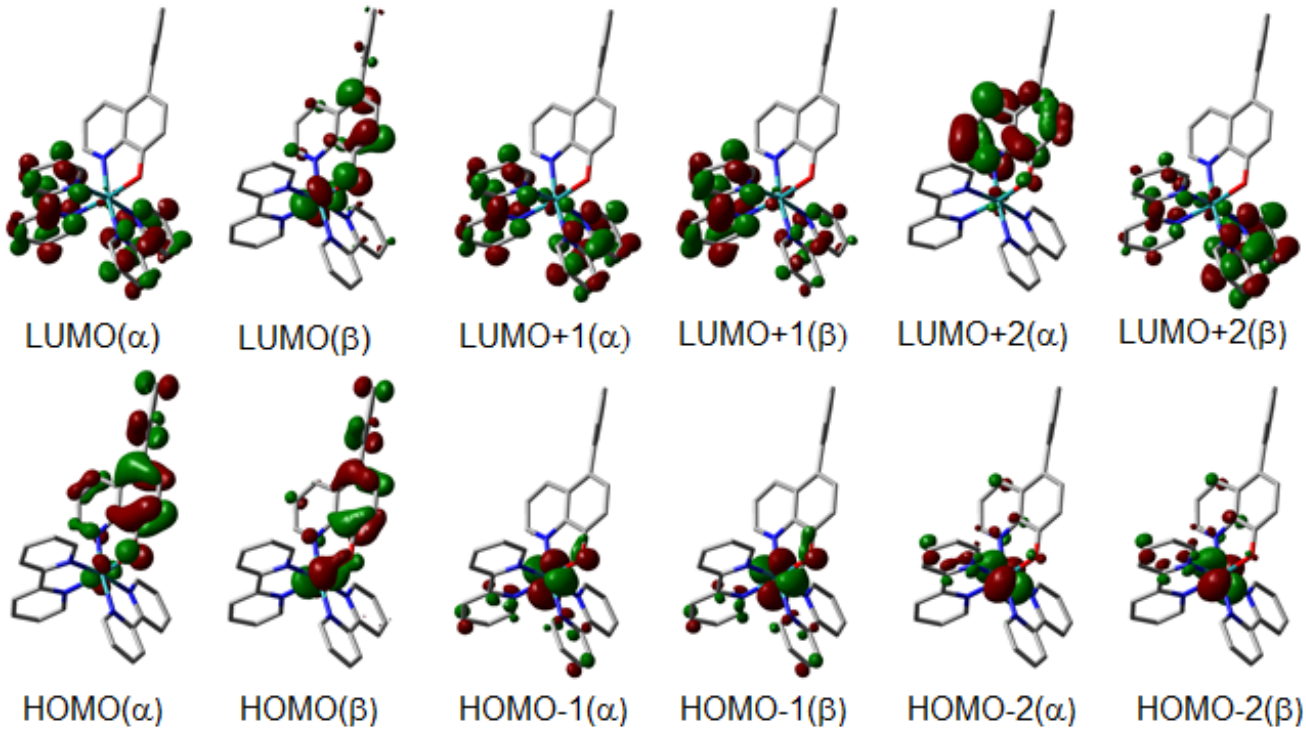

Fig. SI-57 Selected molecular orbitals for $\mathbf{5}^{2+}$.

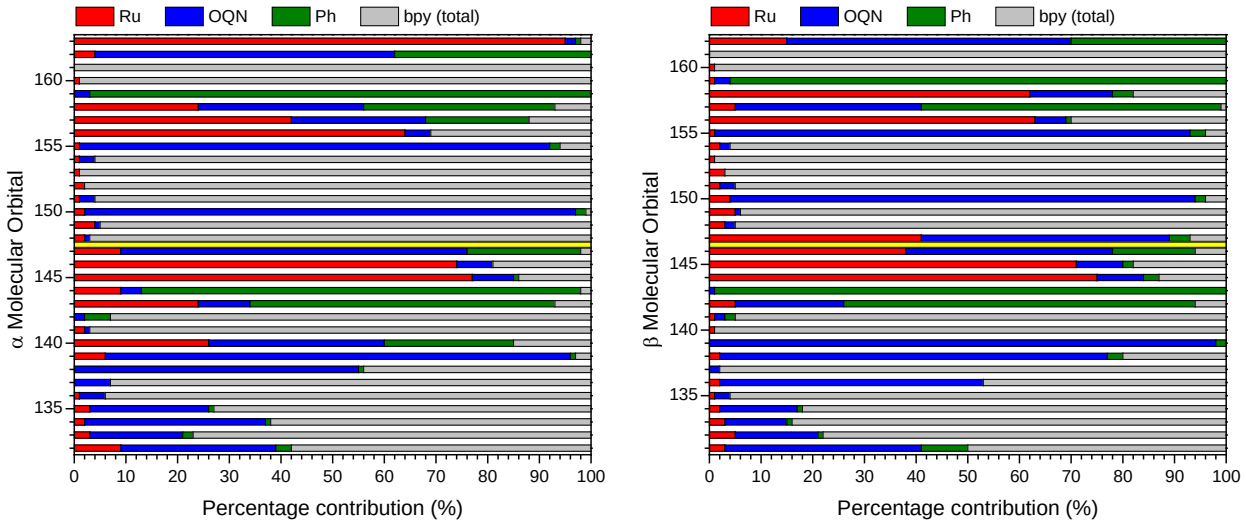

Fig. SI-58 Percentage contributions of Ru, OQN, Ph and bpy fragments for α (left) and β (right) molecular orbitals of $\mathbf{5}^{2+}$. Filled and valence levels are separated by a yellow row between the HOMO (α 147)/LUMO (α 148) and HOMO (β 146)/LUMO (β 147) levels.

6^{2+} $[Ru(bpy)_2(Ph_2OQN)]^{2+}$

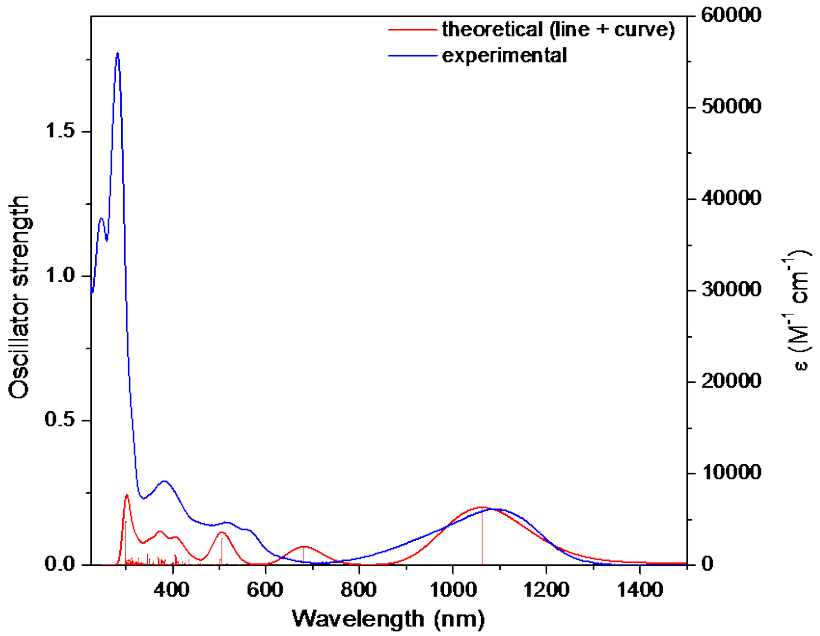

Figure SI-59. An overlay of experimental and theoretical spectra for **6**$^{2+}$.

electronic transition (nm)	MO contributions (%)	oscillator strength (f)
300.09	H(B)->L+8(B) (21%)	0.1508
346.96	H-2(B)->L+3(B) (29%), H-2(A)->L+2(A) (27%), H(A)->L+3(A) (11%)	0.0375
368.42	H-2(A)->L+1(A) (34%), H-2(A)->L(A) (10%)	0.0256
405.56	H(B)->L+3(B) (38%), H-1(A)->L+1(A) (12%), H-1(B)->L+2(B) (11%)	0.0338
408.07	H-1(A)->L(A) (40%), H-1(B)->L+1(B) (22%)	0.0261
506.12	H(A)->L+2(A) (43%), H-6(B)->L(B) (32%)	0.0918
680.67	H-3(B)->L(B) (95%)	0.0638
1062.14	H(B)->L(B) (64%), H-2(B)->L(B) (19%), H-1(B)->L(B) (13%)	0.1997

Table SI-14 Electronic transitions for **6**$^{2+}$ calculated by TD-DFT.

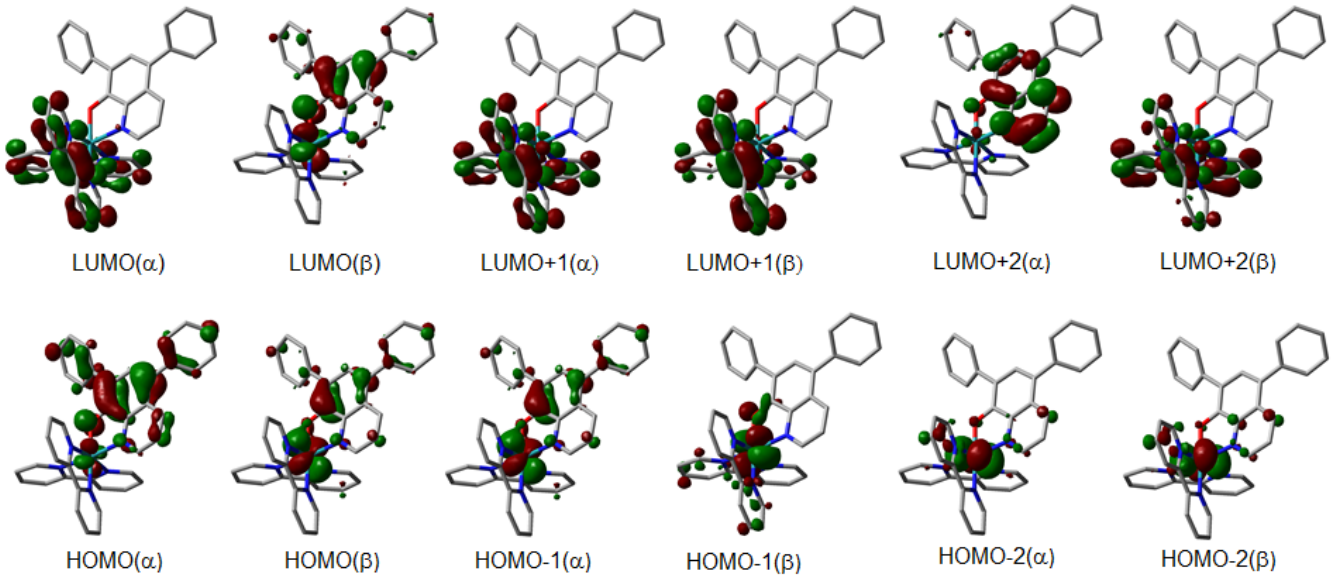

Fig. SI-60 Selected molecular orbitals for $\mathbf{6}^{2+}$.

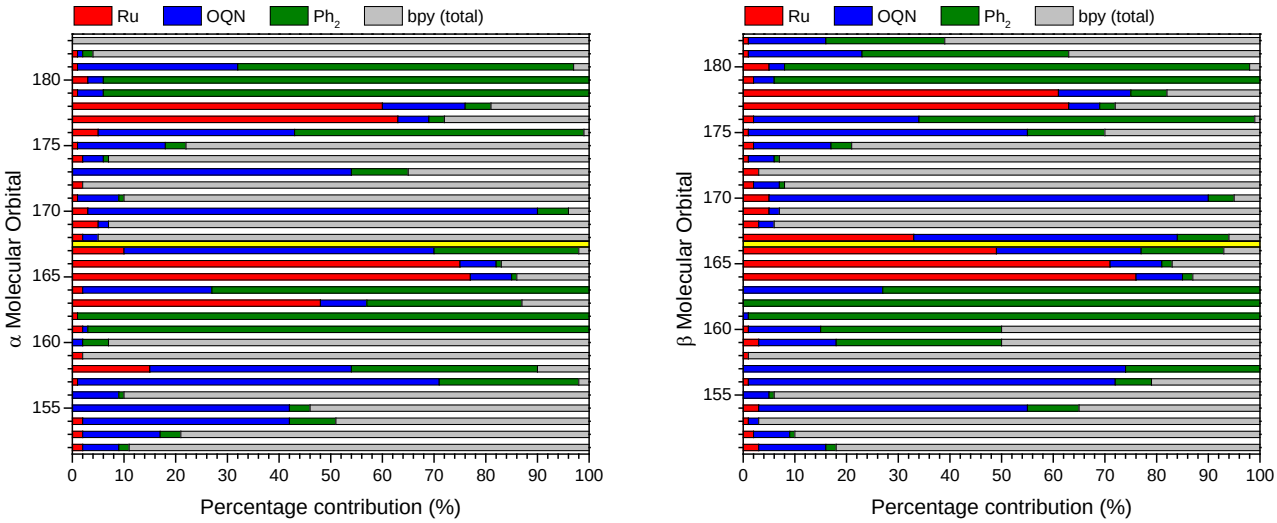

Fig. SI-61 Percentage contributions of Ru, Ph_2, OQN and bpy fragments for α (left) and β (right) molecular orbitals of $\mathbf{6}^{2+}$. Filled and valence levels are separated by a yellow row between the HOMO (α 167)/LUMO (α 168) and HOMO (β 166)/LUMO (β 167) levels.

7^{2+} $\{Ru(bpy)_2[(MeOPh)_2OQN]\}^{2+}$

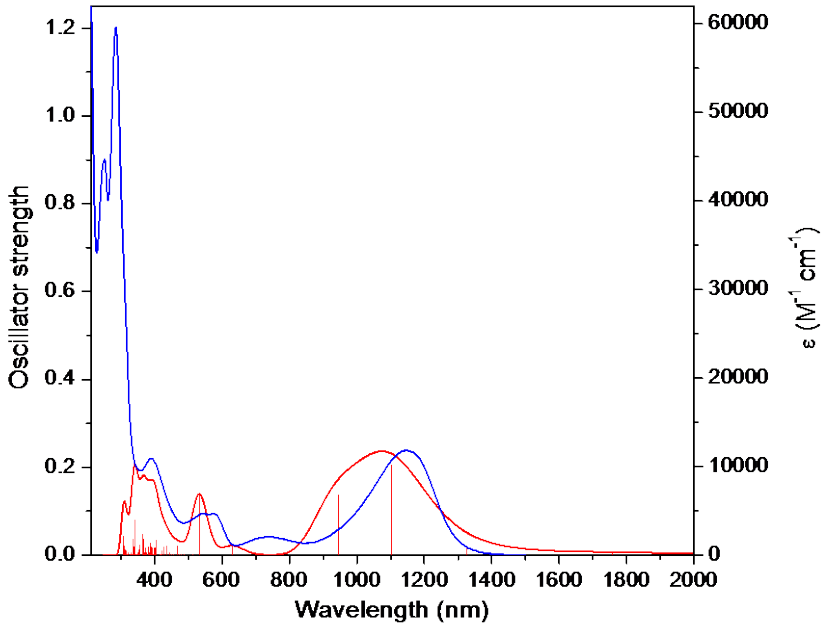

Figure SI-62. An overlay of experimental and theoretical spectra for **7**$^{2+}$.

electronic transition (nm)	MO contributions (%)	oscillator strength (f)
305.97	H-1(B)->L+4(B) (52%)	0.0427
336.34	H(B)->L+10(B) (11%)	0.0362
340.17	H(A)->L+8(A) (13%)	0.0407
341.55	H(A)->L+5(A) (14%)	0.0800
363.42	H-4(A)->L+1(A) (30%), H(A)->L+3(A) (13%)	0.0475
368.31	H-1(B)->L+3(B) (31%), H-10(B)->L(B) (17%)	0.0378
387.63	H-3(A)->L+1(A) (16%)	0.0274
403.15	H-3(A)->L(A) (40%)	0.0348
532.64	H(A)->L+2(A) (64%), H(A)->L(A) (13%)	0.1372
944.63	H-1(B)->L(B) (91%)	0.1378
1102.86	H(B)->L(B) (55%), H-3(B)->L(B) (22%), H-2(B)->L(B) (15%)	0.2047

Table SI-15 Electronic transitions for **7**$^{2+}$ calculated by TD-DFT.

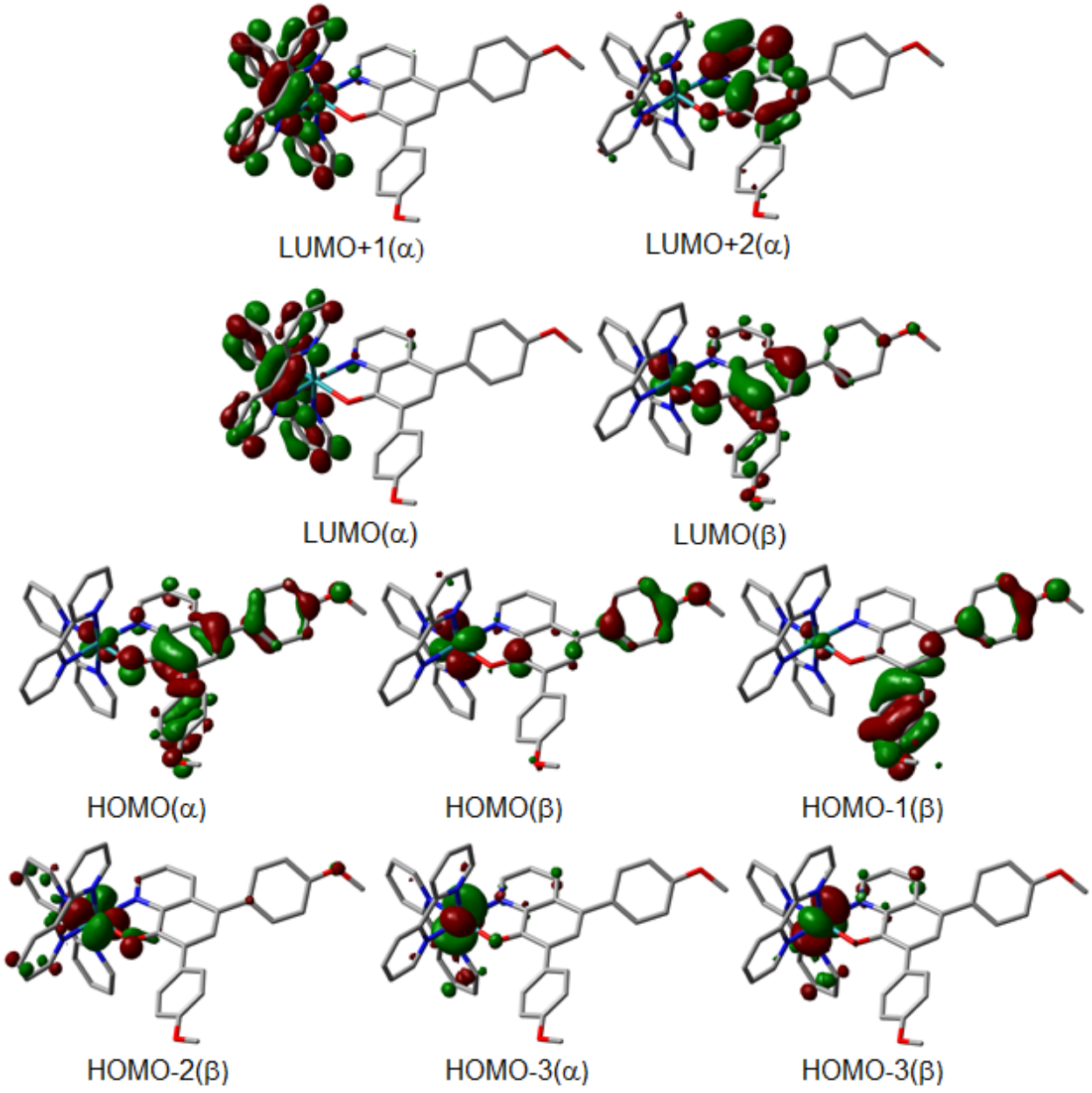

Fig. SI-63 Selected molecular orbitals for $\mathbf{7}^{2+}$.

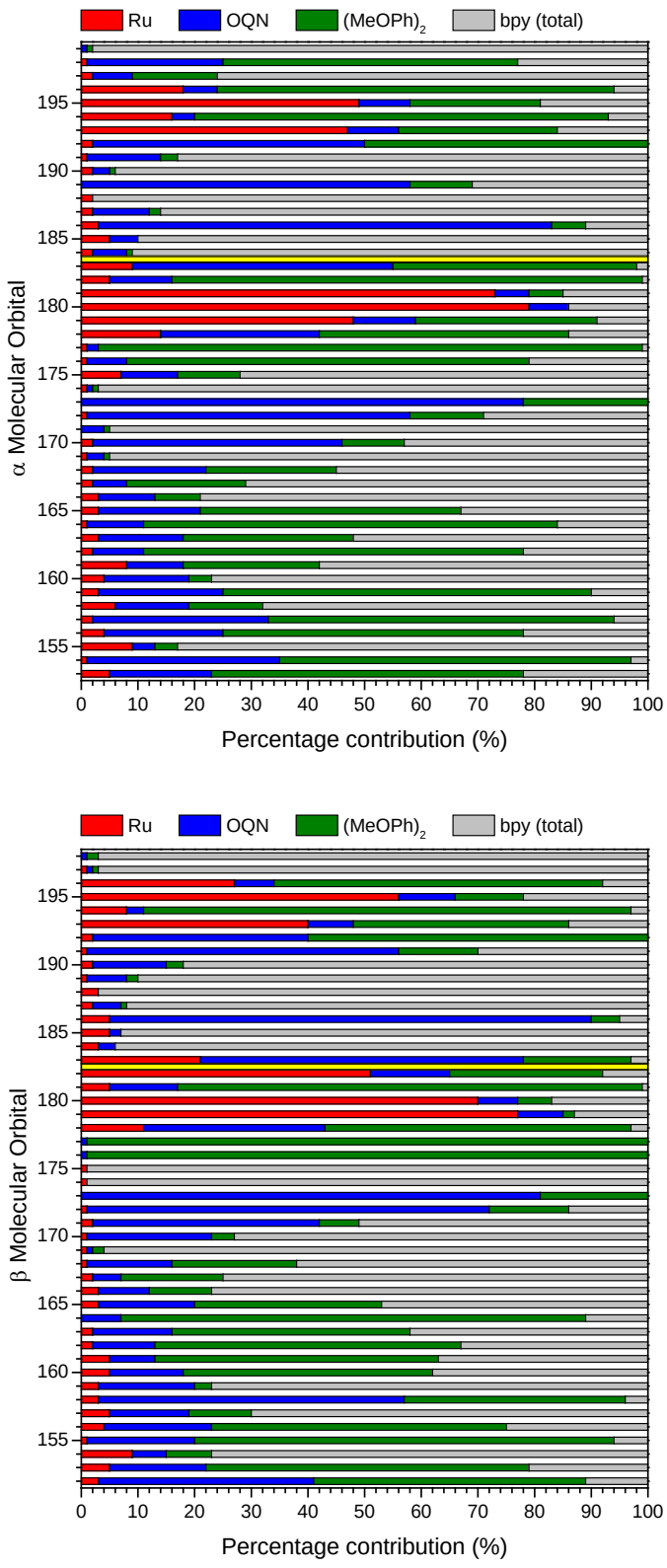

Fig. SI-64 Percentage contributions of Ru, OQN, $(MeOPh)_2$ and bpy fragments for α (top) and β (bottom) molecular orbitals of $\mathbf{3}^{2+}$. Filled and valence levels are separated by a yellow row between the HOMO (α 183)/LUMO (α 184) and HOMO (β 182)/LUMO (β 183) levels.

8^{2+} $[Ru(bpy)_2(TPA_2OQN)]^{2+}$

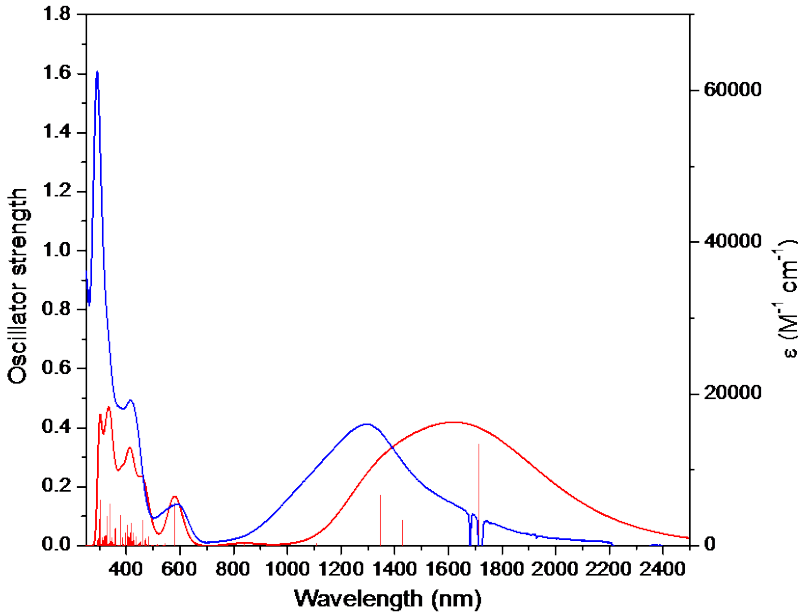

Figure SI-65. An overlay of experimental and theoretical spectra for **8**$^{2+}$.

electronic transition (nm)	MO contributions (%)	oscillator strength (f)
300.63	HOMO(A)->L+11(A) (26%), HOMO(B)->L+12(B) (23%), H-5(B)->L+2(B) (12%), H-1(A)->L+11(A) (10%)	0.0898
301.74	HOMO(A)->L+12(A) (39%), HOMO(B)->L+13(B) (40%)	0.1557
326.90	HOMO(B)->L+9(B) (15%)	0.1016
337.50	HOMO(A)->L+8(A) (16%)	0.1431
360.31	H-1(A)->L+3(A) (44%), HOMO(B)->L+6(B) (15%)	0.0608
376.89	H-3(B)->L+3(B) (20%), H-4(A)->L+2(A) (10%), HOMO(B)->L+4(B) (10%)	0.1045
401.98	HOMO(A)->L+8(A) (16%), HOMO(B)->L+9(B) (14%)	0.0709
418.09	HOMO(A)->L+3(A) (18%), H-17(B)->LUMO(B) (17%), HOMO(A)->L+4(A) (15%), H-2(A)->L+2(A) (13%)	0.0764
459.55	H-1(A)->L+2(A) (41%), H-1(A)->LUMO(A) (18%), H-1(A)->L+1(A) (15%), HOMO(B)->L+3(B) (13%)	0.0864
581.18	HOMO(A)->L+2(A) (51%), HOMO(A)->LUMO(A) (24%)	0.1481
1346.62	H-1(B)->LUMO(B) (58%), H-2(B)->LUMO(B) (36%)	0.1725
1431.02	H-2(B)->LUMO(B) (61%), H-1(B)->LUMO(B) (35%)	0.0870
1713.90	HOMO(B)->LUMO(B) (99%)	0.3442

Table SI-16 Electronic transitions for **8**$^{2+}$ calculated by TD-DFT.

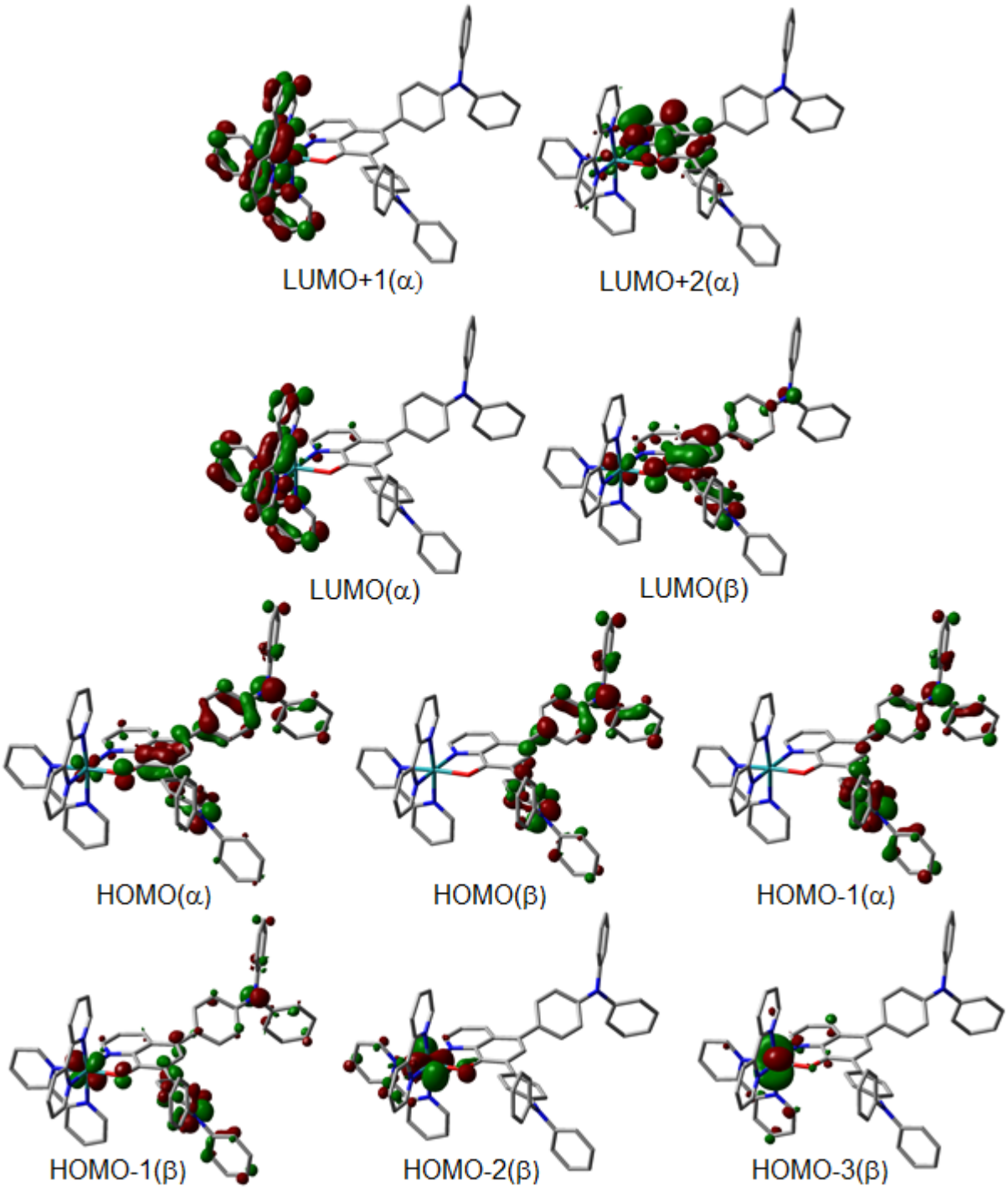

Fig. SI-66 Selected molecular orbitals for $\mathbf{8}^{2+}$.

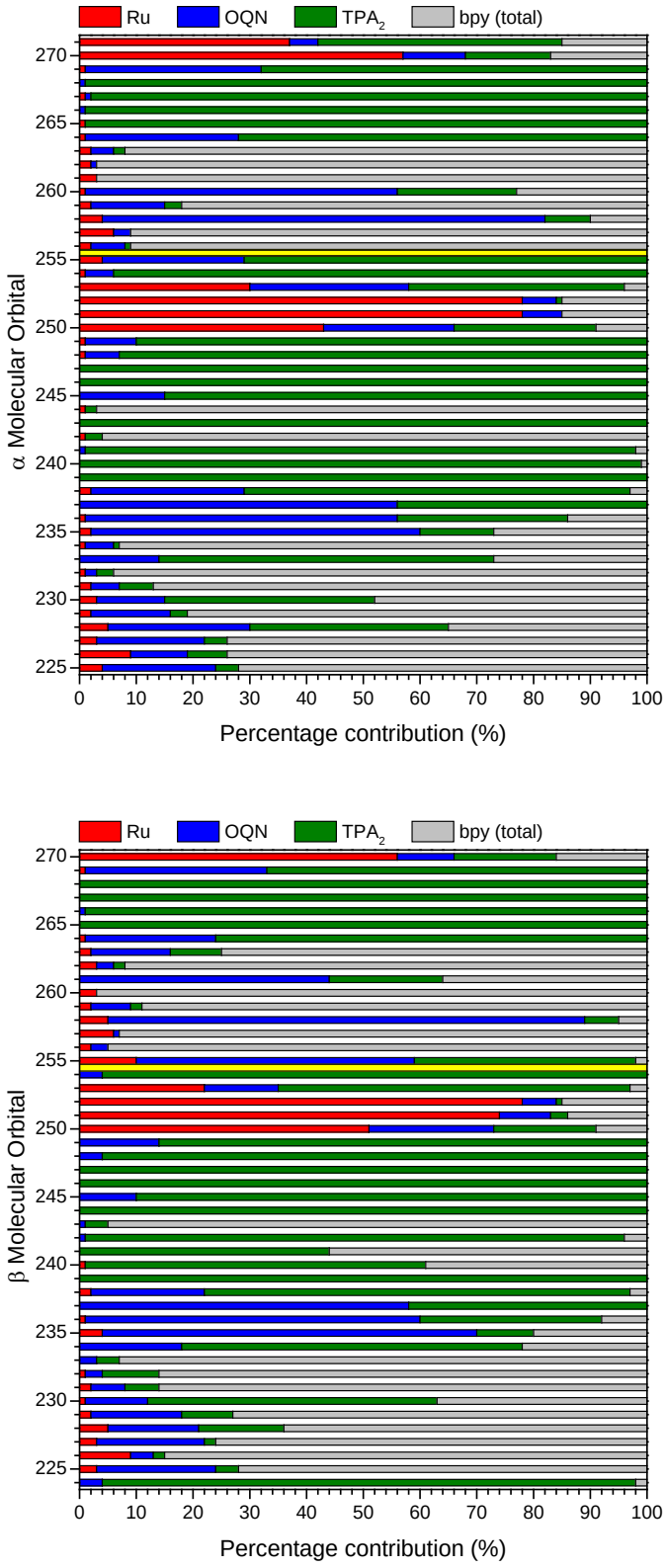

Fig. SI-67 Percentage contributions of Ru, OQN, TPA_2 and bpy fragments for α (left) and β (right) molecular orbitals of $\mathbf{8}^{2+}$. Filled and valence levels are separated by a yellow row between the HOMO (α 255)/LUMO (α 256) and HOMO (β 254)/LUMO (β 255) levels.

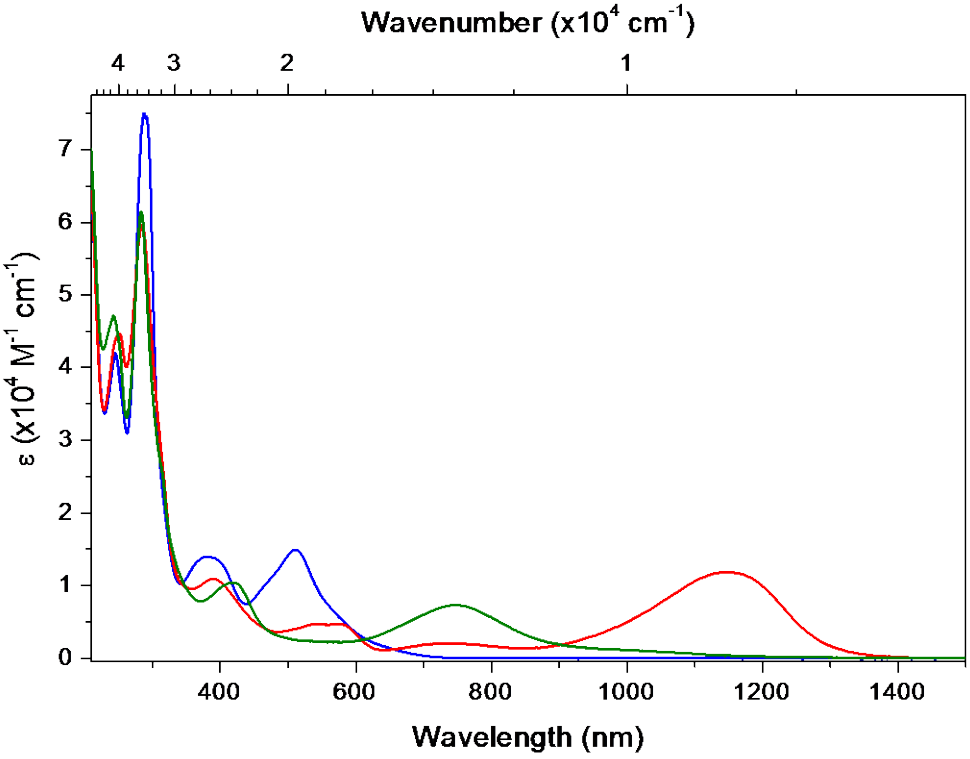

Figure SI-68. UV/Vis-NIR electronic absorption spectra of $\mathbf{7}^{+}$(blue), $\mathbf{7}^{2+}$(red) and $\mathbf{7}^{3+}$(green) prepared in-situ by controlled potential electrolysis in 0.1 M Bu_4NPF_6 acetonitrile electrolyte.

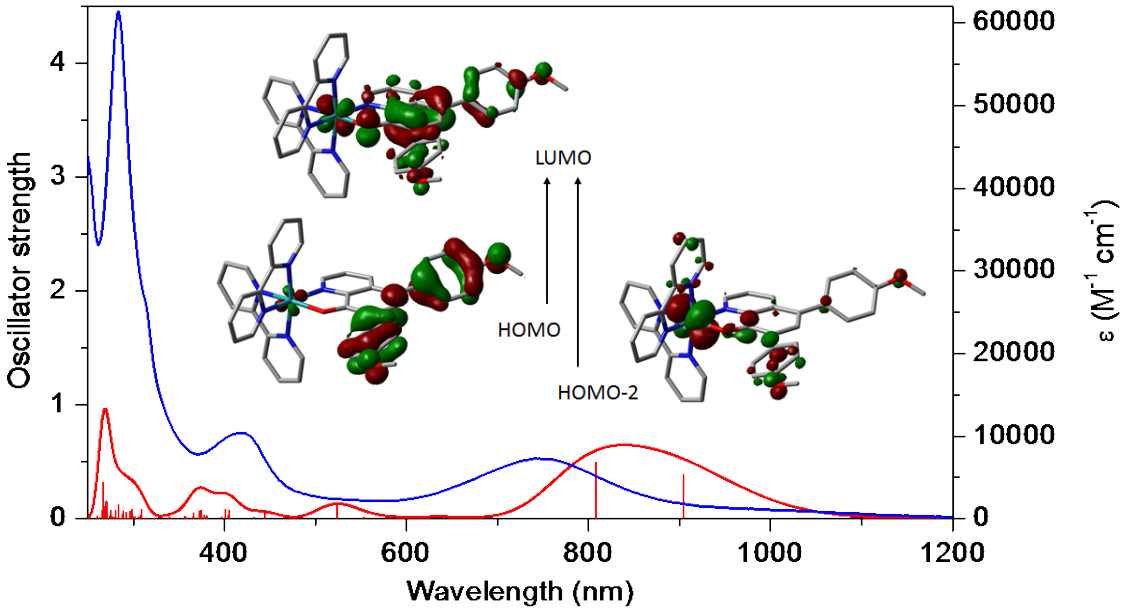

Figure SI-69. Overlay of experimental (blue) and theoretical (red) line and curve spectra for $\mathbf{7}^{3+}$.

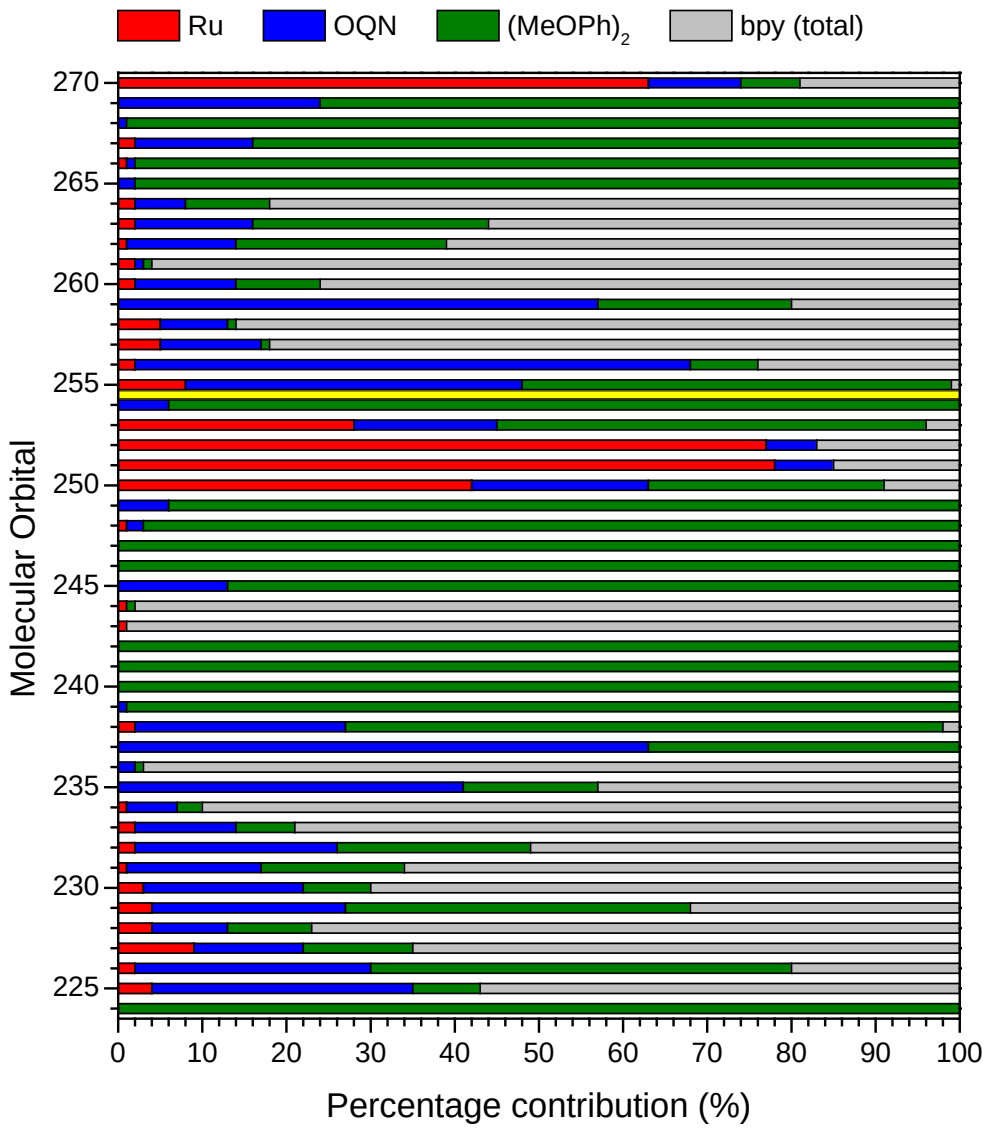

Fig. SI-70 Percentage contributions of Ru, OQN, $(MeOPh)_2$ and bpy fragments for frontier molecular orbitals of $\mathbf{7}^{3+}$. Filled and valence levels are separated by a yellow row between the HOMO (254) and LUMO (255) levels.

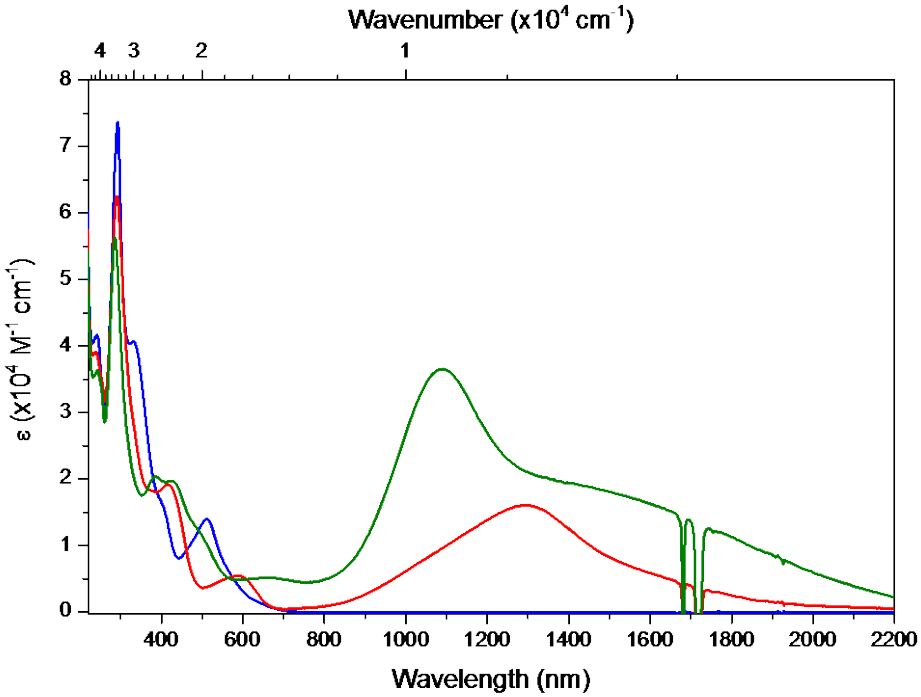

Figure SI-71. UV/Vis-NIR electronic absorption spectra of $\mathbf{8}^{+}$ (blue), $\mathbf{8}^{2+}$ (red) and $\mathbf{8}^{3+}$ (green) prepared in-situ by controlled potential electrolysis in 0.1 M Bu_4NPF_6 acetonitrile electrolyte.

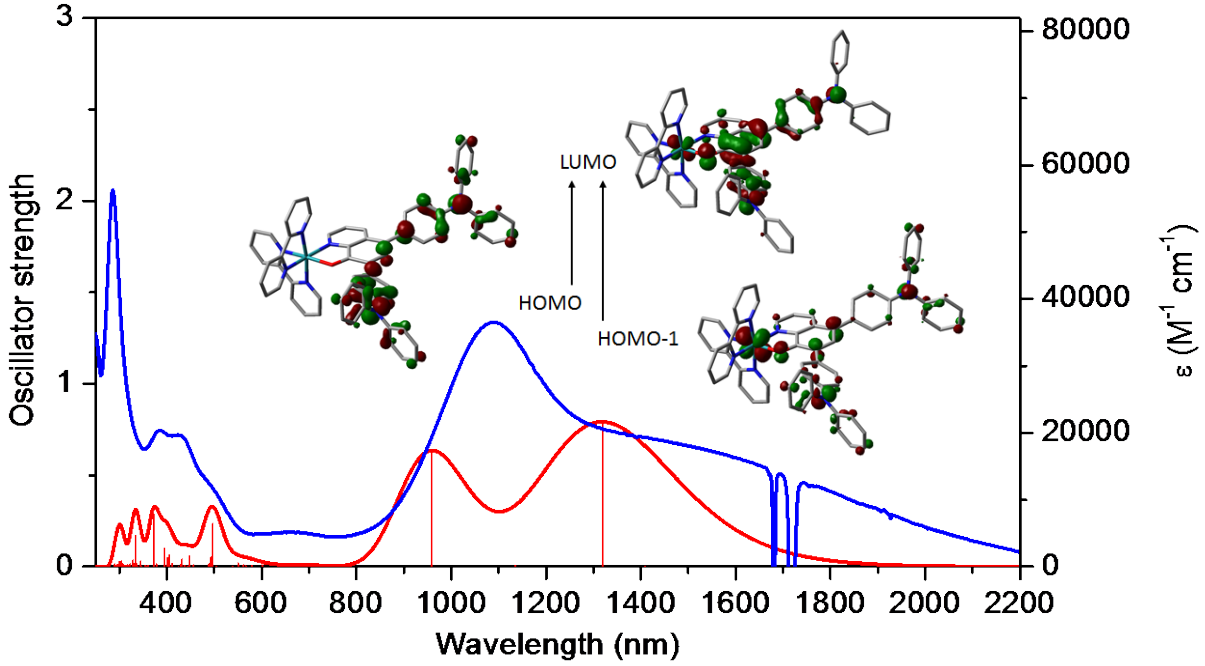

Figure SI-72. Overlay of experimental (blue) and theoretical (red) line and curve spectra for $\mathbf{8}^{3+}$.

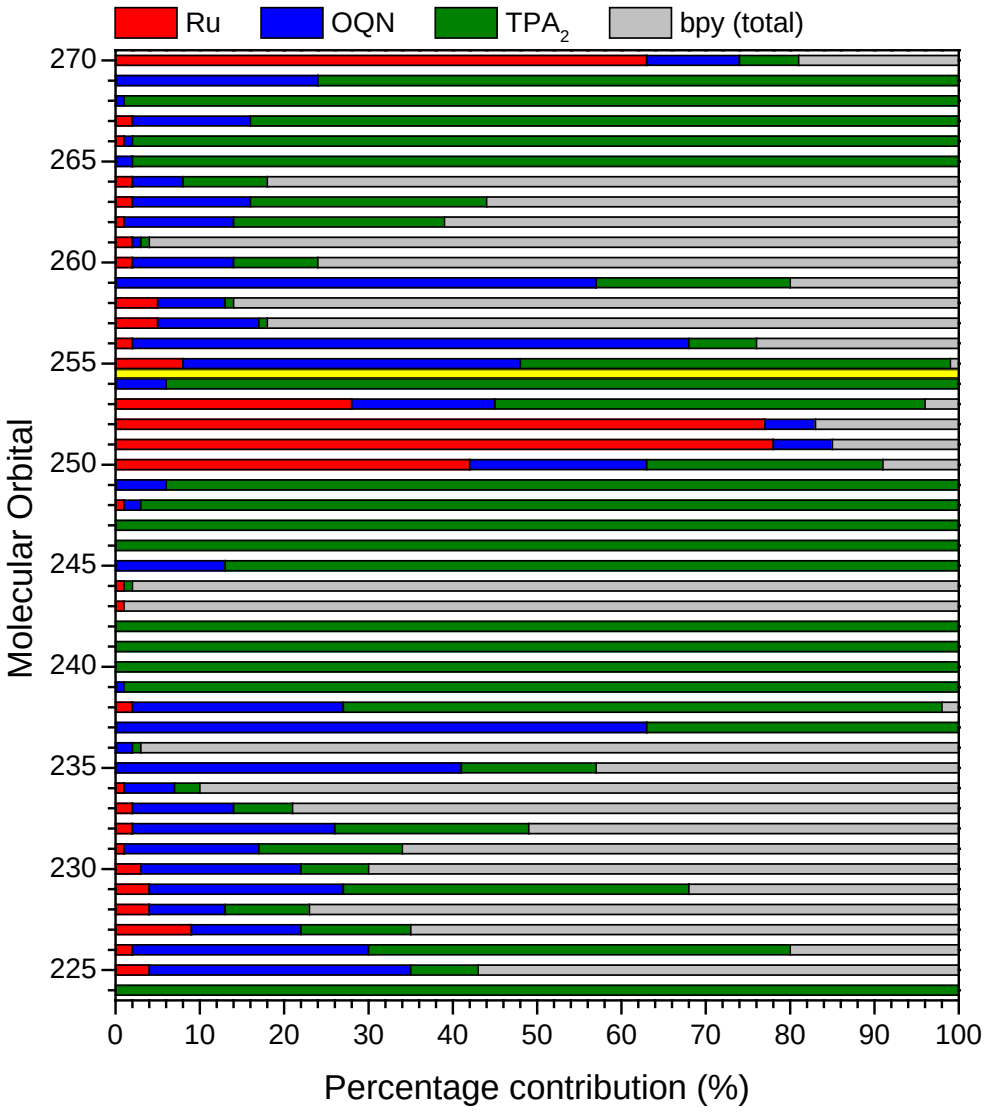

Fig. SI-73 Percentage contributions of Ru, OQN, TPA_2 and bpy fragments for frontier molecular orbitals of $\mathbf{8}^{3+}$. Filled and valence levels are separated by a yellow row between the HOMO (254) and LUMO (255) levels.

Table SI-17. Cartesian coordinates of the optimized complexes $\mathbf{1}^{2+}$ - $\mathbf{8}^{+}$.

$\mathbf{1}^{2+}$ $[Ru(bpy)_3]^{2+}$

Tag	Symbol	X	Y	Z
1	C	-1.32034	0.968148	2.106893
2	C	0.081877	2.036956	0.575745
3	C	-0.15527	3.268077	1.194069
4	C	-0.99974	3.334192	2.297905
5	C	-1.59334	2.162284	2.763909
6	H	-1.75796	0.034736	2.437727
7	H	0.312605	4.168904	0.818529
8	H	-1.18899	4.285074	2.78376
9	H	-2.25778	2.162562	3.620058
10	C	1.836125	0.366253	-2.15602
11	C	2.556038	1.370619	-2.79252
12	C	2.468235	2.672047	-2.30113
13	C	1.663347	2.920769	-1.19371
14	C	0.961996	1.869033	-0.59687
15	H	1.87318	-0.65751	-2.50626
16	H	3.168864	1.127543	-3.65265
17	H	3.015826	3.482063	-2.77026
18	H	1.585066	3.925572	-0.79909
19	C	-4.18246	-1.23682	-1.19275
20	C	-2.9186	-1.34198	-0.6046
21	C	-2.04561	0.179701	-2.14629
22	C	-3.27671	0.322032	-2.7757
23	C	-4.36587	-0.39786	-2.28754
24	H	-5.01857	-1.80062	-0.79984
25	H	-1.17337	0.719208	-2.49309
26	H	-3.36929	0.986188	-3.62703
27	H	-5.3431	-0.30977	-2.74942
28	C	-1.90032	-3.76373	2.713567
29	C	-1.00302	-2.9141	2.077163
30	C	-2.62591	-2.21084	0.552078
31	C	-3.57223	-3.04973	1.148055
32	C	-3.20885	-3.83385	2.238553
33	H	-1.57038	-4.3543	3.560196
34	H	0.022389	-2.82952	2.414241
35	H	-4.5833	-3.0958	0.764532
36	H	-3.9364	-4.48773	2.706664
37	C	0.583627	-4.22139	-2.81302
38	C	1.765014	-4.78774	-2.33742
39	C	2.390444	-4.21434	-1.23478

40	C	1.828008	-3.08814	-0.62706
41	C	0.071023	-3.10302	-2.16581
42	H	0.060486	-4.63189	-3.66873
43	H	2.19475	-5.66166	-2.81457
44	H	3.307042	-4.64471	-0.85231
45	H	-0.8433	-2.63104	-2.50287
46	C	3.620456	-2.80797	1.140874
47	C	4.102462	-2.11386	2.246423
48	C	3.371664	-1.03199	2.735077
49	C	2.18749	-0.68289	2.096516
50	C	2.420901	-2.41092	0.542614
51	H	4.175863	-3.64981	0.748415
52	H	5.032281	-2.41485	2.716432
53	H	3.705221	-0.46148	3.593946
54	H	1.587623	0.149447	2.442537
55	Ru	-0.04565	-0.8646	-0.03232
56	N	-1.34697	-2.15159	1.021232
57	N	-1.8606	-0.62873	-1.08489
58	N	-0.50245	0.895608	1.039053
59	N	1.054493	0.599123	-1.08417
60	N	1.715386	-1.34916	1.025473
61	N	0.670804	-2.54155	-1.09822

2^{+} $[Ru(bpy)_2(OQN)]^{+}$

Tag	Symbol	X	Y	Z
1	Ru	-3.84734	-0.77366	1.140099
2	C	-5.22869	1.091841	-0.69739
3	C	-2.91879	1.389865	-0.86806
4	C	-3.06885	2.403025	-1.80604
5	C	-4.35702	2.77275	-2.19656
6	C	-5.44181	2.107421	-1.63601
7	C	-6.31468	0.318593	-0.0665
8	C	-6.81158	-1.42889	1.412352
9	C	-8.17698	-1.27849	1.199155
10	C	-8.61695	-0.28708	0.320389
11	C	-7.67654	0.516018	-0.31829
12	H	-1.93822	1.07265	-0.53244
13	H	-2.19098	2.888623	-2.21766
14	H	-4.5136	3.561341	-2.92489
15	H	-6.44985	2.375403	-1.92856
16	H	-6.39709	-2.17581	2.081102
17	H	-8.87602	-1.92556	1.7172

18	H	-9.67578	-0.1407	0.134235
19	H	-8.0022	1.288701	-1.00421
20	C	-1.20089	-1.99469	0.660509
21	C	0.158626	-2.29469	0.79853
22	C	0.948896	-1.54254	1.660715
23	C	0.360357	-0.49547	2.370247
24	C	-0.9943	-0.24467	2.191019
25	C	-2.11402	-2.72581	-0.23622
26	C	-1.71933	-3.80486	-1.03466
27	C	-2.64511	-4.42742	-1.86446
28	C	-3.95691	-3.9534	-1.88178
29	C	-4.2896	-2.88121	-1.06393
30	H	0.59758	-3.11242	0.240483
31	H	2.002978	-1.77116	1.777469
32	H	0.933656	0.116411	3.057675
33	H	-1.49697	0.550716	2.728226
34	H	-0.69671	-4.1603	-1.00655
35	H	-2.34815	-5.26695	-2.4841
36	H	-4.71512	-4.40554	-2.51128
37	H	-5.2986	-2.48811	-1.03522
38	N	-5.9003	-0.64919	0.798164
39	N	-3.96397	0.742411	-0.31182
40	N	-1.76701	-0.96838	1.357227
41	N	-3.40014	-2.27374	-0.25558
42	C	-4.27456	-2.48816	4.990509
43	C	-4.16828	-1.71276	3.830689
44	C	-4.20777	-0.28562	3.988255
45	C	-4.35435	0.322839	5.273504
46	C	-4.45698	-0.50778	6.412628
47	C	-4.41486	-1.88324	6.252683
48	H	-4.24561	-3.56876	4.894799
49	C	-4.38558	1.7416	5.311937
50	H	-4.56745	-0.05981	7.394664
51	H	-4.49283	-2.52221	7.127912
52	C	-4.27918	2.467338	4.145817
53	C	-4.13506	1.789341	2.917245
54	H	-4.49459	2.244816	6.268708
55	H	-4.30306	3.551673	4.151976
56	H	-4.0463	2.335832	1.98418
57	N	-4.09554	0.461651	2.838488
58	O	-4.05478	-2.22558	2.621679

3^{+} $[Ru(bpy)_2(Me_2OQN)]^{+}$

Tag	Symbol	X	Y	Z
1	Ru	-0.46814	0.307039	0.362723
2	C	-0.82471	2.938667	1.999184
3	C	-0.80287	4.33664	2.176515
4	C	-0.46192	5.149499	1.117539
5	C	-0.14006	4.58305	-0.14489
6	H	-1.0856	2.276346	2.817004
7	H	-1.05344	4.75028	3.147124
8	H	-0.43898	6.22665	1.245935
9	C	3.49252	-1.3724	0.460952
10	C	2.125846	-1.11331	0.313937
11	C	3.747598	0.769377	1.51006
12	C	4.313706	-0.42438	1.062323
13	H	3.913631	-2.3058	0.109405
14	H	4.345606	1.538028	1.986042
15	H	5.374778	-0.61608	1.1795
16	C	0.569866	-4.15983	-1.32084
17	C	-0.75451	-3.72337	-1.35491
18	C	-1.05602	-2.46293	-0.85402
19	C	1.173832	-2.06273	-0.29103
20	C	1.539525	-3.32003	-0.78308
21	H	0.844434	-5.13637	-1.70468
22	H	-1.54626	-4.34167	-1.76207
23	H	-2.07002	-2.08283	-0.86574
24	H	2.572446	-3.6422	-0.74664
25	C	-3.32795	0.016351	1.049446
26	C	-4.72074	0.069761	0.933832
27	C	-5.29467	0.495464	-0.26042
28	C	-4.46342	0.858756	-1.32101
29	C	-3.08634	0.786722	-1.14714
30	H	-5.35211	-0.21662	1.765545
31	H	-6.37377	0.541222	-0.36004
32	H	-4.86871	1.194542	-2.26868
33	H	-2.3846	1.052984	-1.92943
34	C	-0.52646	-0.81263	3.237904
35	C	-1.10872	-1.25843	4.417936
36	C	-2.50038	-1.28594	4.513073
37	C	-3.25519	-0.86975	3.42132
38	C	-2.61262	-0.43218	2.258825
39	H	0.549762	-0.77224	3.122724
40	H	-0.47719	-1.5749	5.240166
41	H	-2.99015	-1.62643	5.418842

42	H	-4.33657	-0.88729	3.473458
43	N	-0.12288	-1.64205	-0.33382
44	N	-0.52442	2.366518	0.836348
45	N	1.581325	0.0581	0.75125
46	N	-1.24903	-0.40187	2.175716
47	N	-2.52744	0.37824	0.008199
48	C	2.383791	0.969964	1.335029
49	H	1.901343	1.881286	1.666207
50	C	0.459632	3.237002	-2.58175
51	C	-0.18931	3.156677	-0.24051
52	C	0.110072	2.465453	-1.46087
53	O	0.03549	1.148914	-1.49899
54	C	0.220096	5.341283	-1.29499
55	C	0.504719	4.642328	-2.46096
56	H	0.780896	5.212052	-3.34673
57	C	0.773999	2.548445	-3.88419
58	H	1.594836	1.830344	-3.76875
59	H	-0.08612	1.975176	-4.25171
60	H	1.056285	3.269709	-4.65593
61	C	0.288327	6.849482	-1.25021
62	H	-0.67642	7.299811	-0.98503
63	H	1.019602	7.210163	-0.51601
64	H	0.579075	7.248435	-2.22562

4^{+} [Ru(bpy)$_2$(*i*-Ph$_2$OQN)]$^{+}$

Tag	Symbol	X	Y	Z
1	Ru	-1.47265	0.008746	1.223982
2	C	-3.21475	1.674536	-0.48742
3	C	-2.45696	2.937133	1.321716
4	C	-3.1684	4.054799	0.902553
5	C	-3.93093	3.967508	-0.26203
6	C	-3.9521	2.764863	-0.96063
7	C	-3.17085	0.364107	-1.16119
8	C	-2.28528	-1.7958	-1.12406
9	C	-2.96864	-2.14862	-2.28159
10	C	-3.78413	-1.19843	-2.89503
11	C	-3.88437	0.067328	-2.32677
12	H	-1.85631	2.958126	2.221879
13	H	-3.12108	4.968699	1.48347
14	H	-4.49957	4.818438	-0.62098
15	H	-4.53788	2.677683	-1.86684
16	H	-1.64847	-2.50553	-0.61165

17	H	-2.85962	-3.1491	-2.68407
18	H	-4.3353	-1.43717	-3.79809
19	H	-4.51627	0.816505	-2.7865
20	C	1.107727	-0.84305	0.049867
21	C	2.191682	-0.90296	-0.83122
22	C	2.472741	0.184066	-1.65243
23	C	1.662968	1.315964	-1.56725
24	C	0.595998	1.311777	-0.67635
25	C	0.73105	-1.94712	0.951537
26	C	1.508703	-3.09125	1.157916
27	C	1.058119	-4.0809	2.026238
28	C	-0.16735	-3.90835	2.671604
29	C	-0.89325	-2.74797	2.431227
30	H	2.802964	-1.79541	-0.88516
31	H	3.307098	0.146339	-2.34447
32	H	1.844598	2.191115	-2.18068
33	H	-0.05912	2.168874	-0.5818
34	H	2.459922	-3.20365	0.652989
35	H	1.654604	-4.97084	2.195768
36	H	-0.55902	-4.65532	3.352571
37	H	-1.85462	-2.56155	2.894533
38	N	-2.46819	1.769292	0.649856
39	N	-2.37495	-0.57185	-0.56914
40	N	-0.45737	-1.7838	1.597626
41	N	0.3055	0.25911	0.11119
42	C	-4.33543	-0.51412	4.315445
43	C	-3.23777	-0.21968	3.495263
44	C	-2.12147	0.482505	4.07604
45	C	-2.16486	0.898307	5.44611
46	C	-3.29414	0.561228	6.232902
47	C	-4.34827	-0.13333	5.664302
48	C	-1.03233	1.620074	5.948625
49	H	-5.20827	-0.39224	6.276478
50	C	0.034111	1.809918	5.093496
51	C	0.02318	1.346604	3.755387
52	H	0.909902	2.351048	5.433182
53	N	-1.03721	0.713111	3.243367
54	O	-3.19414	-0.58359	2.235632
55	C	1.256454	1.617859	2.954222
56	C	2.287697	0.66967	2.902874
57	C	1.463704	2.882909	2.385441
58	C	3.495643	0.974003	2.271892
59	H	2.148602	-0.30105	3.369576

60	C	2.671031	3.185164	1.753217
61	H	0.683493	3.635926	2.446636
62	C	3.689516	2.231175	1.694873
63	H	4.287483	0.231452	2.239408
64	H	2.817683	4.167649	1.31417
65	H	4.631664	2.468635	1.209744
66	C	-0.96005	2.162426	7.331653
67	C	0.163642	1.89299	8.131542
68	C	-1.96919	2.995151	7.846642
69	C	0.271089	2.431685	9.414145
70	H	0.947422	1.245696	7.749211
71	C	-1.85576	3.539697	9.126012
72	H	-2.83433	3.230942	7.235205
73	C	-0.73791	3.257234	9.915285
74	H	1.142278	2.204527	10.02153
75	H	-2.63996	4.188889	9.504251
76	H	-0.65379	3.678326	10.91274
77	H	-5.17131	-1.05386	3.880532
78	H	-3.31909	0.836947	7.279121

5^{+} $[Ru(bpy)_2(PhOQN)]^{+}$

Tag	Symbol	X	Y	Z
1	Ru	-3.85827	-0.81781	1.184921
2	C	-5.25329	0.959177	-0.72065
3	C	-2.94968	1.329049	-0.83405
4	C	-3.10726	2.310982	-1.80423
5	C	-4.39442	2.623828	-2.24194
6	C	-5.47388	1.938957	-1.69363
7	C	-6.3326	0.176972	-0.08928
8	C	-6.82759	-1.52071	1.443029
9	C	-8.19025	-1.41194	1.191778
10	C	-8.62916	-0.46693	0.263364
11	C	-7.69121	0.33302	-0.38235
12	H	-1.96912	1.057556	-0.46277
13	H	-2.23399	2.815035	-2.20211
14	H	-4.55633	3.385345	-2.99698
15	H	-6.48068	2.164299	-2.02204
16	H	-6.42187	-2.2345	2.150687
17	H	-8.88646	-2.05596	1.716666
18	H	-9.68524	-0.3536	0.043625
19	H	-8.01602	1.070314	-1.10578
20	C	-1.15967	-1.88616	0.605558

21	C	0.220792	-2.09861	0.68158
22	C	0.99172	-1.32429	1.542544
23	C	0.36362	-0.34523	2.312125
24	C	-1.01137	-0.18234	2.194407
25	C	-2.0566	-2.64408	-0.28636
26	C	-1.61926	-3.65515	-1.1483
27	C	-2.53541	-4.31272	-1.96255
28	C	-3.8787	-3.94344	-1.89888
29	C	-4.25312	-2.93225	-1.0225
30	H	0.691793	-2.8622	0.075715
31	H	2.062584	-1.48288	1.608917
32	H	0.921286	0.284257	2.995977
33	H	-1.54122	0.564306	2.77293
34	H	-0.57232	-3.92802	-1.18521
35	H	-2.205	-5.09836	-2.63328
36	H	-4.63028	-4.42588	-2.5131
37	H	-5.28593	-2.61815	-0.93796
38	N	-5.91694	-0.74718	0.821444
39	N	-3.98979	0.662523	-0.29313
40	N	-1.766	-0.92973	1.365318
41	N	-3.37277	-2.29078	-0.22981
42	C	-4.27499	-2.4302	5.100563
43	C	-4.16375	-1.69159	3.916241
44	C	-4.23603	-0.2588	4.035269
45	C	-4.39952	0.391894	5.298219
46	C	-4.47352	-0.40304	6.486619
47	C	-4.42302	-1.78871	6.338814
48	H	-4.23002	-3.51377	5.046775
49	C	-4.52666	1.808251	5.265075
50	H	-4.47797	-2.40424	7.232911
51	C	-4.45112	2.486551	4.069209
52	C	-4.24966	1.769707	2.873547
53	H	-4.69226	2.35182	6.187903
54	H	-4.54775	3.565845	4.028879
55	H	-4.17363	2.280577	1.920378
56	N	-4.14954	0.444098	2.854645
57	O	-4.01813	-2.23913	2.73206
58	C	-4.6017	0.189778	7.844767
59	C	-5.596	-0.26983	8.728083
60	C	-3.71551	1.180426	8.308666
61	C	-5.70354	0.24195	10.02188
62	H	-6.29711	-1.02677	8.387981
63	C	-3.82727	1.698298	9.599902

64	H	-2.91781	1.530747	7.66008
65	C	-4.82193	1.231859	10.46297
66	H	-6.48265	-0.12754	10.68286
67	H	-3.12772	2.458923	9.935249
68	H	-4.90743	1.633705	11.46833

6^{+} $[Ru(bpy)_2(Ph_2OQN)]^{+}$

Tag	Symbol	X	Y	Z
1	Ru	-1.74559	0.153101	1.153226
2	C	-3.05938	1.668439	-1.01685
3	C	-2.29879	3.142606	0.625387
4	C	-2.83701	4.237794	-0.03842
5	C	-3.51384	4.028807	-1.2406
6	C	-3.62202	2.732249	-1.73094
7	C	-3.1118	0.264669	-1.46301
8	C	-2.48253	-1.93267	-0.99571
9	C	-3.08814	-2.40664	-2.15221
10	C	-3.73332	-1.49807	-2.9914
11	C	-3.74216	-0.15275	-2.64049
12	H	-1.77337	3.253988	1.566249
13	H	-2.7298	5.229462	0.38675
14	H	-3.95067	4.859023	-1.78546
15	H	-4.14406	2.549968	-2.66215
16	H	-1.98105	-2.60335	-0.30875
17	H	-3.05596	-3.46594	-2.38108
18	H	-4.22245	-1.8304	-3.90095
19	H	-4.24038	0.566857	-3.27837
20	C	0.975725	-0.99913	0.985631
21	C	2.327905	-1.15468	0.660844
22	C	2.957676	-0.22084	-0.15465
23	C	2.214481	0.858073	-0.63659
24	C	0.876742	0.962109	-0.27847
25	C	0.221199	-1.94797	1.825916
26	C	0.765222	-3.10127	2.401182
27	C	-0.04634	-3.93814	3.161426
28	C	-1.3921	-3.60783	3.330046
29	C	-1.87878	-2.4488	2.736534
30	H	2.885217	-2.00198	1.041725
31	H	4.005783	-0.33408	-0.41064
32	H	2.658962	1.610172	-1.27898
33	H	0.26199	1.784559	-0.62509
34	H	1.811103	-3.34511	2.259326

35	H	0.365979	-4.83383	3.614106
36	H	-2.05888	-4.23244	3.913984
37	H	-2.91202	-2.12951	2.824086
38	N	-2.39961	1.882393	0.157677
39	N	-2.48657	-0.63164	-0.64748
40	N	-1.0927	-1.63541	2.004159
41	N	0.256831	0.066271	0.517915
42	C	-4.89811	0.557571	3.983723
43	C	-3.72125	0.572147	3.203677
44	C	-2.5551	1.193056	3.763023
45	C	-2.55937	1.82986	5.044202
46	C	-3.77946	1.861608	5.784851
47	C	-4.8808	1.216616	5.236701
48	C	-1.3212	2.345817	5.506631
49	H	-5.8129	1.254221	5.791992
50	C	-0.18925	2.247789	4.725549
51	C	-0.2726	1.627413	3.465179
52	H	-1.27244	2.807485	6.486443
53	H	0.765606	2.6317	5.067774
54	H	0.598854	1.536984	2.825265
55	N	-1.40932	1.117512	2.998799
56	O	-3.62935	0.003826	2.016425
57	C	-4.41526	1.866099	8.212343
58	C	-3.8976	2.549691	7.098978
59	C	-3.53979	3.900547	7.256813
60	C	-3.68582	4.541254	8.48734
61	C	-4.19879	3.847069	9.584604
62	C	-4.56617	2.507856	9.441297
63	H	-4.68705	0.819102	8.112051
64	H	-3.17116	4.459373	6.401012
65	H	-3.4107	5.587526	8.585233
66	H	-4.31446	4.346504	10.54177
67	H	-4.96499	1.959063	10.28954
68	C	-8.53047	-1.39851	2.741696
69	C	-7.7362	-0.73733	1.802579
70	C	-6.55103	-0.11434	2.189842
71	C	-6.13527	-0.12907	3.534254
72	C	-6.94468	-0.80376	4.467367
73	C	-8.12693	-1.43081	4.077395
74	H	-9.45218	-1.88477	2.436002
75	H	-8.04441	-0.70234	0.761092
76	H	-5.94071	0.394378	1.454224
77	H	-6.63477	-0.85428	5.507153

78	H	-8.73039	-1.94831	4.817622

7^{+} {Ru(bpy)$_2$[(MeOPh)$_2$OQN]}$^{+}$

Tag	Symbol	X	Y	Z
1	Ru	-1.59077	-0.06615	1.190042
2	C	-2.99992	1.683746	-0.7368
3	C	-2.25689	2.94623	1.08064
4	C	-2.82232	4.107219	0.56746
5	C	-3.50508	4.041339	-0.64701
6	C	-3.59162	2.817697	-1.30294
7	C	-3.02281	0.349704	-1.36456
8	C	-2.342	-1.87637	-1.19101
9	C	-2.939	-2.20455	-2.40213
10	C	-3.60509	-1.20708	-3.11381
11	C	-3.64496	0.080014	-2.58797
12	H	-1.71932	2.949928	2.020743
13	H	-2.7267	5.037462	1.115566
14	H	-3.96168	4.925756	-1.0779
15	H	-4.11613	2.747721	-2.24735
16	H	-1.8198	-2.62113	-0.60334
17	H	-2.87978	-3.22219	-2.77064
18	H	-4.08528	-1.4253	-4.06151
19	H	-4.15658	0.867274	-3.127
20	C	1.147985	-1.04926	0.664313
21	C	2.47177	-1.09306	0.215693
22	C	2.993807	-0.02244	-0.50258
23	C	2.17439	1.076579	-0.76174
24	C	0.868263	1.064711	-0.28856
25	C	0.504588	-2.14008	1.419776
26	C	1.14479	-3.3303	1.779961
27	C	0.440714	-4.30394	2.481888
28	C	-0.89527	-4.06976	2.810118
29	C	-1.4776	-2.86772	2.42612
30	H	3.090017	-1.95723	0.423706
31	H	4.01946	-0.04778	-0.85411
32	H	2.533506	1.933533	-1.32003
33	H	0.199056	1.897747	-0.46457
34	H	2.181539	-3.49734	1.516197
35	H	0.928308	-5.23006	2.766444
36	H	-1.48137	-4.8009	3.355005
37	H	-2.50961	-2.62507	2.650158
38	N	-2.33788	1.756591	0.453167

39	N	-2.37744	-0.63304	-0.67356
40	N	-0.79965	-1.9219	1.748469
41	N	0.35442	0.034601	0.414337
42	C	-4.59649	-0.04213	4.234246
43	C	-3.45097	0.031002	3.406265
44	C	-2.25031	0.586533	3.972825
45	C	-2.17726	1.050857	5.322284
46	C	-3.35164	0.976829	6.134718
47	C	-4.49442	0.429804	5.564597
48	C	-0.91197	1.513807	5.771736
49	H	-5.38036	0.359205	6.188886
50	C	0.162145	1.547965	4.910196
51	C	-0.00319	1.1142	3.581128
52	H	-0.79554	1.83579	6.800095
53	H	1.134573	1.90007	5.235998
54	H	0.819649	1.143468	2.876042
55	N	-1.16214	0.64552	3.127897
56	O	-3.43142	-0.37532	2.157002
57	C	-5.89767	-0.55885	3.740282
58	C	-7.10764	0.002069	4.183034
59	C	-5.98748	-1.64066	2.837956
60	C	-8.35054	-0.48471	3.771052
61	C	-7.21538	-2.13775	2.421288
62	C	-8.41075	-1.56682	2.885171
63	C	-3.38309	1.442663	7.547473
64	C	-3.86576	0.607439	8.566014
65	C	-2.98727	2.745147	7.91411
66	C	-3.95377	1.032923	9.894257
67	C	-3.06189	3.182135	9.230978
68	C	-3.5464	2.328565	10.23463
69	H	-7.27212	-2.97716	1.73473
70	H	-5.07893	-2.09425	2.462888
71	H	-7.08843	0.855659	4.854193
72	H	-9.25282	-0.00952	4.13724
73	H	-4.17184	-0.40552	8.320222
74	H	-4.32936	0.348916	10.64597
75	H	-2.76164	4.189321	9.502883
76	H	-2.63617	3.434082	7.151332
77	O	-9.56388	-2.12749	2.415707
78	O	-3.58284	2.850479	11.49518
79	C	-10.8046	-1.58525	2.859028
80	H	-10.9145	-0.5358	2.560896
81	H	-11.5822	-2.17928	2.377413

82	H	-10.9116	-1.66306	3.947495
83	C	-4.07908	2.029812	12.54944
84	H	-3.46612	1.130386	12.68117
85	H	-4.02622	2.637133	13.45369
86	H	-5.11977	1.733875	12.37206

8^{+} $[Ru(bpy)_2(TPA_2OQN)]^{+}$

Tag	Symbol	X	Y	Z
1	Ru	1.185623	-0.03402	0.183167
2	C	1.799653	1.797801	2.426142
3	C	0.176303	0.255848	3.087073
4	C	0.074649	0.830261	4.348248
5	C	0.871922	1.934533	4.649259
6	C	1.742303	2.418806	3.678314
7	C	2.699184	2.229036	1.340227
8	C	3.429863	1.816684	-0.83826
9	C	4.324893	2.878551	-0.79164
10	C	4.399988	3.641636	0.373316
11	C	3.579269	3.310936	1.446565
12	H	-0.42233	-0.60329	2.81043
13	H	-0.61756	0.415409	5.071901
14	H	0.819836	2.410231	5.622565
15	H	2.371076	3.272848	3.895645
16	H	3.334795	1.201876	-1.7245
17	H	4.943911	3.096237	-1.65437
18	H	5.084635	4.479592	0.446865
19	H	3.624231	3.892277	2.358637
20	C	3.059487	-2.18591	-0.58755
21	C	4.015332	-3.20198	-0.49091
22	C	4.554154	-3.52807	0.749301
23	C	4.124736	-2.82483	1.875039
24	C	3.171674	-1.82619	1.717975
25	C	2.439816	-1.76482	-1.85796
26	C	2.730305	-2.33538	-3.10146
27	C	2.098097	-1.85217	-4.24314
28	C	1.185883	-0.80309	-4.12077
29	C	0.936193	-0.27699	-2.85883
30	H	4.33765	-3.7336	-1.37741
31	H	5.295749	-4.31492	0.833604
32	H	4.516455	-3.04024	2.86253
33	H	2.807683	-1.25746	2.564836
34	H	3.442249	-3.1474	-3.17996

35	H	2.31602	-2.28797	-5.21217
36	H	0.672569	-0.3953	-4.98403
37	H	0.242174	0.539596	-2.6961
38	N	1.014459	0.720308	2.139455
39	N	2.630175	1.490691	0.195661
40	N	1.544125	-0.74365	-1.75121
41	N	2.639696	-1.50585	0.520824
42	C	-2.71786	1.469046	-0.71258
43	C	-1.54196	0.760563	-0.36687
44	C	-1.68186	-0.62169	0.01158
45	C	-2.94795	-1.2797	0.074621
46	C	-4.12637	-0.52381	-0.22041
47	C	-3.96069	0.798886	-0.61209
48	C	-2.9344	-2.66462	0.388644
49	H	-4.85699	1.377867	-0.81416
50	C	-1.7442	-3.30581	0.652949
51	C	-0.54097	-2.57683	0.60775
52	H	-3.86652	-3.21727	0.4093
53	H	-1.71505	-4.36305	0.891792
54	H	0.409068	-3.05104	0.825983
55	N	-0.50692	-1.28449	0.295382
56	O	-0.33977	1.285452	-0.4099
57	C	-6.42678	-0.94132	-1.14769
58	C	-5.49483	-1.09236	-0.10489
59	C	-5.93492	-1.74823	1.060095
60	C	-7.23078	-2.2436	1.173044
61	C	-8.15429	-2.0779	0.127359
62	C	-7.73214	-1.41157	-1.03517
63	H	-6.12271	-0.44234	-2.06344
64	H	-5.25533	-1.86521	1.899049
65	H	-7.53615	-2.75033	2.082442
66	H	-8.42902	-1.26949	-1.85456
67	C	-2.70561	5.598788	-2.02089
68	C	-1.78044	5.148375	-1.064
69	C	-1.77507	3.821663	-0.64532
70	C	-2.68453	2.880133	-1.1671
71	C	-3.59661	3.343249	-2.13561
72	C	-3.61788	4.671507	-2.54953
73	H	-1.06339	5.846785	-0.64454
74	H	-1.04786	3.501067	0.090035
75	H	-4.30401	2.650382	-2.58158
76	H	-4.34001	4.9923	-3.29318
77	N	-2.71427	6.954065	-2.44697

78	N	-9.4815	-2.56873	0.244732
79	C	-2.54224	8.000508	-1.50007
80	C	-3.17105	7.93941	-0.24477
81	C	-1.7405	9.113715	-1.80511
82	C	-2.9922	8.96486	0.683054
83	H	-3.7988	7.088252	-0.00266
84	C	-1.58205	10.14276	-0.87765
85	H	-1.24476	9.167089	-2.76875
86	C	-2.20162	10.07479	0.373196
87	H	-3.48701	8.900575	1.64808
88	H	-0.95848	10.99545	-1.13125
89	H	-2.07038	10.87471	1.095435
90	C	-2.90839	7.265089	-3.82133
91	C	-2.25753	6.520309	-4.81937
92	C	-3.75466	8.31994	-4.20264
93	C	-2.45861	6.820965	-6.16601
94	H	-1.59641	5.708638	-4.53394
95	C	-3.93585	8.62463	-5.5513
96	H	-4.26742	8.89593	-3.43937
97	C	-3.29422	7.876243	-6.54188
98	H	-1.94702	6.23449	-6.92401
99	H	-4.59429	9.443361	-5.82757
100	H	-3.44321	8.11184	-7.59118
101	C	-10.1144	-3.18749	-0.86891
102	C	-11.457	-2.90582	-1.17234
103	C	-9.40833	-4.09116	-1.68058
104	C	-12.0777	-3.52318	-2.25773
105	H	-12.0081	-2.20387	-0.55518
106	C	-10.032	-4.68982	-2.77474
107	H	-8.37353	-4.32143	-1.44928
108	C	-11.3703	-4.41482	-3.06858
109	H	-13.1166	-3.29356	-2.47732
110	H	-9.47071	-5.3864	-3.39112
111	H	-11.8548	-4.88848	-3.91685
112	C	-10.1808	-2.4436	1.477386
113	C	-10.9575	-3.50678	1.96763
114	C	-10.1063	-1.25511	2.223135
115	C	-11.6482	-3.37672	3.172041
116	H	-11.016	-4.4311	1.402427
117	C	-10.7857	-1.14083	3.435492
118	H	-9.51538	-0.42572	1.848768
119	C	-11.5642	-2.19703	3.916497
120	H	-12.2437	-4.2093	3.535854

121	H	-10.7163	-0.21431	3.998447
122	H	-12.0977	-2.10221	4.857281

Complete reference # 57

Frisch, M. J.; Trucks, G. W.; Schlegel, H. B.; Scuseria, G. E.; Robb, M. A.; Cheeseman, J. R.; Scalmani, G.; Barone, V.; Mennucci, B.; Petersson, G. A.; Nakatsuji, H.; Caricato, M.; Li, X.; P., H. H.; Izmaylov, A. F.; Bloino, J.; Zheng, G.; Sonnenberg, J. L.; Hada, M.; Ehara, M.; Toyota, K.; Fukuda, R.; Hasegawa, J.; Ishida, M.; Nakajima, T.; Honda, Y.; Kitao, O.; Nakai, H.; Vreven, T.; Montgomery, J. J. A.; Peralta, J. E.; Ogliaro, F.; Bearpark, M.; Heyd, J. J.; Brothers, E.; Kudin, K. N.; Staroverov, V. N.; Kobayashi, R.; Normand, J.; Raghavachari, K.; Rendell, A.; Burant, J. C.; Iyengar, S. S.; Tomasi, J.; Cossi, M.; Rega, N.; Millam, N. J.; Klene, M.; Knox, J. E.; Cross, J. B.; Bakken, V.; Adamo, C.; Jaramillo, J.; Gomperts, R.; Stratmann, R. E.; Yazyev, O.; Austin, A. J.; Cammi, R.; Pomelli, C.; Ochterski, J. W.; Martin, R. L.; Morokuma, K.; Zakrzewski, V. G.; Voth, G. A.; Salvador, P.; Dannenberg, J. J.; Dapprich, S.; Daniels, A. D.; Farkas, Ö.; Foresman, J. B.; Ortiz, J. V.; Cioslowski, J.; Fox, D. J.; Revision A.1 ed.; Gaussian Inc.: Wallingford, CT., 2009.